

INFLUENCE OF MINERALOGICAL CHARACTERISTICS ON
RHEOLOGICAL BEHAVIOR OF TAILINGS SLURRIES

A THESIS SUBMITTED TO
THE GRADUATE SCHOOL OF NATURAL AND APPLIED SCIENCES
OF
MIDDLE EAST TECHNICAL UNIVERSITY

BY

BERKE BESTE AKTAŞ

IN PARTIAL FULFILLMENT OF THE REQUIREMENTS
FOR
THE DEGREE OF MASTER OF SCIENCE
IN
MINING ENGINEERING

AUGUST 2022

Approval of the thesis:

**INFLUENCE OF MINERALOGICAL CHARACTERISTICS ON
RHEOLOGICAL BEHAVIOR OF TAILINGS SLURRIES**

submitted by **BERKE BESTE AKTAŞ** in partial fulfillment of the requirements
for the degree of **Master of Science in Mining Engineering, Middle East
Technical University** by,

Prof. Dr. Halil Kalıpçılar
Dean, Graduate School of **Natural and Applied Sciences**

Prof. Dr. Naci Emre Altun
Head of the Department, **Mining Engineering, METU**

Prof. Dr. Naci Emre Altun
Supervisor, **Mining Engineering, METU**

Examining Committee Members:

Assoc. Prof. Dr. Nurullah Metin Can
Mining Engineering, Hacettepe University

Prof. Dr. Naci Emre Altun
Mining Engineering, METU

Assoc. Prof. Dr. Mustafa Erkayaoğlu
Mining Engineering, METU

Date: 19.08.2022

I hereby declare that all information in this document has been obtained and presented in accordance with academic rules and ethical conduct. I also declare that, as required by these rules and conduct, I have fully cited and referenced all material and results that are not original to this work.

Name Last name : Berke Beste Aktaş

Signature :

ABSTRACT

INFLUENCE OF MINERALOGICAL CHARACTERISTICS ON RHEOLOGICAL BEHAVIOR OF TAILINGS SLURRIES

Aktaş, Berke Beste
Master of Science, Mining Engineering
Supervisor : Prof. Dr. N. Emre Altun

August 2022, 86 pages

The gradual depletion of high-grade ores force mining operations to process ores to finer particles to extract valuable minerals. With the increased amount of fine particles and, in some cases, high clay mineral content presence, complex rheological behaviors in phases including suspensions, such as high viscosity and high yield stress have been observed, causing a decrease in the performance of certain mineral processing operations. Through the study, rheological characteristics of ore tailings slurries with respect to the mineralogy and with special emphasis on the presence of clay minerals were investigated for backfill purposes of tailings from mineral processing plants. Also, this study aims to identify the influence of clay presence, on the flow behavior of ore tailings slurries, as a key information for slurry involving phases in downstream processes. Pure mineral suspensions and tailings samples were investigated in terms of surface charge properties to establish a rheological classification. In addition to surface charge property experiments, the rheological properties of the tailings samples with greater and less extent of clay minerals were examined to enable the real simulations of rheological properties of clay minerals in complex multi-component ore systems where different clay particles are locked in valuable mineral particles.

The tailings samples were examined to identify their viscosity and yield stress values at different pulp conditions. The rheological data produced were evaluated using “Bingham Plastic” and “Casson” models. The significant findings were obtained thanks to rheological measurements. First of all, regardless of the vein of the tailings samples, the samples showed thixotropic behavior. Secondly, it was obtained that solid content plays an important role in viscosity regardless of which veins the tailings samples were sourced. The small amount of increase in the solid content caused a significant decrease in the flow by increasing viscosity. In addition to these findings, it was revealed that the mineralogical characteristics have a significant effect on the rheological behavior of tailings slurries. In this context, the ore tailings sample from the clayey vein of the deposit showed higher viscosity than that of the normal vein of the same deposit despite similar solid content. The higher values of surface charges caused the more dispersed state whereas the particles with relatively lower values of surface charges were prone to interparticle interactions and agglomeration in suspensions. As a result, this would result in suspensions of higher viscosity and yield stress than in the dispersed state. To conclude, the transportation of “clayey” tailings was observed to be more challenging. Therefore, it becomes more critical to optimize rheological behavior of ore tailings slurries by arranging solid content especially for “clayey” tailings. In other words, the mineralogical characteristics of tailings slurries, and the processing conditions are critical for the transportation of the tailings from the minerals processing plant for backfill purposes. Therefore, the real simulation and the optimization of the rheological behavior of ore tailings slurries are of great importance so that the problems encountered during the transportation of tailings can be eliminated, and the desired processing plant conditions with high command can be provided.

Keywords: Rheology, Yield Stress, Viscosity, Surface Charge, Clay Minerals

ÖZ

MİNERALOJİK ÖZELLİKLERİN ATIK ÇAMURLARININ REOLOJİK DAVRANIMINA ETKİSİ

Aktaş, Berke Beste
Yüksek Lisans, Maden Mühendisliği
Tez Yöneticisi: Prof. Dr. N. Emre Altun

Ağustos 2022, 86 sayfa

Yüksek tenörlü cevherlerin giderek tükenmesi nedeniyle, madencilik operasyonları, değerli madenlerin işletilebilmesi için cevherleri daha ince boyutlara öğütmek zorunda kalmaktadır. Giderek artan ince tanecik miktarı ve bazı durumlarda mevcut yüksek kil minerali içeriği ile atık çamurları içeren operasyonlarda yüksek viskozite ve akma direnci gibi karmaşık reolojik davranımlar gözlemlenmiş ve bu da cevher hazırlama operasyonlarının performansının düşmesine neden olmuştur ve olmaktadır. Bu çalışmada atık çamurlarının akış davranımlarının cevherin mineralojik karakteristiklerine ve özellikle kil mineralleri içeriğine göre değişimleri incelenmiş ve cevher hazırlama tesis atıklarının yer altı yöntemleriyle işletilen madenlerde geri dolgu malzemesi olarak kullanımı irdelenmiştir. Ayrıca, bu çalışma kil minerallerinin atık çamurlarının akış davranışlarına olan etkilerinin belirlenmesine ve süspansiyon içeren proses aşamalarındaki davranımının anlaşılmasına yardımcı olmasını amaçlamaktadır. Saf kil mineralleri ve aynı cevherin farklı damarlarından alınan iki atık çamuru örneği reolojik bir sınıflandırma ortaya koymak için mineralojik özellikleri ve yüzey yükü özellikleri açısından karşılaştırılmalı olarak incelenmiştir. Atık çamuru örneklerden birisi diğerine göre daha yüksek miktarda kil mineralleri içermektedir. Her iki örnek

reolojik tetkik ve testlere tabi tutularak çamur örneklerinin farklı pülp koşullarında viskozite ve akma direnci değerleri belirlenmiş ve reolojik bulgular “Bingham Plastic” ve “Casson” modelleri kullanılarak değerlendirilmiştir. Öncelikle, cevher zonundan bağımsız olarak, atık çamurlarının tiksotropik davranıma sahip olduğu gözlemlenmiştir. Diğer önemli bulgu, yine cevher zonundan bağımsız olarak, çamur katı içeriğinin viskoziteye yani akışkanlığa belirgin şekilde etki ettiğiidir. Çamurun katı içeriği reolojik davranım bakımından kritik öneme sahip olup, katı içeriğindeki sınırlı artışlar akışkanlığı önemli ölçüde azaltmaktadır. Bu bulgulara ek olarak, cevher süspansiyonlarının reolojik davranımın üzerinde mineralojik özelliklerin önemli bir etkiye sahip olduğu ortaya konmuştur. Bu bağlamda gözlemsel olarak kil mineralleri içeren ve “killi” olarak tabir edilen cevher zonuna ait atık çamur örneği, benzer miktarda katı içeriğine rağmen, normal cevher zonuna göre daha düşük akışkanlık göstermektedir. Yüksek yüzey yüklerinin daha dağınık duruma neden olurken, nispeten daha düşük yüzey yüklerine sahip taneciklerin süspansiyonlarda tanecikler arası etkileşime ve aglomerasyona ve dolayısıyla düşük akışkanlık ve yüksek akma direncine neden olduğu anlaşılmıştır. Tüm bulgular kil içeren atık çamurlarının nakliyesinin çok daha zorlayıcı bir işlem olacağına işaret etmektedir. Dolayısıyla atık çamurunun katı içeriğinin ayarlanması/optimize edilmesi, özellikle kil içerikli çamurlar için daha kritik hale gelmektedir. Yani, atık çamurunun geri dolgu malzemesi olarak kullanıldığı tesislerde cevher mineralojisi, proses şartları, vb. meydana gelebilecek değişimler, çamurun nakliyesini ciddi şekilde etkileyebilecek koşullar olarak ortaya çıkmaktadır. Atık çamurunun sorunsuz şekilde nakliye edilebilmesi, çamur pompalarının ve nakliye hatlarının öngörülen tesis şartlarında çalışabilmeleri bakımından, atık çamurlarının testlerle belirlenen reolojik davranımlarının kontrolü ve korunması büyük önem taşımaktadır.

Anahtar Kelimeler: Reoloji, Akma Direnci, Viskozite, Yüzey Yükü, Kil Mineralleri

Dedicated to My Beloved Family

ACKNOWLEDGMENTS

First of all, I kindly would like to express my deep and sincere thanks and appreciation to my supervisor, Prof. Dr. Naci Emre Altun for his supervision, support, and patience during my thesis study. I also would like to thank my examining committee members, Assoc. Prof. Dr. Mustafa Erkayaođlu, Assoc. Prof. Dr. Nurullah Metin Can for their valuable contributions.

I want to express my special thanks to my colleagues and friends Asena Hande Sarı, Elif Uslu, Batur Toka, Murat Can Ataş, Mehmet Emircan Emci, Sena Şenses, Hazal Melis Baydar and my dear friends Esra Baytekin, Gizem Derinci for their endless support and motivation whenever I need them.

Finally, I wish to express my deep thanks to my father Fahrettin Aktaş, my mother Deniz Aktaş, and my sister Eylül Nisa Aktaş for their endless support and encouragement during my hard times. I owe my greatest thanks to my sister and always best friend Ayşe Aktaş. It would have been impossible for me to finish this thesis without their support and endless love.

TABLE OF CONTENTS

ABSTRACT	v
ÖZ.....	vii
ACKNOWLEDGMENTS	x
TABLE OF CONTENTS.....	xi
LIST OF TABLES.....	xiii
LIST OF FIGURES	xiv
LIST OF ABBREVIATIONS	xix
LIST OF SYMBOLS	xx
CHAPTERS	
1 INTRODUCTION	1
2 PROBLEM STATEMENT AND SCOPE OF THESIS	3
3 THEORY AND LITERATURE REVIEW	5
3.1 Clay Minerals.....	5
3.2 The Electrical Double Layer.....	8
3.3 Rheology.....	10
3.3.1 Characterizing Rheological Behavior of Fluids.....	12
3.3.2 Rheological Behavior of Clay Including Suspensions	16
3.3.3 Measurement of Rheological Properties	18
3.3.4 Description of Rheological Models	21
3.3.5 Rheology in Mineral Processing.....	23
4 MATERIALS AND METHODS.....	27
4.1 Materials	27

4.1.1	Pure Clay Minerals.....	27
4.1.2	Complex Gold Ore Tailings Samples.....	28
4.2	Material Characterization	29
4.2.1	Characterization of Pure Clay Minerals	29
4.2.2	Characterization of the Ore Tailings	34
4.3	Methods	36
4.3.1	Zeta Potential Measurements.....	36
4.3.2	Potentiometric Titration Measurements	38
4.3.3	Rheology Measurements	38
4.3.3.1	Yield Stress Measurements	39
4.3.3.2	Viscosity Measurements.....	41
5	RESULTS AND DISCUSSION.....	43
5.1	Surface Charge Properties of Clay Minerals	43
5.2	Surface Charge Properties of Quartz and Calcite	46
5.3	Surface Charge Properties of Complex Gold Ore Tailings Samples	48
5.4	Rheological Properties of Complex Gold Ore Tailings Samples	49
5.4.1	Yield Stress of Clayey Vein Tailings Samples	49
5.4.2	Yield Stress of Normal Vein Tailings Samples	60
5.4.3	Viscosity of Ore Tailings Samples.....	73
6	CONCLUSION AND RECOMMENDATION	77
	REFERENCES.....	79

LIST OF TABLES

TABLES

Table 3.1 Classification of purely viscous fluids	13
Table 3.2 Rheological models (Concha, 2014; Rao, 2014)	22
Table 4.1 The particle size distributions of the less and higher clayey ore tailings samples.....	28
Table 4.2 Moisture contents and average moisture content of the higher clayey tailings samples obtained from thickener underflow.....	39
Table 4.3 Moisture contents and average moisture content of the less clayey tailings samples obtained from thickener underflow.....	40
Table 4.4 The solid contents of the ore tailings samples with less extent of clays .	41
Table 4.5 The solid contents of the ore tailings samples with higher extent of clays	42
Table 4.6 The solid contents of the ore tailings samples after homogenization	42
Table 5.1 Yield stress values depending on solid contents of clayey and normal vein tailings samples obtained from thickener underflow	70
Table 5.2 Relative viscosity values of ore tailings samples with higher and less extent of clay minerals	75

LIST OF FIGURES

FIGURES

Figure 3.1 The Stern-Gouy-Chapman model of the electrical double layer of a negatively charged particle (Forbes & Chryss, 2017)	9
Figure 3.2 Deformation of a fluid under simple shear stress (Tilton, 2008).....	11
Figure 3.3 Variation of shear stress with shear rate for different types of fluids (Liptak & Kim, 2003)	14
Figure 3.4 Representation of typical rheological behavior, viscosity, of inelastic fluids (Liptak & Kim, 2003)	16
Figure 3.5 Representation of shear stress vs shear rate for different fluids, especially Bingham Plastic Fluid (Farrokhpay, 2012).....	18
Figure 3.6 Schematic diagram of (A) the vane, (B) the vane apparatus (Nguyen & Boger, 1983).....	19
Figure 3.7 Simple rotational viscometer (Liptak & Kim, 2003)	20
Figure 4.1 The XRD pattern of kaolinite sample	30
Figure 4.2 The XRD pattern of illite sample.....	30
Figure 4.3 The XRD pattern of bentonite sample	31
Figure 4.4 The XRD pattern of muscovite sample	32
Figure 4.5 The XRD pattern of talc sample	32
Figure 4.6 The XRD pattern of quartz sample	33
Figure 4.7 The XRD pattern of calcite sample.....	33
Figure 4.8 The XRD pattern of normal vein sample	34
Figure 4.9 The XRD pattern of clayey vein sample	35
Figure 4.10 Malvern Zetasizer Nano Z (Malvern, 2013).....	37
Figure 4.11 Disposable Cuvette of Malvern Zetasizer Nano Z and Particle Movement toward the Electrode of Opposite Charge (Malvern, 2013)	37
Figure 4.12 Brookfield DV-II+ Pro viscometer	41
Figure 5.1 The zeta potential curves of clay minerals	44
Figure 5.2 The potentiometric titration curves of clay minerals	45

Figure 5.3 The zeta potential curves of quartz and calcite.....	47
Figure 5.4 The zeta potential curves of ore tailings samples with higher and less extent of clay minerals	49
Figure 5.5 The plot of shear rate vs shear stress of clayey vein tailings sample including 35% solids by weight based on Bingham rheological model	50
Figure 5.6 The plot of shear rate vs shear stress of clayey vein tailings sample including 35% solids by weight based on Casson rheological model	50
Figure 5.7 The plot of shear rate vs shear stress of clayey vein tailings sample including 40% solids by weight based on Bingham rheological model	51
Figure 5.8 The plot of shear rate vs shear stress of clayey vein tailings sample including 40% solids by weight based on Casson rheological model	51
Figure 5.9 The plot of shear rate vs shear stress of clayey vein tailings sample including 45% solids by weight based on Bingham rheological model	52
Figure 5.10 The plot of shear rate vs shear stress of clayey vein tailings sample including 45% solids by weight based on Casson rheological model	52
Figure 5.11 The plot of shear rate vs shear stress of clayey vein tailings sample including 48% solids by weight based on Bingham rheological model	53
Figure 5.12 The plot of shear rate vs shear stress of clayey vein tailings sample including 48% solids by weight based on Casson rheological model	53
Figure 5.13 The plot of shear rate vs shear stress of clayey vein tailings sample including 51% solids by weight based on Bingham rheological model	54
Figure 5.14 The plot of shear rate vs shear stress of clayey vein tailings sample including 51% solids by weight based on Casson rheological model	54
Figure 5.15 The plot of shear rate vs shear stress of clayey vein tailings sample including 54% solids by weight based on Bingham rheological model	55
Figure 5.16 The plot of shear rate vs shear stress of clayey vein tailings sample including 54% solids by weight based on Casson rheological model	55
Figure 5.17 The plot of shear rate vs shear stress of clayey vein tailings sample including 57% solids by weight based on Bingham rheological model	56

Figure 5.18 The plot of shear rate vs shear stress of clayey vein tailings sample including 57% solids by weight based on Casson rheological model	56
Figure 5.19 The plot of shear rate vs shear stress of clayey vein tailings sample including 60% solids by weight based on Bingham rheological model	57
Figure 5.20 The plot of shear rate vs shear stress of clayey vein tailings sample including 60% solids by weight based on Casson rheological model	57
Figure 5.21 The plot of shear rate vs shear stress of clayey vein tailings sample including 65% solids by weight based on Bingham rheological model	58
Figure 5.22 The plot of shear rate vs shear stress of clayey vein tailings sample including 65% solids by weight based on Casson rheological model	58
Figure 5.23 The plot of shear rate vs shear stress of clayey vein tailings sample including 70% solids by weight based on Bingham rheological model	59
Figure 5.24 The plot of shear rate vs shear stress of clayey vein tailings sample including 70% solids by weight based on Casson rheological model	59
Figure 5.25 The plot of shear rate vs shear stress of normal vein tailings sample including 35% solids by weight based on Bingham rheological model	60
Figure 5.26 The plot of shear rate vs shear stress of normal vein tailings sample including 35% solids by weight based on Casson rheological model	60
Figure 5.27 The plot of shear rate vs shear stress of normal vein tailings sample including 40% solids by weight based on Bingham rheological model	61
Figure 5.28 The plot of shear rate vs shear stress of normal vein tailings sample including 40% solids by weight based on Casson rheological model	61
Figure 5.29 The plot of shear rate vs shear stress of normal vein tailings sample including 45% solids by weight based on Bingham rheological model	62
Figure 5.30 The plot of shear rate vs shear stress of normal vein tailings sample including 45% solids by weight based on Casson rheological model	62
Figure 5.31 The plot of shear rate vs shear stress of normal vein tailings sample including 48% solids by weight based on Bingham rheological model	63
Figure 5.32 The plot of shear rate vs shear stress of normal vein tailings sample including 48% solids by weight based on Casson rheological model	63

Figure 5.33 The plot of shear rate vs shear stress of normal vein tailings sample including 51% solids by weight based on Bingham rheological model	64
Figure 5.34 The plot of shear rate vs shear stress of normal vein tailings sample including 51% solids by weight based on Casson rheological model	64
Figure 5.35 Th The plot of shear rate vs shear stress of normal vein tailings sample including 54% solids by weight based on Bingham rheological model	65
Figure 5.36 The plot of shear rate vs shear stress of normal vein tailings sample including 54% solids by weight based on Casson rheological model	65
Figure 5.37 The plot of shear rate vs shear stress of normal vein tailings sample including 57% solids by weight based on Bingham rheological model	66
Figure 5.38 The plot of shear rate vs shear stress of normal vein tailings sample including 57% solids by weight based on Casson rheological model	66
Figure 5.39 The plot of shear rate vs shear stress of normal vein tailings sample including 60% solids by weight based on Bingham rheological model	67
Figure 5.40 The plot of shear rate vs shear stress of normal vein tailings sample including 60% solids by weight based on Casson rheological model	67
Figure 5.41 The plot of shear rate vs shear stress of normal vein tailings sample including 65% solids by weight based on Bingham rheological model	68
Figure 5.42 T The plot of shear rate vs shear stress of normal vein tailings sample including 65% solids by weight based on Casson rheological model	68
Figure 5.43 The plot of shear rate vs shear stress of normal vein tailings sample including 70% solids by weight based on Bingham rheological model	69
Figure 5.44 The plot of shear rate vs shear stress of normal vein tailings sample including 70% solids by weight based on Casson rheological model	69
Figure 5.45 The changes in yield stress values depending on the solid content of clayey vein tailings based on Bingham and Casson models	71
Figure 5.46 The changes in yield stress values depending on the solid content of normal vein tailings based on Bingham and Casson models	71
Figure 5.47 Viscosity-time graph of tailings sample having higher extent of clay with 65.58% solids by wt. – Test 1 and Test 2.....	73

Figure 5.48 Viscosity-time graph of tailings sample having higher extent of clay with 54.60% solids by wt. – Test 1 and Test 2..... 73

Figure 5.49 Viscosity-time graph of tailings sample having less extent of clay with 65.36% solids by wt. – Test 1 and Test 2 74

Figure 5.50 Viscosity-time graph of tailings sample having less extent of clay with 54.43% solids by wt. – Test 1 and Test 2 74

LIST OF ABBREVIATIONS

Abbreviations	Description
Mt	Megatonne
IEP	Isoelectric point
PZC	Point of zero charge
wt	weight
EE	Edge-edge interaction
FF	Face-face interaction
ICDD	International Center for Diffraction Data
XRD	X-ray diffraction
Na ⁺ Mt	Sodium montmorillonite
MMT	Montmorillonite
M-R method	Mular-Roberts method

Units	Description
%	percentage
μm	micrometer
Pa	pascal
mPa	megapascal
kV	kilovolt
mA	milliampere
kW	kilowatt
°C	Celsius degree
M	Molar
rpm	revolution per minute
mV	millivolt
dyn/cm ²	dyne/centimeter square
cP	centipoise

LIST OF SYMBOLS

Symbols	Description
ψ_0	Surface potential
ψ_δ	Stern potential
ζ	Zeta potential
$1/\kappa$	Debye length
κ	Debye-Hückel parameter
T	Absolute temperature
F	Faraday's constant
ϵ	Permittivity of solution
ϵ_r	Relative permittivity
R	Universal gas constant
ϵ_0	Permittivity of free space
I	Ionic strength
C_i	Concentration of ions
Z_i	Charge of ions
τ	Shear stress
$\dot{\gamma}$	Shear rate
γ	Shear strain
η	Viscosity
τ_y	Yield stress
n	Flow index
K	Consistency index
Θ	Contact angle, °
He-Ne	Helium-Neon
λ	Lambda, nm
HCl	Hydrochloric acid
NaOH	Sodium hydroxide

CHAPTER 1

INTRODUCTION

The increasing mining production and consumption of various minerals is one of the biggest concerns worldwide due to the increasing population and gross domestic product per capita of developing countries. Gold ores considered by production was reported as 2.78 Mt in 2012 and 3.35 Mt in 2019 (Brown et al., 2018, 2021), i.e. the gold production increased by more than 20% even in 7 years. Mining operations, on the other hand, must proceed and develop for the functioning of modern societies and economies in the future.

In recent years, with a decreasing number of high-grade, easy-to-process ores, mining operations are at the verge of processing low-grade, mineralogically complex, finely disseminated ores to compensate the increasing demand for raw materials. As a result, mining and mineral processing operations are increasingly evolving to grind these complex ores to ever finer particle sizes to achieve sufficient liberation of the valuable minerals locked with unwanted gangue components. This makes the knowledge of gangue mineralogy essential in industrial applications and processes for the success of ore beneficiation.

Many low grade ores include phyllosilicate group minerals as a common gangue component. Phyllosilicate group minerals are broadly classified as ‘clays’ in mineral processing (Ndlovu et al., 2013). Clays are described as naturally occurring, fine-grained minerals of any composition that show certain physical properties (Gräfe et al., 2017).

While clay minerals sustain their importance as raw materials, their negative impacts on mineral processing value chain for a wide range of commodity raw materials are in undeniable extent. The ‘sticky’ nature of phyllosilicates cause difficulties, such as decrease in production performance, grinding efficiency,

flotation performance and recovery during leaching, pumping challenges, dewatering challenges, complex tailings treatment (Ndlovu et al., 2014). Thus, the knowledge of the fundamental analysis of the flow behavior of phyllosilicate mineral suspensions and potential solutions to phyllosilicate related processing problems are areas of growing interest, especially for low grade ore beneficiation (Ndlovu et al., 2013).

The term “Rheology” was first invented by Professor Bingham of Lafayette College, Easton, PA thanks to the advice of a colleague, the Professor of Classics (Barnes et al., 1989). “Rheology” is the science of the deformation and flow behavior of fluid under applied stress (Boger, 2000). Over the years, several researchers have emphasized the significance of rheology in the mineral processing industry (e.g. Boger, 2000; Farrokhpay, 2012; Ndlovu et al., 2013; Zhang & Peng, 2015). Research into the rheological behavior of mineral suspensions provide information about the level of inter-particle interaction and aggregation, so it can be useful as a processing control parameter in long-term solutions required for processing problems (Farrokhpay, 2012).

Due to the platy structure of phyllosilicate minerals, phyllosilicates particles expose crystallographically distinct surfaces, the flat basal surface and the edge surface. Because phyllosilicate minerals have different particle planes, different surface charge characteristics are observed, which causes the particles to be charged anisotropically. As a result, these particles have a complex mode of inter-particle association due to the electrostatic attraction and therefore clay particles coat the surface of a number of valuable minerals (Forbes & Chryss, 2017; Zhang & Peng, 2015).

CHAPTER 2

PROBLEM STATEMENT AND SCOPE OF THESIS

Because of the gradual depletion of high grade ores, mining operations are being forced to process ores to finer particles to extract valuable minerals. With the increased amount of fine particles and in some cases, high clay mineral content presence, complex rheological behaviors in phases including ore tailings slurries, such as high viscosity and high yield stress due to the possible particle interactions have been observed, causing decrease in the performance of mineral processing value chain. Therefore, it is required to examine the rheological properties of ore tailings slurries, and modify when needed. It can also not be disregarded that this situation brings some environmental issues due to the increasing amounts of mining process tailings produced. Disposal and storage of process tailings have become an increasingly problematic in recent years due to the increased costs of disposal and storage of high amounts of process tailings and insufficient volumes of tailings dams caused by processing of low-grade ores. In addition, the overflow and collapse of tailings dams around world cause the dewatering of tailings after mineral processing operations and disposal of these tailings along with new technologies instead of conventional methods to gain importance. An alternative method increasingly applied is the backfill of paste material obtained by mixing of dewatered tailings with a binder to help support underground mines.

Through the study, rheological characteristics of ore tailings suspensions with respect to the mineralogy and with special emphasis to the presence of clay minerals was investigated for the backfill purposes of tailings from mineral processing plants. In this respect, gold ore tailing slurries having different mineralization characteristics from two different veins of the same deposit were inspected for the differences in their rheological behavior. The tailing slurries used in this study were obtained from a mine operating in Turkey. As mentioned, one of

the samples is characterized with its higher extent of clay minerals. The gold ore tailings samples, with higher extent of clays and with less extent of clays, were examined to determine rheological behavior of the suspensions by identifying surface charge properties of suspensions with the help of zeta potential measurements and potentiometric titration measurements as a function of pH. Also, resulting rheological properties called viscosity and yield stress values at different solids concentration were identified to correlate surface charge properties specific to each of clay minerals, and so most likely particle interactions to have a better understanding of possible particle packing. The rheological tests were conducted by using a rheometer that works simultaneously with a software.

CHAPTER 3

THEORY AND LITERATURE REVIEW

3.1 Clay Minerals

In industrial applications, it would be misleading to suppose that only clay minerals group among phyllosilicates show adverse effects. In fact, talc and serpentine minerals are known to show deleterious effects in mineral processing value chain and they are generally named as ‘clay minerals’. It can be clear to say that ‘clay minerals’ term is commonly used instead of phyllosilicates in general (Forbes & Chryss, 2017).

Talc is known to be potentially problematic gangue minerals in many base metal sulfide ore deposits because of their hydrophobicity which renders them naturally floatable. In flotation circuit, talc and chlorite can easily float into the mineral concentrates uniquely, increasing the viscosity in froth phase. This not only decrease concentrate grade and recovery but also cause operational problems during smelting (Becker et al., 2009; Burdukova et al., 2007; Ndlovu et al., 2014; Yuan et al., 2019).

Micas especially muscovite is known to be commonly occurring minerals in many types of igneous and metamorphic rocks (Deer et al., 2013). Muscovite underlines with brittle and flaky morphology (Ndlovu et al., 2013). There has been little research regarding rheological behavior of suspensions including mica. Ndlovu et al. (2011) investigated rheological properties (suspension yield stress and viscosity) of muscovite suspensions relative to a non-phyllosilicate mineral, quartz. The results showed that the yield stress of muscovite suspensions is inconsiderably higher than that of quartz, whilst low viscosities is observed in muscovite suspensions like that of quartz because complex structure is broken upon yielding. The other research conducted by Farrokhpay et al. (2018) on the behavior of mica

in copper ore flotation revealed that high amount of muscovite (30%) influences pulp rheology with high yield stress, reduce copper flotation grade because of entrainment. However, it was observed that the influence of high amount of muscovite on copper recovery is negligible.

Clay minerals such as kaolinite, illite, montmorillonite, which are intrinsically composed of very small particles, so they are classified as slimes in mineral processing. Clay minerals can be classified as swelling (smectites and vermiculites) and non-swelling clay minerals (kaolinites and illites). The other classifications can include talc into the clay mineral group. “Clay” term is commonly used instead of “clay fraction” to represent grain size less than about 2 μm (some say 4 μm). In mineralogical usage, whereas “clay” term is used as sediment which involves clay minerals and accessory non-clay minerals, “clay minerals” are pure sheet silicates, giving plasticity in wet conditions and hardness in dry or heated conditions to clay body (Deer et al., 2013).

Kaolinite group minerals occur as common gangue minerals in many ore deposits around world especially in many porphyry copper deposits and Australian hematite/goethite iron ores (Ndlovu et al., 2014). Kaolinite is the most important member of the kaolinite group (Deer et al., 2013). They have platy morphology like talc, illite and some other phyllosilicate minerals. Because of their wide use in ceramic industry, as well as paints and coatings applications, their surface properties and rheological properties have been studied extensively (Burdukova et al., 2007). Ndlovu et al. (2014) revealed in their investigations that kaolinite suspensions exhibit high yield stress and comparatively low viscosities, and kaolinite bearing ores don't pose a threat in viscosity related issues at high shear conditions.

Many sedimentary rocks include illite as a common accessory mineral (Klein & Hurlbut, 1993). Also, in many porphyry copper ores, kaolinite, chlorite, illite and montmorillonite are present (Jorjani et al., 2011). Ndlovu et al. (2014) investigated pure talc, kaolinite, and illite suspensions in their research, and they have revealed that yield stress of illite suspensions is lower than that of talc and kaolinite.

However, there are no observed viscosity related problems thanks to their relatively low viscosities. As a result, ores containing illite are unlikely to present problems during beneficiation.

Smectites are included in a group of clay minerals which exhibit high swelling property by absorption of water between their structural layers. Montmorillonite is the well-known clay mineral among smectite group. If Na^+ cation is predominant in montmorillonite surface, the clay is known as Na-montmorillonite. On the other hand, if Ca^{2+} cations exist in the interlayer region, it is called as Ca-montmorillonite (Luckham & Rossi, 1999). “Bentonite” is a type of clay comprised of mainly montmorillonite clay mineral and can contain non-clay minerals like quartz (Ndlovu, 2013). Due to the swelling behavior of smectites, there are operational challenges in dewatering, pumping and impoundment because this behavior causes low settling rates and poor compaction rates (McFarlane et al., 2005). In addition, challenges related with smectite group minerals in coal flotations have been investigated by Xu et al. (2003). The tests performed confirmed that slime coverage of montmorillonite on coal is detrimental to coal flotation by depressing coal. Another research conducted by Ndlovu et al. (2011) have shown that smectite suspensions are likely to have relatively low yield stresses but have high viscosities, due to dominant role of hydration.

The rheological properties of muscovite were studied by Ndlovu et al. (2011), demonstrating their complex behavior relative to quartz. The yield stress of muscovite suspensions was only slightly higher than that of quartz at the same solid content. Therefore, muscovite resulted in the least rheologically complex suspensions. Additionally, the rheology of montmorillonite suspensions was discussed in terms of their thixotropic behavior observed during the processing of ores containing montmorillonite. This behavior makes montmorillonite much more complicated than other clay minerals with the highest yield stress and viscosity values. In addition, the rheological behavior of pure talc, kaolinite, illite and quartz suspensions as a function of solid contents was also investigated by Ndlovu et al. (2014) comparatively. The results showed that pure kaolinite, illite, and talc

demonstrated higher yield stress and viscosity values relative to pure quartz. Pure quartz suspensions were characterized by very low yield stress values, close to zero. Pure talc and kaolinite suspensions demonstrated higher Bingham yield stress values than pure illite suspensions at the same solid content. When pure talc and kaolinite suspensions were evaluated comparatively, there was a slight difference at same solid content. The lower value of yield stress of illite suspensions can be attributed to the lower degree of charge anisotropy as derived by differences in IEP and PZC. A comparison of viscosities of talc, kaolinite, and illite suspensions showed that there was a clear difference in the viscosity values. The higher viscosity values of talc and kaolinite suspensions were observed than illite suspensions.

3.2 The Electrical Double Layer

An excess of positive or negative charge developed at the solid surface, regardless of the origin of surface charge, lead to the distribution of nearby ions in the solution. Counter-ions in solution are electrostatically attracted towards the oppositely charged surface while co-ions are repelled away from the surface to maintain electrical neutrality (Fatehah et al., 2014; Gregory, 2006). The adsorbed layer, also called as Stern layer is created by the oppositely charged counter-ions by forming an inner layer close to the particle surface. The concentration of counter-ions decreases with an increasing distance away from the particle surface together with co-ions, forming the diffuse layer or Gouy-Chapman layer. The outer plane of the adsorbed layer, located about a hydrated ion radius from the surface, is called as Stern plane or inner Helmholtz plane. Usually, the thickness of adsorption-layer, the distance between the particle surface and stern plane, is denoted by δ . The electrical potential at the surface of the particle is called as surface potential and given by ψ_0 , on the other hand, the electrical potential at the Stern plane is known as Stern potential and given by ψ_δ . The potential decreases exponentially to zero from Stern plane into the bulk of the solution, through the diffuse layer. When there is motion of the solution relative to the mineral surface,

shear occurs at a plane close to the boundary between the Stern layer and diffuse layer. The electrical potential at this shear plane, also called as outer Helmholtz plane, is called as *the zeta potential* (ζ). The charge potential of the particle surface is commonly approximated by the zeta potential. The significant point at which the zeta potential becomes zero is known as *isoelectric point* (IEP) (Allagui et al., 2021; Fatehah et al., 2014; Gregory, 2006; Luckham & Rossi, 1999; Oldham, 2008). This combined system is known as the Stern-Gouy-Chapman model of *the electrical double layer* as depicted in Figure 3.1.

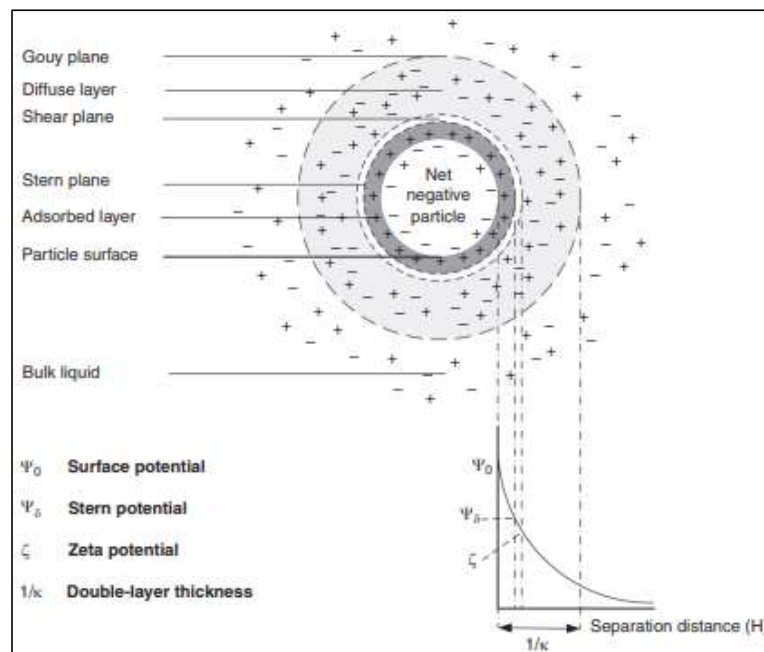


Figure 3.1 The Stern-Gouy-Chapman model of the electrical double layer of a negatively charged particle (Forbes & Chryss, 2017)

The thickness of the double layer around a particle is called as *Debye length* ($1/\kappa$), as shown in Figure 3.4, where the parameter κ is called as *Debye-Hückel parameter*. It plays an important role in the interaction of charged particles in a suspension (Adamson & Gast, 1997; Gregory, 2006). To calculate the Debye length, some parameters are needed to know as described by Equation 1, where T is the absolute temperature, F is Faraday's constant, ϵ is the permittivity of the solution, which is equal to the relative permittivity (or dielectric constant), ϵ_r , R is the universal gas constant, ϵ_0 is the permittivity of vacuum or the permittivity of free space, and I is

the ionic strength of the aqueous medium. I is shown by Equation 2, where C_i is the concentration of ions in suspension and z_i is the charge (valence) of all significant ions in suspension (de Moraes et al., 2021; Gregory, 2006; Luckham & Rossi, 1999).

$$\kappa^{-1} = \left(\frac{RT\epsilon_r\epsilon_0}{2F^2I} \right)^{1/2} \quad (1)$$

$$I = \frac{1}{2} \sum z_i^2 C_i \quad (2)$$

It can be seen from the above equations that valence and concentration of ions are two important factors affecting the thickness of the electrical double layer. The increasing the ionic strength causes the decrease in the thickness (compression) of the double layer, especially diffuse layer (Gregory, 2006).

3.3 Rheology

The term ‘‘Rheology’’ was invented by Professor Eugene C. Bingham of Lafayette College, and he commenced the first society of Rheology, American Society of Rheology, in 1929 (Barnes, 1999; Barnes et al., 1989). Rheology is the science of deformation and flow behavior of matter under applied stress. The greatest overlap matter between rheology and mineral processing is a particulate fluid (i.e., a suspension) (Boger, 2000).

The flow behavior of a fluid is characterised by the relationship between the stress (shear stress, τ [Pa]), and the resultant rate of deformation (shear rate, $\dot{\gamma}$ [1/s]). The shear stress, τ , is defined as the applied tangential force per unit area, and the shear rate, $\dot{\gamma}$, is described as the change of shear strain, γ , per unit time. The ratio of shear stress, τ , to shear rate, $\dot{\gamma}$, is called as viscosity, η [Pa.s] (Equation 3) (Luckham & Rossi, 1999; Nelson, 2019).

$$\eta = \frac{\tau}{\dot{\gamma}} \quad (3)$$

Hence, viscosity is a measure of a fluid's resistance to flow. Also, it can be defined as the lack of slipperiness. Figure 3.2 represents the behavior of a fluid under a simple shear stress, resulting in a simple shear flow (i.e., deformation). The fluid is between two parallel plates of area A , and the distance between two parallel plates is known to be H . The bottom plate is fixed, and the upper plate having an area A is subjected to a tangential force F . This causes the fluid at the upper plate to move at a velocity V while the lower plate has a velocity of zero under a no-slip condition. The force per unit area required to produce the motion, F/A , is shear stress, τ . As the shear stress is applied, the fluid is subjected to an infinite deformation different from solid. Consequently, this will result in a velocity gradient, dv/dy , which is called as the shear rate, $\dot{\gamma}$ (Hiemenz & Rajagopalan, 1997; Nelson, 2019; Tilton, 2008).

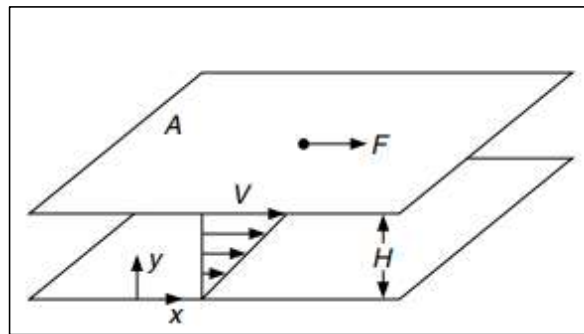


Figure 3.2 Deformation of a fluid under simple shear stress (Tilton, 2008)

The simple fluid flow pattern obeys Newton's postulate for liquids introduced in 1687. Glycerine with 1 Pa.s viscosity, and water with 1 mPa.s viscosity are common Newtonian viscous liquids. A Newtonian viscous liquid is a consistent three-dimensional theory developed by Navier and Stokes independently after Newton's postulate. In the case of a Newtonian liquid, a shear stress results in a shear rate, and therefore, flow. The flow persists as long as the stress is applied. Newtonian liquids obey Newton's law of viscosity. The ratio of shear stress to shear rate is constant, and it is defined as the viscosity. The viscosity is independent of the shear rate (Barnes et al., 1989; George & Qureshi, 2013).

Experiences gained so far show that fluid flow is often more complex than that just described, and the one shown in Figure 3.2. Fluid rheology is usually characterized by a rheogram, which is the plot of the shear stress, τ , versus the shear rate, $\dot{\gamma}$. “Yield stress” and “Viscosity” are two important rheological terms often associated with rheology studies. Yield stress is defined as the intercept of the flow curve on the shear stress axis at zero shear rate, and viscosity is the slope of the line connecting the particular point on the flow curve with the origin (Barnes, 1999; Farrokhpay, 2012; Nelson, 2019).

3.3.1 Characterizing Rheological Behavior of Fluids

Most solids deform elastically, which means the energy required for the deformation is fully recovered and show reverse deformation, i.e., it immediately recovers its original shape, when the stress is removed (Shaw, 1992). Fluids that don't exhibit any solid-like, elastic behavior are called as *purely viscous fluids*. When shear stress is removed, purely viscous fluids don't undergo any reverse deformation. The energy required for the deformation cannot be recovered by removing the stress because the energy is dissipated inside the fluid as it flows. On the other hand, the fluids that exhibit a behavior between viscous and elastic are defined as *viscoelastic fluids* (Nelson, 2019; Schramm, 2000; Tilton, 2008).

The broad characterization of inelastic fluids, i.e., purely viscous fluids, may be either time-independent or time-dependent as given in Table 3.1. In the time-independent case, the shear stress depends only on the instantaneous shear rate. For the second case, the shear stress depends on the history of the rate of deformation, and shear stress changes with shear duration because there is structure or orientation rearrangement, buildup or breakdown, during deformation (Nelson, 2019; Tilton, 2008). Whereas “thixotropic”, and “rheopectic” are the time-dependent inelastic fluids, the time-independent inelastic fluids can be classified as “Newtonian” and “non-Newtonian”. Non-Newtonian fluids can be further classified as “pseudoplastic”, “dilatant” and “plastic solid”.

Table 3.1 Classification of purely viscous fluids

Group	Type of fluids
Purely Viscous Fluids	
Time Independent Fluids	Newtonian Fluids Non-Newtonian Fluids <ul style="list-style-type: none"> • Pseudoplastic • Dilatant • Plastic Solid
Time Dependent Fluids	Thixotropic Rheopectic

The flow curves of time-independent inelastic fluids shown by clay suspensions, which are Newtonian, Pseudoplastic, Dilatant, and the flow curves of the other typical fluids are given in the rheogram in Figure 3.3. The rheogram for Newtonian fluid is linear, meaning the viscosity, η , is constant and unaffected by shear rate. Also, it intercepts the origin of the graph. Newtonian behavior is observed commonly in water, and some low-concentration clay including suspensions. On the other hand, the viscosity of non-Newtonian fluids varies with shear rate, shown in Figure 3.3, even at constant pressure and temperature. Therefore, the viscosity of non-Newtonian fluids at any point is referred to as *apparent viscosity* (Forbes & Chrissy, 2017; Liptak & Kim, 2003; Nelson, 2019; Tilton, 2008).

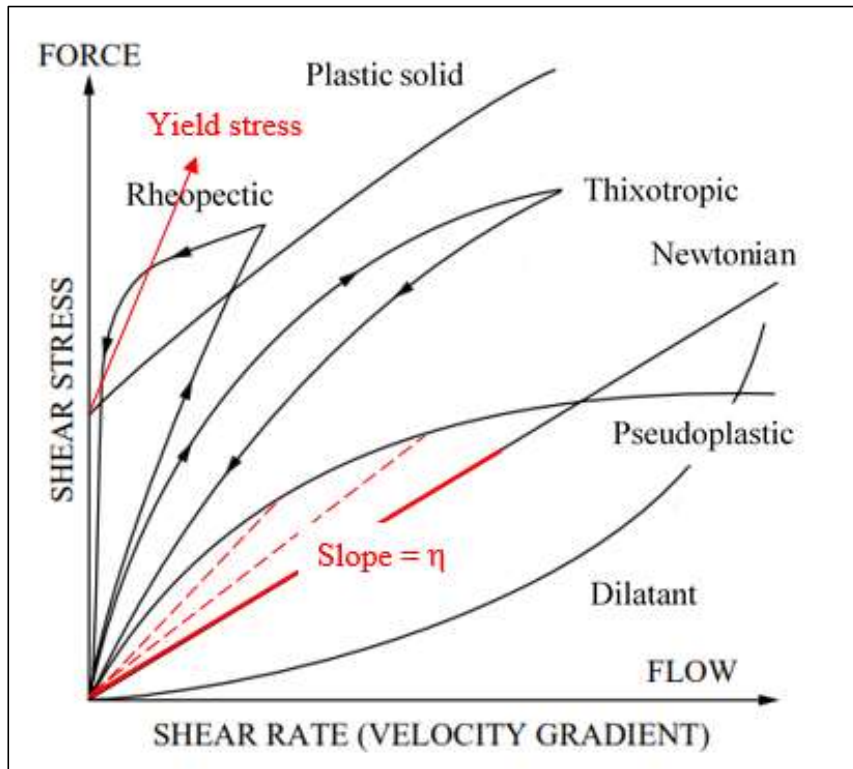


Figure 3.3 Variation of shear stress with shear rate for different types of fluids
(Liptak & Kim, 2003)

The variation of viscosity with the increasing shear rate of inelastic fluids are given in Figure 3.4. Pseudoplastic fluids are shear-thinning, which means apparent viscosity gradually decreases with increasing shear rate, as shown in Figure 3.4. The updated terminology used for this type of fluids are shear-thinning, instead of pseudoplastic. Dilute clay including suspensions or drilling fluids containing polymers show pseudoplastic behavior (Forbes & Chryss, 2017; Luckham & Rossi, 1999; Tilton, 2008). Shear-thinning fluid exhibiting a yield stress is called as yield pseudoplastic, which means a minimum shear stress must be exceeded to commence the flow. Yield pseudoplastic is the most common behavior observed for clay including suspensions. In pseudoplastic fluids, a unit increase in shear stress results in more and more flow thanks to the decrease in apparent viscosity, as shown in Figure 3.4. Dilatant fluids show increasing apparent viscosity with rising shear rate, i.e., shear-thickening. Dilatant terminology is outdated, and the term shear-thickening is used to prevent confusion with dilatancy, meaning increase in

volume observed in some clay minerals. More shear stress is required to obtain same increase in flow as pseudoplastic fluids due to the increase in apparent viscosity, as shown in Figure 3.4. Shear-thickening behavior is only observed in multi-phase mixtures having moderate to high solid concentration. Clay including suspensions usually doesn't show shear-thickening behavior. However, this behavior may be observed if highly concentrated suspension contains a coarse solid phase. Finally, plasticity is similar to the shear-thinning. However, they behave as viscous fluids when the applied shear stress reaches the yield point, shown in Figure 3.3 (Forbes & Chryss, 2017; Liptak & Kim, 2003; Nelson, 2019).

Some fluids can be time-dependent, where shear stress depends on the history of the rate of deformation, and it changes with shear duration. Time-dependent phenomena can be further classified as thixotropic and rheopectic. Thixotropic fluids, such as mayonnaise, are usually shear-thinning, but they show a hysteresis loop as shown in Figure 3.4. Shear stress decreases with time at constant shear rate as shown in Figure 3.3. Their viscosity decreases with time, and the reverse case is observed by ceasing the shear. They seem to “remember” their history. When they are reagitated, they will require less power than was required during the first agitation. The classical example of thixotropic behavior is given by many clays, particularly bentonite clays, and it occurs in some more concentrated clay including suspensions such as “red mud” from bauxite processing. Thixotropic behavior can be observed as a consequence of mixing, pumping or pipeline transport due to shearing. If the reverse behavior occurs, it is anti-thixotropy, called as rheopectic. As opposite to the thixotropic, rheopectic behavior shows increasing shear stress with time at constant shear rate as shown in Figure 3.3. Rheopectic fluids show shear-thickening, but they also display hysteresis. Their viscosity appears to increase, and in some duration of agitation, viscosity will set as shown in Figure 3.4. Rheopectic behavior is generally observed in bentonite and in gypsum suspensions in water (Forbes & Chryss, 2017; Liptak & Kim, 2003; Nguyen & Boger, 1985b; Shaw, 1992; Tilton, 2008).

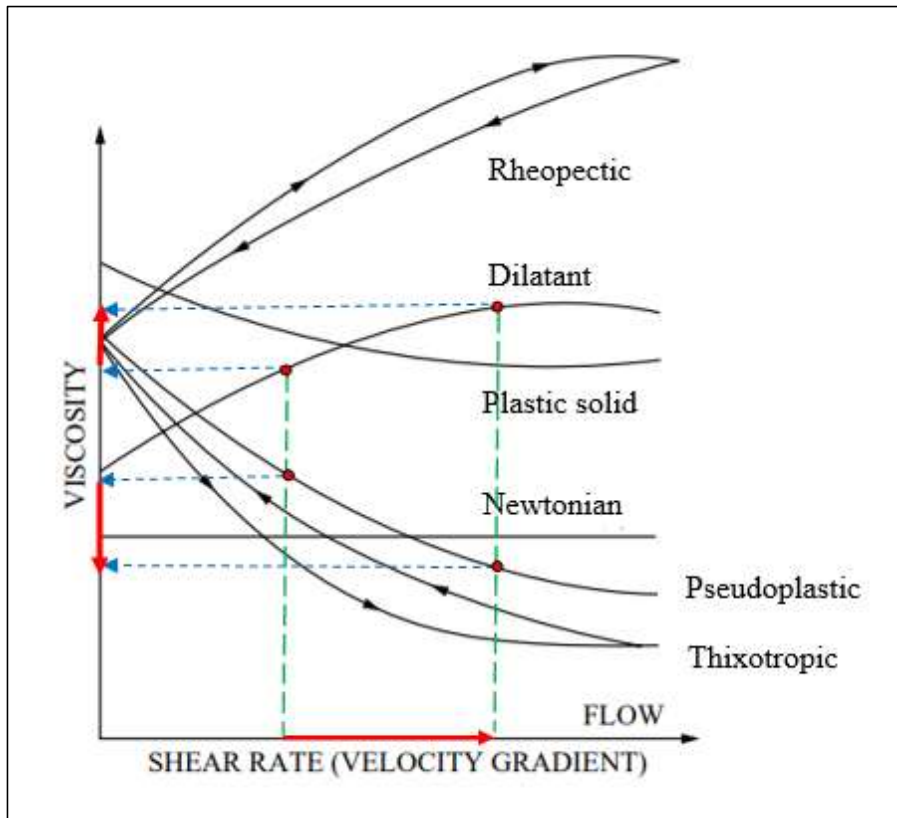


Figure 3.4 Representation of typical rheological behavior, viscosity, of inelastic fluids (Liptak & Kim, 2003)

3.3.2 Rheological Behavior of Clay Including Suspensions

The existing debate is what flow behaviors clay including suspensions exhibit. There is a relationship between the amount of solid in mineral suspensions and resulting rheological behavior. When there is an increase in the amount of solid, rheological behavior of the suspensions shifts from Newtonian to non-Newtonian behavior. As shifting from Newtonian to non-Newtonian, a yield stress appears and viscosity increases exponentially (Farrokhpay et al., 2010; Prestidge, 1997). As discussed above, clay including suspensions exhibit Newtonian, shear-thinning, shear thickening and Bingham plastic based on the concentration of suspensions. Red mud from bauxite processing and bentonite clay including suspensions, also rheopectic behavior is observed, exhibits thixotropic behavior.

In very low concentrated colloidal clay including suspensions can exhibit Newtonian behavior with constant viscosity (Forbes & Chryss, 2017). On the other hand, pseudoplastic behavior can be exhibited by dilute clay including suspensions. When particle aggregation occurs in the system, further increase in the shear rate will cause the gradual breakdown of the aggregates. This in turn results in a decrease in the apparent viscosity. Shear-thinning behavior is common to suspensions containing phyllosilicate particles, which are randomly oriented. At low shear conditions, particles disturb the flow lines to a greater extent. In contrast, at high shear conditions where high velocity gradients exist particles are more aligned in the direction of flow (Forbes & Chryss, 2017; Luckham & Rossi, 1999; Shaw, 1992).

In moderately concentrated clay including suspensions, particle-particle interactions dominate due to the net attractive force. When the system is subjected to shear stress, it will resist to flow because it behaves as an elastic solid until a limiting shear stress is exceeded. This finite stress, yield stress, must be applied to the system to initiate flow. At this point, the network of particle-particle interactions fails, and more liquid-like, dispersed, state is observed. Suspensions where the networked structure fails, and they shift to a more dispersed state are defined as Bingham plastic fluids. When the greater stresses than yield stress are applied to Bingham plastic fluids, the flow will be Newtonian in which the shear stress is proportional to shear rate. Many real fluids closely approximate this type of behavior (Barnes, 1999; Luckham & Rossi, 1999). The rheogram of Bingham plastic fluid and that of others are given in Figure 3.5 for comparison.

Shear-thickening is observed in highly concentrated clay including suspensions. Hoffman (1972) has showed that shear-thickening behavior arises from a transition occurring from a two-dimensional ordered state to disordered state. This transition results in increased friction between particles, and apparent viscosity is considerably higher.

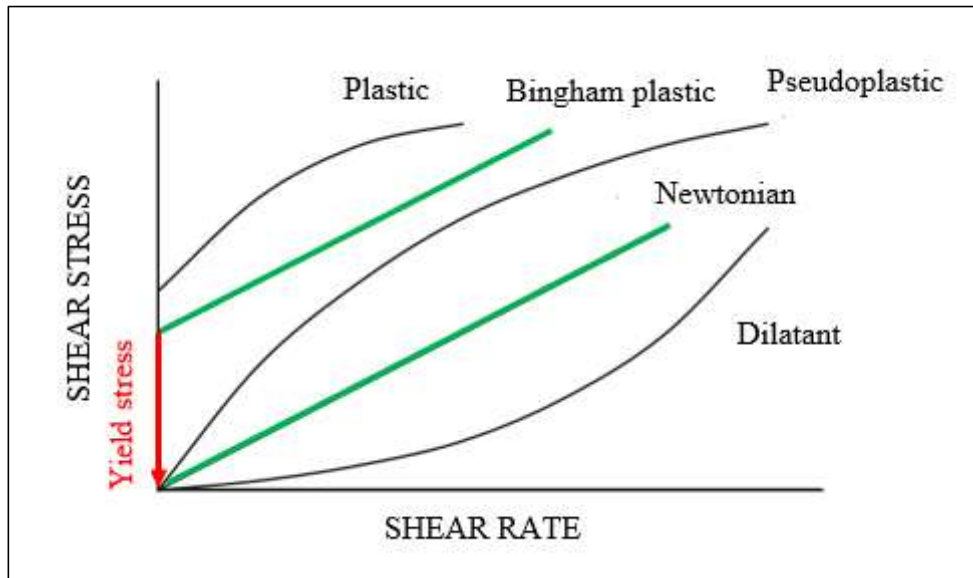


Figure 3.5 Representation of shear stress vs shear rate for different fluids, especially Bingham Plastic Fluid (Farrokhpay, 2012)

3.3.3 Measurement of Rheological Properties

Yield stress, τ_y [Pa], and viscosity, η [Pa.s], are two most important rheological properties in the case of purely viscous suspensions in mineral processing applications. To understand the overall rheological behavior of a suspensions in combination with surface charge properties, measures of yield stress and viscosity are fundamental. The yield stress is an indirect measure of the strength of the flocculated network structure occurring due to interparticle forces (Nguyen & Boger, 1983). There are various number of definitions of yield stress, τ_y [Pa]. “The lowest stress at which strain increases without increase in stress” and “the level of stress at which substantial deformation suddenly takes place” can be the best definition for yield stress described by Parker (1991) and Robinson (1996), respectively. A finite stress, yield stress, must be applied to some systems described above to initiate flow (Barnes, 1999). On the other hand, viscosity, η [Pa.s], is a measure of the suspension resistance to flow as a function of applied shear stress.

Yield stress measurement has been a challenging study for many years. It can be measured in two ways: directly or indirectly. Direct measurement of yield stress with the vane is developed by Nguyen & Boger (1983). There are advantages and disadvantages of the vane method. The first advantage is that the vane geometry, consisting of usually 2-8 thin blades arranged at equal angles around a small cylindrical shaft (Figure 3.6), eliminates the serious wall-slip effects in yield stress measurement in contrast to rotating cylinder viscometers (Nguyen & Boger, 1983). In addition, the vane geometry contributes to the reduction in sample disturbance and time-dependent structural breakdown caused by the introduction of the vane into the sample (Fisher et al., 2007; Kelessidis & Maglione, 2008; Nguyen & Boger, 1983). On the other hand, the vane method is required to measure at a low shear rate ($<1 \text{ s}^{-1}$), so it is generally difficult to conduct such a measurement due to the practical limitations. Also, the vane method is preferable when the yield stress value is greater than 10 Pa (Alderman et al., 1991).

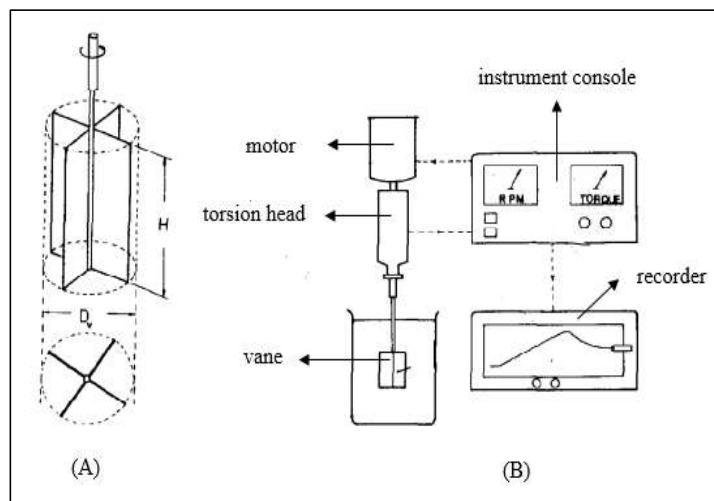


Figure 3.6 Schematic diagram of (A) the vane, (B) the vane apparatus (Nguyen & Boger, 1983)

Due to the practical limitations of the vane method, indirect measurement of yield stress values must be considered. Mathematical models can be used to estimate yield stress based on the steady shear data. The steady shear data can be obtained by measuring a range of shear rates and shear stresses for a given suspension using

a suitable rheometer. The older type of ubiquitous Brookfield, Fann or Hercules viscometers lack a defined range of shear, so they cannot measure true rheology. Generally, rotational rheometers, shown in Figure 3.7, using cone and plate, parallel plate or Couette (concentric cylinder) geometries are used for clay including suspensions. However, there is a limitation with the cone-plate and parallel plate geometries. If larger particles or structures exist in the suspension, it is not suitable to use this type of geometries. Consequently, rotational rheometer with Couette geometry can be used for many mineral suspensions (Forbes & Chryst, 2017; Tadros, 2010).

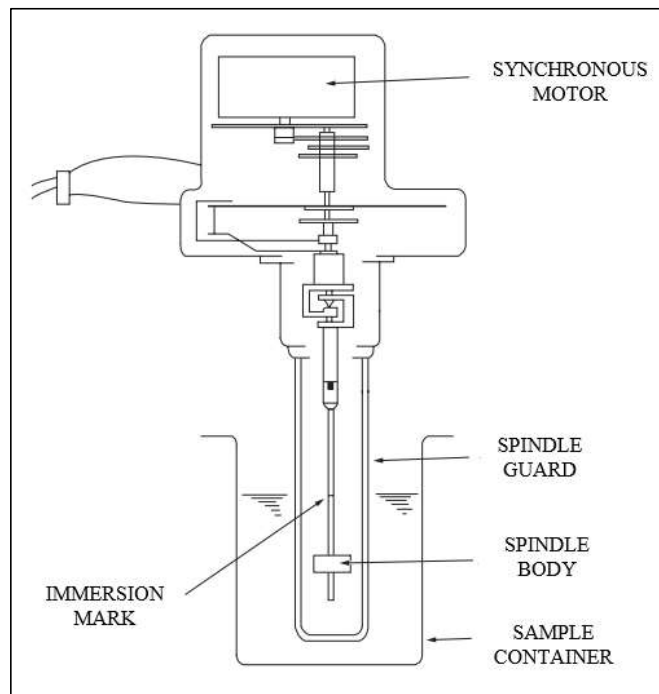


Figure 3.7 Simple rotational viscometer (Liptak & Kim, 2003)

The rotational viscometer illustrated in Figure 3.7 is probably the most widely used rheometer for the determination of shear stress as a function of applied uniform or nearly uniform shear rate. Also, it enables to determine viscosity thanks to corresponding shear data. Rotational viscometers have three parts in common: a mechanical means of driving a spindle at a constant speed, a torque measuring device, and a means of correlating shear rate (spindle diameter and speed of rotation). The properly equipped rotational viscometers can measure the

suspensions of viscosities ranging from 10^{-5} to 10^7 Pa.s. Also, the measurement is possible at a range of shear rates from 10^{-4} to 10^4 sec^{-1} . The most significant advantage of this rheometer is that it enables the continuous measurements under varying conditions on the same sample. As a result, the suspensions exhibiting non-Newtonian behavior can be investigated by rotational viscometers (Liptak & Kim, 2003).

3.3.4 Description of Rheological Models

Instead of direct measurement, shear stress and shear rate data can be used in combination with mathematical models to obtain one of the most significant rheological property, yield stress. In other words, yield stress value of a suspension under certain conditions from flow curves can be calculated by extrapolation using model fits. It is discussed by Nguyen & Boger (1985a) that the rheological data at low shear rates is more reliable in the case of vane method. The calculated yield stress by model fitting cannot give the accurate value due to the lowest measured shear rate. However, Dinkgreve et al., (2016) stated that new sufficiently sensitive rheometers remove this problem from most practical cases. It enables to measure accurately even at lowest shear rate.

Shear data from the rheograms is typically fitted to one or more of empirical rheological models to approximate rheological properties of suspensions, provided in Table 3.2. Materials with a constant viscosity behave as Newtonian fluids. Newtonian fluid is characterized by the Newton model (Equation 4). On the other hand, the Bingham, Casson, and Power Law models describe non-Newtonian fluids. The Herschel-Bulkley (Equation 5) is a generalized model for non-Newtonian fluids. The flow index, n , represents the presence of shear thickening or shear thinning behavior. The Power Law model (Equation 6) is developed for both shear-thinning and shear-thickening behavior depending on the magnitude of flow index, n . The conditions at which flow index is smaller than 1, pseudoplastic behavior is characterized by the Power Law. On the other hand, when flow index is greater than 1, shear-thickening behavior is characterized. Bingham plastic

behavior is characterized by the Bingham model (Equation 7) when flow index is equal to 1 in the presence of a yield value. Finally, yield pseudoplastic behavior is characterized by the Casson model (Equation 8) if flow index is smaller than 1 in the presence of a yield stress (Concha, 2014; Luckham & Rossi, 1999; Rao, 2014). The Bingham and Casson are mostly used models in mineral processing to estimate the yield stress value for a given suspension (Cruz et al., 2019; Farrokhpay, 2012).

Table 3.2 Rheological models (Concha, 2014; Rao, 2014)

Model	Equation	Variables	Units	
Newton	$\tau = \eta \dot{\gamma}$	τ —shear stress	[Pa]	(4)
		η —viscosity	[Pa.s]	
		$\dot{\gamma}$ —shear rate	[s ⁻¹]	
Herschel-Bulkley	$\tau = \tau_y + K\dot{\gamma}^n$	τ —shear stress	[Pa]	(5)
		τ_y —yield stress	[Pa]	
		K—consistency index	[Pa.s ²]	
		$\dot{\gamma}$ —shear rate	[s ⁻¹]	
		n—flow index	-	
Power Law	$\tau = K\dot{\gamma}^n$	τ —shear stress	[Pa]	(6)
		K—consistency index	[Pa.s ²]	
		$\dot{\gamma}$ —shear rate	[s ⁻¹]	
		n—flow index	-	
Bingham	$\tau = \tau_y + \eta \dot{\gamma}$	τ —shear stress	[Pa]	(7)
		τ_y —yield stress	[Pa]	
		η —plastic viscosity	[Pa.s]	
		$\dot{\gamma}$ —shear rate	[s ⁻¹]	
		n—flow index	-	
Casson	$\tau^{1/2} = \tau_y^{1/2} + (\eta\dot{\gamma})^{1/2}$	τ —shear stress	[Pa]	(8)
		τ_y —yield stress	[Pa]	
		η —plastic viscosity	[Pa.s]	
		$\dot{\gamma}$ —shear rate	[s ⁻¹]	

3.3.5 Rheology in Mineral Processing

Because the availability of high grade, easy-to-process ores are decreasing, it is required to process low grade, complex ores to compensate the increasing demands for raw materials. This challenging situation causes the complex ores with a high clay minerals content to be ground to finer sizes, and this leads to changes in slurry rheology. Because the properties of the clay mineral particles in suspension (size, shape, surface charge, concentration etc.) affects the rheology of mineral slurries considerably, the knowledge of slurry rheology with special emphasis to their mineralogy has gained importance to control flow behavior, which enables to improve and optimize many unit operations.

Comminution is known to constitute the highest operating costs and low mechanical efficiency among unit operations. This makes the understanding in the effect of slurry rheology essential. Thus, the research on rheology focused on ore grinding in literature is considerably limited. Some research has focused on the effect of fine particle size in wet grinding (Shi & Napier-Munn, 2002). However, the mineralogical effects of clay minerals are not considered by most of the rheology studies in wet grinding although morphology and surface charges of clay minerals are important properties to investigate rheology for clay mineral bearing ores. Bobicki et al. (2014) have investigated low-grade ultramafic nickel ores with high serpentine and 1 wt% chrysotile content in terms of the effects on slurry rheology. The charge anisotropy and the non-spherical particle shape of serpentine, and the fibrous property of chrysotile resulted in challenging slurry rheology causing high viscosity and yield stress, which can be potential problem in comminution. Therefore, microwave radiation treatment before grinding was proposed to reduce slurry viscosity and yield stress.

The motion of grinding media is a key parameter for the efficiency of grinding. High viscosity can cause a decrease in the velocity and kinetic energy of grinding media while increasing power consumption. On the other hand, low viscosity can increase the movement of both slurry and grinding media, causing the decrease in

particle attrition. As a result, optimum viscosity is needed (Cruz et al., 2019; Gao & Forssberg, 1993; He et al., 2004).

In closed grinding circuits, wet classification is performed by hydrocyclones. The flow behavior of slurries is known to affect hydrocyclone efficiency, and the rheology of the slurries is widely agreed to affect the performance of hydrocyclones. Wills & Finch (2016) have reported that if fibrous mineral chrysotile exists in slurries, rheology of slurries become more complex, and wet classification of asbestos can reveal unusual overall partition curves. In addition, the study conducted by Boylu et al. (2010) has confirmed that swelling clays cause the increase in viscosity that results from mixing with water limits the performance of hydrocyclones, so a sodium bentonite sample was used to perform a series of hydrocyclone testing to develop an effective separation procedure.

Because flotation pulps include much lower solids concentration than in wet grinding, it can be assumed that rheological properties don't affect flotation performance. However, the conditions at which yield stress presents can affect gas dispersion, bubble-particle attachment and detachment due to the direct relationship between yield stress and the strength of bonds. This direct relationship is also an indication of the number of bonds between particles that needed to be broken for higher grade and recovery (Cruz et al., 2019). Cruz et al. (2015) was investigated the interaction of two clay minerals, kaolinite and bentonite, comparably in the flotation of a copper-gold ore. When bentonite and kaolinite were mixed with copper-gold ore, it was found that the value of viscosity was higher in the case of bentonite mixing at even low shear rates. Also, it was concluded that because bentonite formed edge-edge (EE) interactions, causing more rheologically complex slurries, the hydrodynamics in the flotation cell might be affected by decreasing the flotation recovery. On the other hand, the aggregates of kaolinite consisted of face-face (FF) association, causing low yield stress requirements, did not affect flotation hydrodynamics.

Gungoren et al. (2020) investigated the influence of kaolinite, illite, and bentonite clays on coal flotation because they are known to be the major components of ash-forming mineral matters, and they adversely affect the flotation of coal. The ability of clay minerals to make hydrophilic by coating coal surface inhibits particle-bubble attachment. In addition, froth stability can be affected due to the mineralogical properties of clay minerals by increasing pulp viscosity. The results showed that slime coating on bentonite clay on coal is detrimental to coal flotation because it caused significant coal depression. In contrast, the depression of coal flotation with the addition of kaolinite and illite was not observed.

The rheology in dewatering focuses on the modification of the surface chemistry to promote particle aggregation by using flocculants and coagulants in order to enable the separation of particles from water. As was discussed, clay minerals can aggregate in different modes because they have distinct mineralogical characteristics (being fibrous, swelling, etc.), complicating the dewatering operations. McFarlane et al., (2005) investigated the dewatering behavior of Na-exchanged smectite clay dispersions by using CaCl_2 as coagulant and anionic polyacrylamide copolymer (PAM-A) and non-ionic polyacrylamide homopolymer (PAM-N) as flocculants because the smectites are known to present more difficulty than other clay minerals in the dewatering because of their swelling properties. This difficulty can stem from the large surface area, low settling rates, and high flocculant demand. It was concluded that rapid exchange of Ca^{2+} with Na^+ in the clay led to the suppression of swelling, which provides in turn low yield stress, and improved dewaterability. On the other hand, the use of PAM-A causes the faster settling flocs than that of PAM-N. When the rheological properties were observed, PAM-A flocculated pulp presented higher yield stress than PAM-N flocculated pulps. However, under shear, the yield stress of the PAM-A flocs reduced to lower value than those of PAM-N flocs, indicating PAM-A flocs were weak.

Clay and other gangue minerals, tailings, dispersed in an effluent, containing process chemicals are problematic in transport, dewatering, and water recovery processes. Clay minerals having distinct properties can alter the tailings rheology

differently by affecting settling rate and increasing pumping energy requirements. They can also change the angle of the tailings deposit, and high clay content will decrease the shear strength of the deposited tailings, consequently, causing possible collapse (Chryss, 2017).

The rheological properties of slurries mainly yield stress and viscosity plays an important role in the design and operation of pumping systems. While the acquisition of yield stress is significant to ensure a successful start-up of a pumping system from a static shut-down condition, the viscosity is a useful indication of the pumping requirements for the ease of flow (de Kretser et al., 1997).

Because of the increasing depth of the South African gold mines and so the increasing cost of ventilation, the cheaper and alternative methods for fill of stopes have been investigated. The rheological characteristics of high concentration waste slurries or pastes and their transportation for backfill purposes was discussed by Verkerk & Marcus (1988). It was recognized from the results that hydraulic transportation of high concentration of the reduction plant tailings slurries provides cost-effective fill by providing the required strength, the required conveying distance, and the pumping requirements.

In the light of these effects, the presence of gangue and clay minerals should be properly considered in mineral processing unit operations because they affect the slurry rheology adversely due to their unique morphology, colloidal size, and surface charges. However, this is most valid for the phyllosilicates. The further understanding of their mineralogical characteristics will help improving the rheological effects, and their availability for the backfill purposes.

CHAPTER 4

MATERIALS AND METHODS

Through this study, pure mineral suspensions and gold ore tailings samples were investigated in terms of their mineralogy and surface charge properties to establish a rheological classification. Also, the rheological properties of the tailings samples with higher and less extent of clay minerals were determined to enable the real simulations of rheological properties of phyllosilicate minerals in complex multicomponent ore systems where different clay particles locked in valuable mineral particles.

4.1 Materials

4.1.1 Pure Clay Minerals

Pure phyllosilicate minerals (kaolinite, illite, montmorillonite, talc, and muscovite) and non-phyllosilicate minerals (quartz and calcite) were comparatively and individually investigated to reveal the effects of the mineralogy and surface charge properties in rheological classification. Each pure mineral was supplied from different regions of Turkey to be investigated in the Mineral Processing Laboratory of Middle East Technical University. Kaolinite was obtained from Bilecik-Bozüyük region from Turkey. The studied illite sample was sourced from Yılanlı Burnu quarry in Bartın-Turkey. In order to negate the effect of particle size distribution, kaolinite and illite samples were first crushed by roll crusher, and then, dry-ground in a titanium ring mill under controlled conditions to yield smaller than 75 μm fraction, which is used for all experimental work. Montmorillonite, talc, and calcite from Tokat-Reşadiye, Sivas, Eskişehir regions of Turkey, respectively, were supplied in pre-ground forms. Quartz and muscovite were obtained from Aydın-

Çine-Milas region of Turkey. Quartz had -4 mm + 2.5 mm size distribution. On the other hand, muscovite was supplied in an exfoliated form. Muscovite and quartz were pre-ground in a titanium ring mill to obtain -75 μm fraction.

4.1.2 Complex Gold Ore Tailings Samples

Two gold ore tailings slurries having different mineralization characteristics from different veins of the same deposit were inspected for the differences in their rheological behavior, and surface charge properties were examined to understand the effect of mineralogical properties on rheological behavior of ore tailings slurries. One of the gold ore tailings samples is characterized with its higher extent of clay minerals whereas the other includes less extent of clays. The samples used in this study were provided by a mine operating in Turkey.

In keeping within the scope of the study, pH for zeta potential measurements and solids concentration for rheology measurements were used as only parameters. Thus, all other variables, such as particle size, temperature, and ionic strength were kept constant in order to minimize their effects on rheological behavior of tailings slurries. The particle size distribution measurements were performed using Malvern Mastersizer 2000 instrument. The particle size distributions of the ore tailings samples from the different veins of the same deposit are given in Table 4.1. It can be concluded that the particle size distributions of the samples used in this study are almost identical.

Table 4.1 The particle size distributions of the less and higher clayey ore tailings samples

Samples	d_{10} (μm)	d_{50} (μm)	d_{80} (μm)	d_{90} (μm)
Normal zone	3.25	27.58	73.67	105.59
Clayey zone	3.66	27.48	77.11	109.96

4.2 Material Characterization

4.2.1 Characterization of Pure Clay Minerals

In order to characterize the purity of minerals, mineralogical analyses were evaluated. XRD (X-ray Diffraction) analysis were performed to identify the compositional characteristics of the minerals qualitatively. XRD spectra of each mineral was obtained using Rigaku Ultima-IV Diffractometer. The samples were micronized prior to X-ray Diffraction. Powders were placed in a flat glass holder and scanning was taken using $\text{CuK}\alpha$ radiation over the 2θ ranging from 5° to 85° . Analyses were performed at the analytical conditions where X-ray tube voltage is 40 kV, tube current is 30 mA, and tube rating is 1.28 kW. The phases were identified based on the powder diffraction databases issued by the International Center for Diffraction Data (ICDD) using Bruker Diffrac.Suit software, which searches and matches diffraction patterns to reference patterns for easy X-ray powder diffraction data acquisition and evaluation, together with the table of key lines provided by Chen (1977). The reference patterns are compiled by the Joint Committee on Powder Diffraction Standards – International Center for Diffraction Data (JCPDS – ICDD) and released on software as a database of Powder Diffraction Files.

Figure 4.1 shows the XRD diffractogram of kaolinite. The diffractogram and peak intensities verified that kaolinite was the dominant mineral phase in the sample. Also, trace amount of silicate, clay and iron-containing minerals was detected in the XRD spectra. It was confirmed by the supplied mining site that kaolinite mineral had a purity of 90-100 wt%.

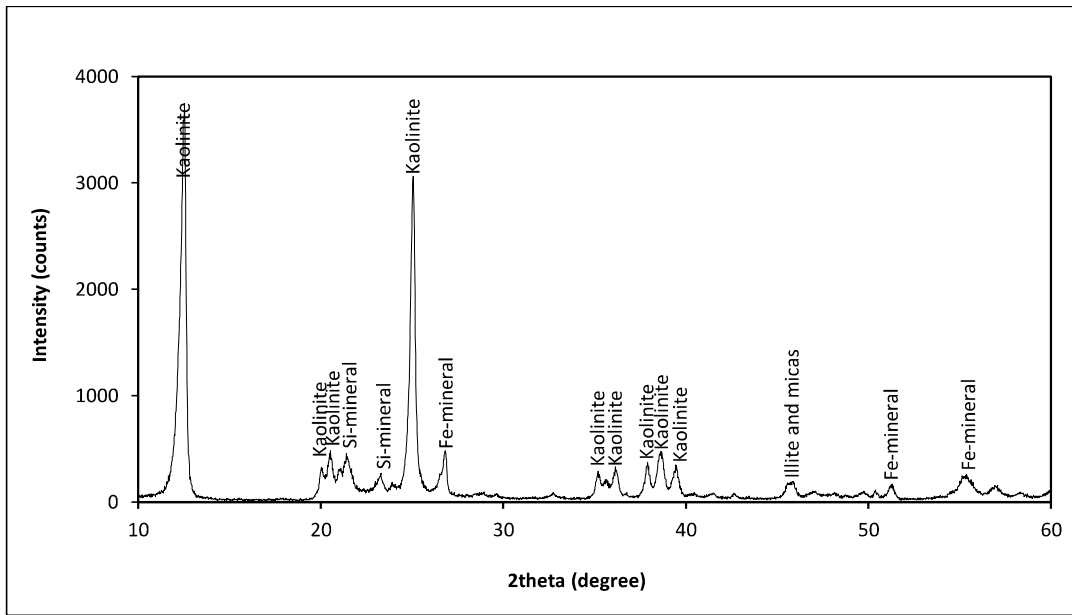


Figure 4.1 The XRD pattern of kaolinite sample

The sample taken from Yılanlı Burnu quarry was comprised mainly of high-grade illite. According to the XRD pattern shown in Figure 4.2, illite was responsible for the most intense peaks. On the other hand, lower intense characteristic peaks of other silicate and non-silicate minerals were detected as impurities.

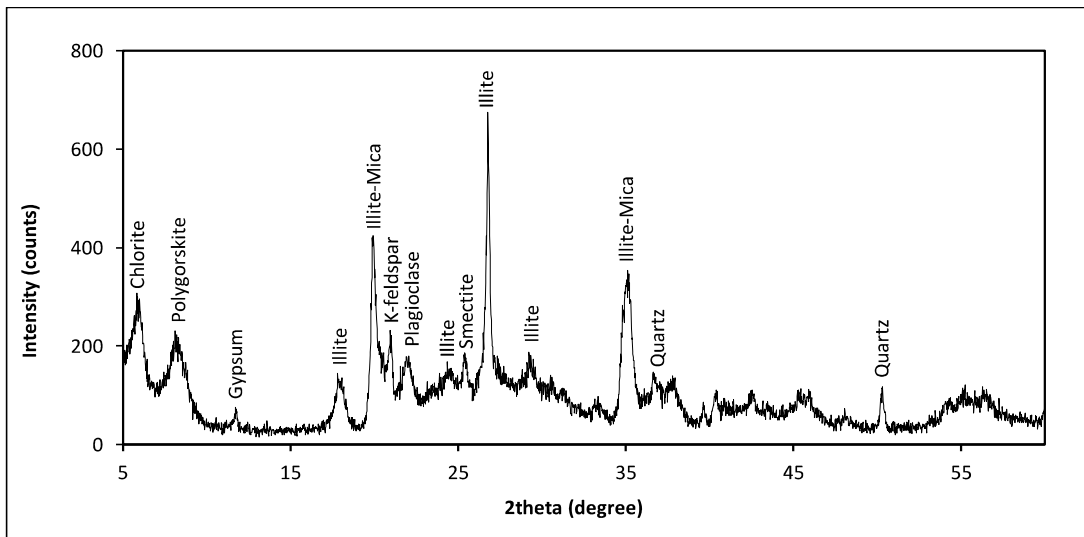


Figure 4.2 The XRD pattern of illite sample

Bentonite clay sample used in this study was composed of mainly sodium montmorillonite (Na^+Mt). Mineralogical analysis of bentonite sample illustrated in Figure 4.3 verified that the dominating mineral was sodium montmorillonite, and it was responsible for the most intense peaks. The other peaks are impurities corresponding to iron-containing minerals and kaolin group minerals. It was confirmed by the supplied mining site that the bentonite sample had a purity of over 85% in terms of Na^+Mt content.

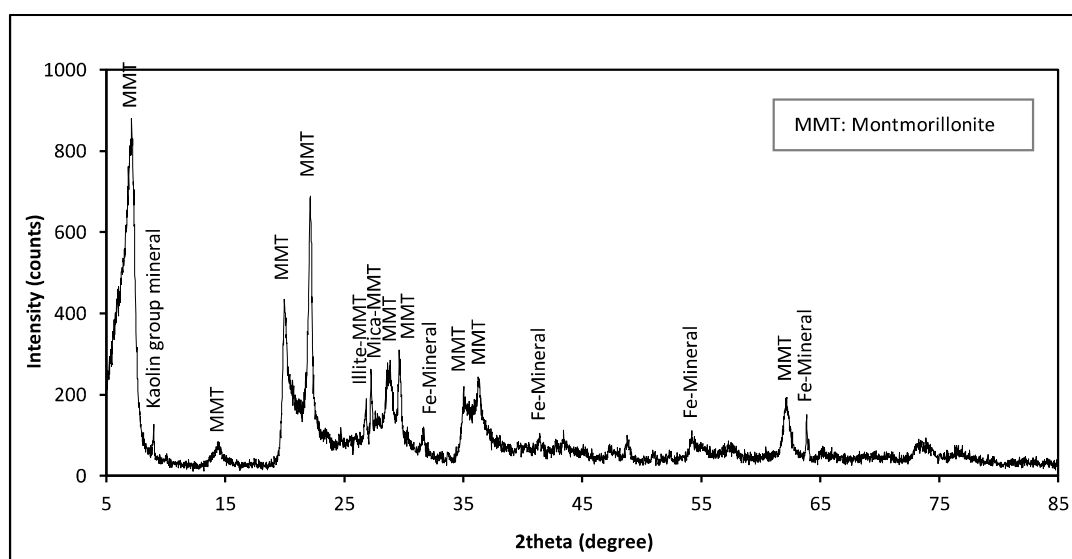


Figure 4.3 The XRD pattern of bentonite sample

Muscovite, talc, quartz, and calcite were analyzed by XRD shown in Figure 4.4, 4.5, 4.6, 4.7, respectively. All mentioned mineral samples were supplied in almost pure forms from different regions of Turkey. As seen in Figure 4.4, XRD peaks of the tested muscovite sample confirmed that it was mainly muscovite. X-ray diffraction analysis conducted on the talc sample, as shown in Figure 4.5, confirmed that talc is the dominant mineral phase. In both cases, the impurity comprised mainly of quartz in trace amounts. In addition, X-ray diffraction (XRD) analysis of the quartz and calcite powders revealed that the minerals were pure quartz and pure calcite as seen in Figure 4.6 and 4.7.

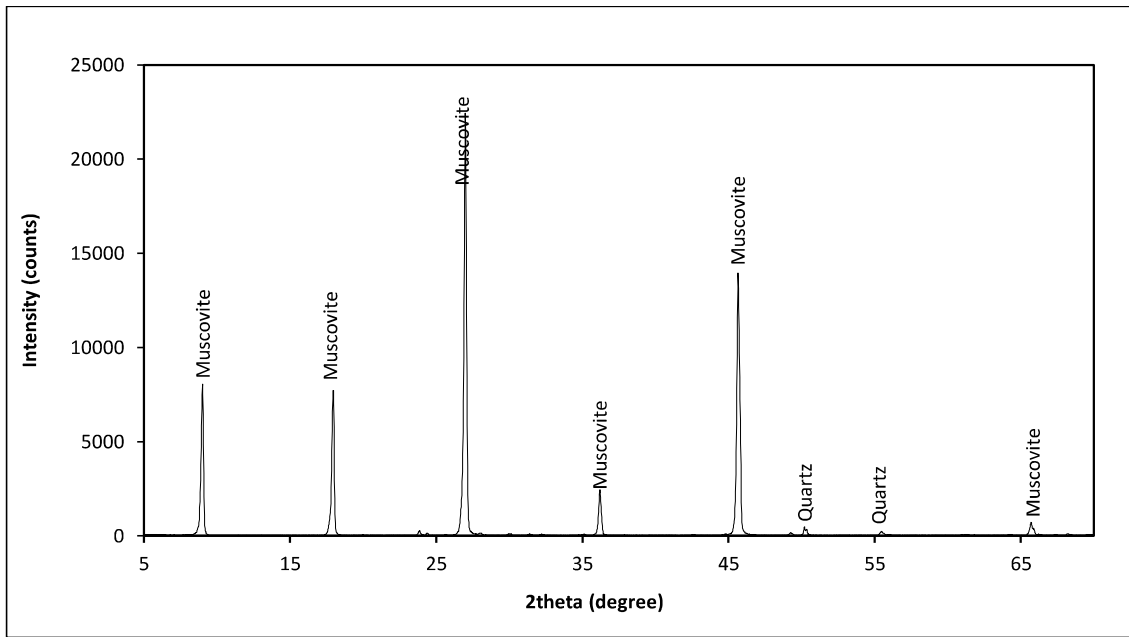


Figure 4.4 The XRD pattern of muscovite sample

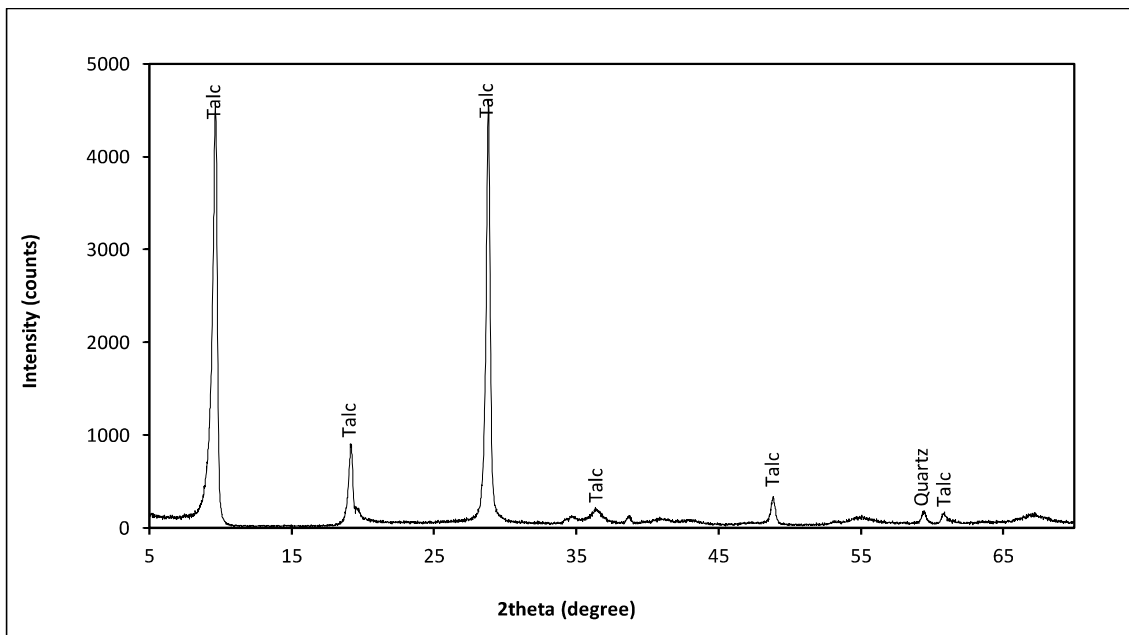


Figure 4.5 The XRD pattern of talc sample

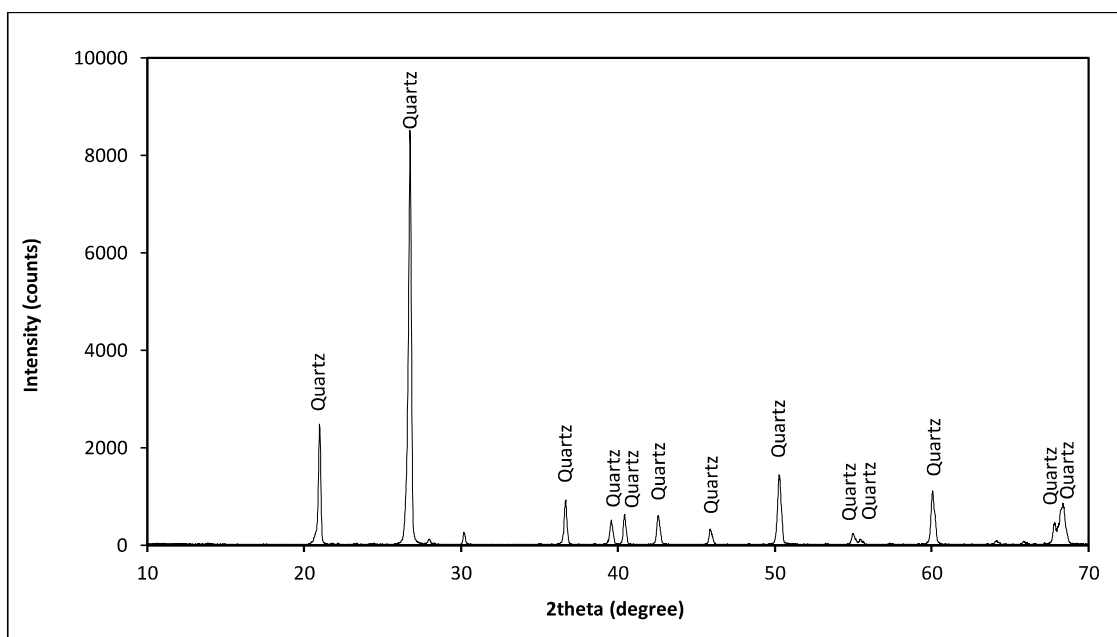


Figure 4.6 The XRD pattern of quartz sample

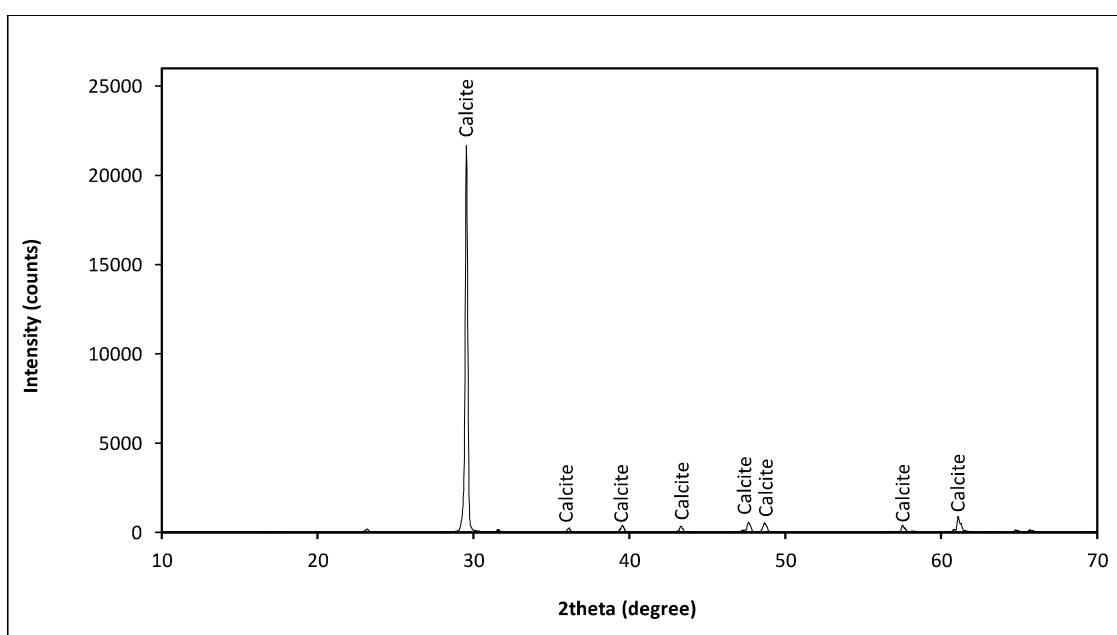


Figure 4.7 The XRD pattern of calcite sample

4.2.2 Characterization of the Ore Tailings

In order to reveal the differences in mineralogical properties and to define the major minerals of the studied commercial gold ores, XRD (X-ray Diffraction) analyses were performed on two gold ore tailings samples taken from different veins of the same deposit because it was mentioned that one of the gold ore tailings samples are characterized with higher extent of clay minerals. XRD spectra of the ore tailings samples (Figure 4.8 and Figure 4.9) were obtained using Rigaku Ultima-IV Diffractometer. Interpretations were based on the powder diffraction databases issued by the International Center for Diffraction Data (ICDD) using Bruker Diffrac.Suit software together with the table of key lines provided by Chen (1977).

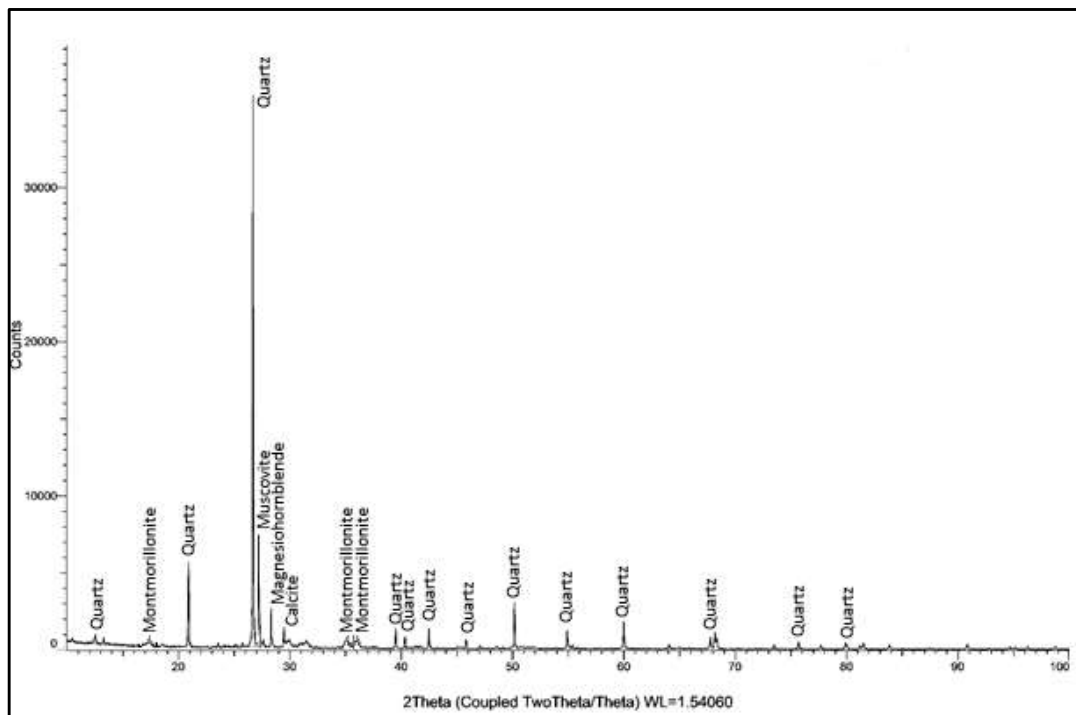


Figure 4.8 The XRD pattern of normal vein sample

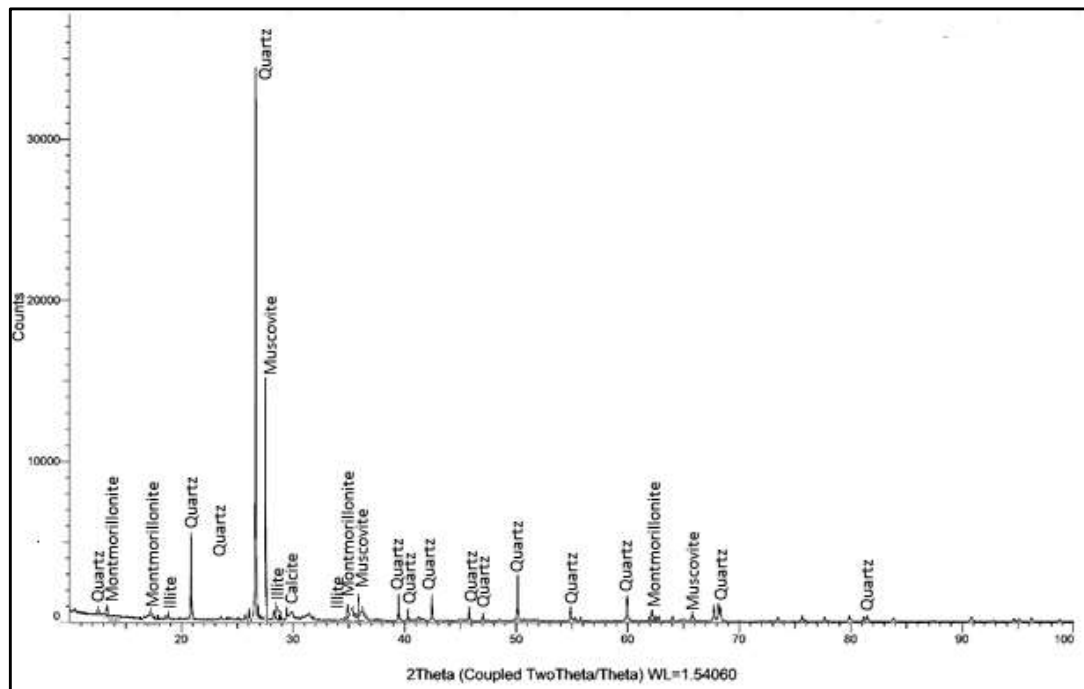


Figure 4.9 The XRD pattern of clayey vein sample

Two gold ore tailings samples from different veins of the same deposit were used in this study. When mineralogical analysis of normal vein sample and clayey vein sample illustrated in Figure 4.8 and Figure 4.9 respectively are compared, it was verified that clay minerals were responsible for the most intense peaks in the case of clayey vein sample. Different from normal vein sample, clayey vein sample also contained illite mineral. When XRD pattern of normal vein sample (Figure 4.8) is examined, it was observed that quartz was responsible for the most intense peaks, and montmorillonite and muscovite was observed in small amounts as clay minerals. On the other hand, XRD pattern of clayey vein sample shows that muscovite, montmorillonite, and illite was responsible for the most intense peaks as clay minerals besides quartz as non-phyllsilicate mineral.

4.3 Methods

4.3.1 Zeta Potential Measurements

Zeta potential measurements are experimental measurements that have been extensively studied for the surface charge properties of the minerals. Zeta potential measurements were carried out to present the differences in surface charge properties of kaolinite, illite, montmorillonite, talc, and muscovite with respect to quartz and calcite. In addition, the tailings samples were inspected for the differences in surface charge properties. The zeta potential measurements were conducted using a Malvern Zetasizer Nano Z instrument (Figure 4.8) . The Zetasizer Nano Z series of analyser uses He-Ne (Helium-Neon) red laser beam (λ (lambda): 632.8 nm). The instrument can be utilized for zeta potential measurements in 3.8 nm to 100 μm size range (Malvern, 2013). The instrument automatically calculates the electrophoretic mobility of particles and converts it to zeta potential using Smoluchowski's equation.

For each mineral and the tailings samples, 0.5% solid by weight dilute suspension was prepared in 50 ml ultrapure water. In order to obtain a well-dispersed suspension, the suspensions were mixed and dispersed continuously with a magnetic stirrer for 10 minutes. The pH of the suspensions was adjusted to the pre-determined values (between pH 2 and pH 12) with droplets of acid and alkali (0.1 M HCl and 0.1 M NaOH) solutions. However, the zeta potential measurements of calcite were performed in a narrow pH range, pH = 7 – 12, due to the dissolution of calcite in acidic environment. The pH of the suspensions was altered to desired values based on the pristine pH of the suspensions using 0.1 M HCl and 0.1 M NaOH solutions. For each new pH value, the suspensions were continuously mixed with a magnetic stirrer for 5 minutes, allowing to equilibrate prior to measurement to ensure consistency. Also, at each pH condition, individually prepared suspensions were used in order to minimize the subsequent adsorption of the leached ions on the same surfaces. After that, pH of the suspensions was measured and recorded. Subsequently, the suspension was settled for about 2 min to allow the

coarse particles to settle down. An aliquot of approximately 1 ml from the supernatant of the suspension was injected into the disposable cuvette (Figure 4.9) of the instrument and placed in the Zetasizer to determine the zeta potential at each pH condition. Each sample at each pH condition was measured at least three times and the average was reported as the final zeta potential value. The measurements were conducted at room temperature (24-25 °C), controlled by the instrument. The pH at which zeta potential is zero is known as iso-electric point (IEP) of the mineral.



Figure 4.10 Malvern Zetasizer Nano Z (Malvern, 2013)

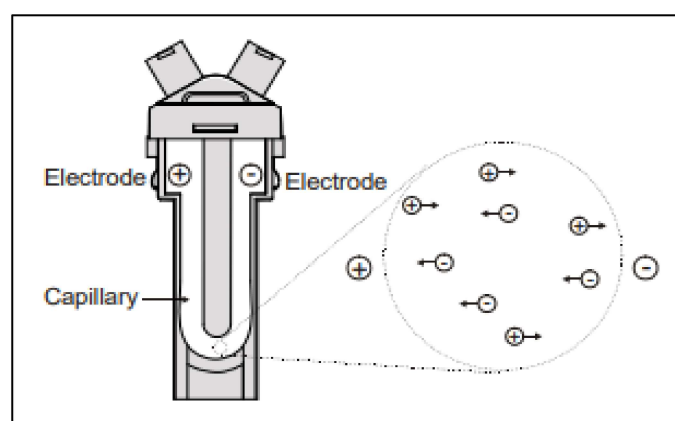


Figure 4.11 Disposable Cuvette of Malvern Zetasizer Nano Z and Particle Movement toward the Electrode of Opposite Charge (Malvern, 2013)

4.3.2 Potentiometric Titration Measurements

The surface charge properties of minerals were also investigated with the help of Mular-Roberts potentiometric titration technique. The point of zero charge of each mineral was determined. This method relies on the change in the surface charge as the concentration of background electrolyte is changed, with the pH measured at different ionic strengths of the suspension.

The PZC determination via the Mular-Roberts (M-R) method is a pH-salt addition measurement. For each mineral, suspensions consisting of 1.00 g representative samples in 50 ml aliquots of 0.001 M NaCl were prepared. Each suspension was prepared at different pre-determined pH values (ranging from pH 2 to pH 11) using 0.1 M HCl and 0.1 M NaOH solutions, and the initial pH was measured. The ionic strength of each suspension was raised from 0.001 M to 0.1 M by the addition of the appropriate amount of dry NaCl solids. When the new pH reading was stable, the pH of the resulting suspension was then recorded to give a final pH. The difference in the initial and final pH values (ΔpH) was plotted as a function of the final pH. The pH value at which ΔpH is equal to zero corresponds to the point of zero charge of each mineral.

4.3.3 Rheology Measurements

The rheology of tailings slurries with less and higher extent of clay minerals was investigated in terms of their yield stress and viscosity properties under changing conditions. The yield stress of tailings samples was investigated as a function of solids concentration, such that the suspensions varied from dilute to highly concentrated. The yield stress behavior of suspensions was explained in terms of Bingham Plastic and Casson rheological models. On the other hand, viscosity of suspensions was determined as a function of time at a certain solid content for both normal vein and clayey vein samples.

4.3.3.1 Yield Stress Measurements

Rheology measurements were carried out on the tailings samples obtained from thickener underflow having less extent of clays and higher extent of clays. The tailings sample with higher extent of clays were obtained in three separate packages. This tailings samples were blended, and five representative samples were taken to determine moisture content. The tailings sample with less extent of clays were also obtained and five representative samples were taken to determine moisture content and solid content by weight.

The moisture content of five representative samples of two different tailings samples are presented in Table 4.2 and Table 4.3. As shown in Table 4.2, the moisture contents were changing from 21.26% to 21.60% in the case of the higher clayey tailings samples taken from thickener underflow. Also, the average moisture content is 21.41%, and the solid content by weight was found as 78.59%. On the other hand, the moisture contents of the less clayey tailings samples were found considerably close to each other. The average moisture content was 15.75%, and the solid content was 84.25%.

Table 4.2 Moisture contents and average moisture content of the higher clayey tailings samples obtained from thickener underflow

Samples	Moisture Content %	Solid Content by wt. %
Sample 1	21.32	78.68
Sample 2	21.37	78.63
Sample 3	21.26	78.74
Sample 4	21.52	78.48
Sample 5	21.60	78.40
Average	21.41	78.59

Table 4.3 Moisture contents and average moisture content of the less clayey tailings samples obtained from thickener underflow

Samples	Moisture Content %	Solid Content by wt. %
Sample 1	14.79	85.21
Sample 2	16.62	83.38
Sample 3	15.51	84.49
Sample 4	15.83	84.17
Sample 5	16.00	84.00
Average	15.75	84.25

The yield stress of tailings samples with less and higher clayey content were determined with respect to change in solid content. The average moisture content was considered in order to prepare ore tailings slurries with different amount of solid content. In this respect, with the addition of required amount of pure water, tailings suspensions including 35, 40, 45, 48, 51, 54, 57, 60, 65, 70% solids by weight were prepared. Tailings suspensions having different amount of solid content were analyzed using Brookfield DV-II+Pro type viscometer (shown in Figure 4.10) that works simultaneously with “Reocalc” rheology software. The most suitable type of rheometer spindle was determined as Brookfield Ametek SC4-27 thanks to preliminary analysis conducted on two tailings samples using suspensions with highest and lowest solid content. Yield stress was obtained using shear stress and shear rate data in combination with “Bingham Plastic” and “Casson” mathematical models because “Bingham Plastic” and “Casson” rheological models give consistent and evaluable results for settling suspensions. In this respect, rotational rate was increased from 20 rpm to 200 rpm ($6.8 - 68 \text{ s}^{-1}$) gradually for each suspension, and at each shear rate, shear stress value was recorded. The obtained shear stress was plotted as a function of shear rate at each solid content to determine yield stress of tailings suspensions obtained from thickener underflow.



Figure 4.12 Brookfield DV-II+ Pro viscometer

4.3.3.2 Viscosity Measurements

Tailings samples from higher and less clayey veins were obtained from different shifts in four different packages. The solid contents of each sample were determined and presented in Table 4.4 and Table 4.5. Based on the results, it was observed that the solid contents of both tailings samples were approximately 65-66% by weight and 54-55% by weight in two groups. Therefore, it was decided to blend the samples having similar solid contents, and they were homogenized. The solid contents of tailings samples after homogenization are presented in Table 4.6. The homogenized samples were used to conduct viscosity measurements.

Table 4.4 The solid contents of the ore tailings samples with less extent of clays

	NZ1	NZ2	NZ3	NZ4
Solid Content (by wt. %)	66.02	65.11	54.96	54.12

Table 4.5 The solid contents of the ore tailings samples with higher extent of clays

	KZ1	KZ2	KZ3	KZ4
Solid Content (by wt. %)	65.82	65.46	54.78	54.62

Table 4.6 The solid contents of the ore tailings samples after homogenization

Normal		Clayey	
Mineralization	Solid Content	Mineralization	Solid Content
Vein Tailings	(by wt. %)	Vein Tailings	(by wt. %)
Samples		Samples	
NZ1	65.36	KZ1	65.58
NZ2	54.43	KZ2	54.60

Viscosity measurements were conducted using Brookfield DV-II+ Pro viscometer (Figure 4.10) with appropriate spindle. The experiments were conducted at constant rotational rate of 50 rpm, and each measurement was continued for 1020 seconds. Also, each measurement was conducted two times, and the average was taken as relative viscosity.

CHAPTER 5

RESULTS AND DISCUSSION

The surface charge properties of phyllosilicate minerals (kaolinite, illite, montmorillonite, talc, muscovite) and non-phyllosilicate minerals (quartz and calcite) were investigated using the electrophoretic zeta potential measurements and Mular-Roberts titration technique in tandem. The charge deviation was demonstrated through the measured isoelectric point (determined by the zeta potential measurement) and point of zero charge (determined by titration) for those minerals. In addition, zeta potential measurements of gold ore tailings samples with higher and less extent of clay minerals were performed. As a result, the particle interactions likely to form in ore tailings slurries as a function of pH depending on the developed surface charge distributions were proposed to have better understanding of the rheological behavior of ore tailings slurries. The rheological properties (yield stress and viscosity) are useful indicators of the degree of aggregation and dispersion of particles within the suspensions as would be dictated by the surface charge properties.

5.1 Surface Charge Properties of Clay Minerals

The electrophoretic zeta potential measurements of clay minerals were performed as a function of pH over the range of pH 2- pH 12, with the results presented in Figure 5.1. The isoelectric points (IEP) of kaolinite, illite, muscovite, and talc were measured at pH 3.7, 2.5, 5.5, and 2.5, respectively. For kaolinite, it means the zeta potential is zero at pH 3.7. It can be seen that kaolinite, illite, muscovite, and talc particles were positively charged at low pH, but the increase in the suspension pH resulted in an increase in the negative charge of particles. At low pH values, an excess of positive sites left on the surface of kaolinite due to protonation provided

to be positively charged. On the other hand, an excess of negative sites due to dissociation of H^+ at high pH values resulted in negatively charged surface. However, the isoelectric point (IEP) of montmorillonite was not detected. Along the measured pH range, montmorillonite particles were negatively charged. The increase in the suspension pH resulted in an increase in the negative charge of montmorillonite. An excess of negative sites due to dissociation of H^+ at high pH values resulted in negatively charged surface.

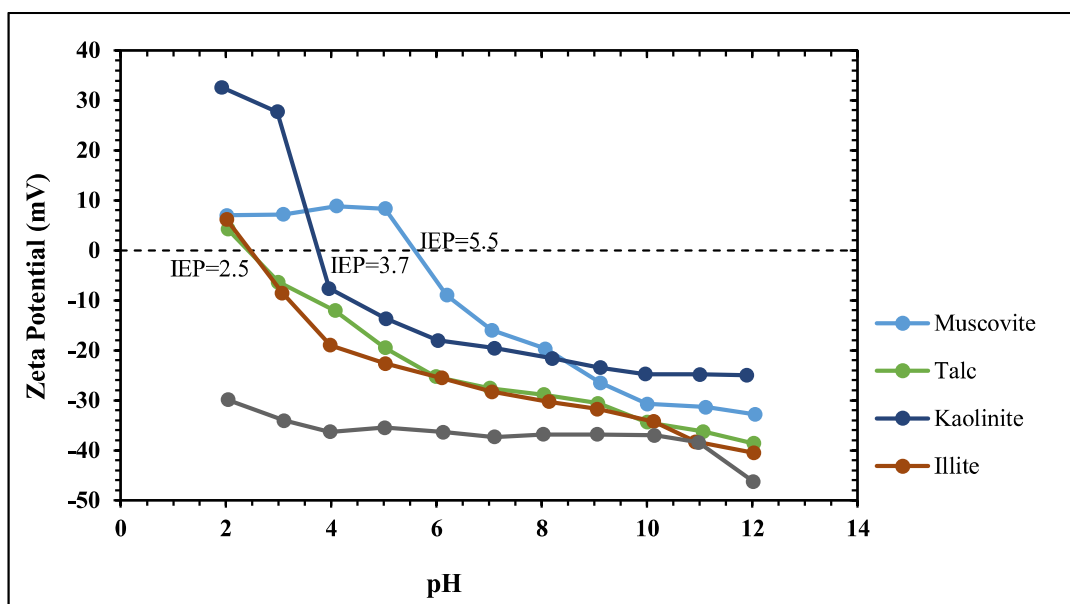


Figure 5.1 The zeta potential curves of clay minerals

Mular-Roberts titration measurements of kaolinite were performed over the pH range of pH 2- pH 10. The M-R titration measurements of illite and muscovite were performed over the pH range of pH 2- pH 9 different from kaolinite, talc and montmorillonite. For talc and montmorillonite minerals, the measurements were performed over the pH range of pH 2- pH 11. The results, given in Figure 5.2, show that the point of zero charges (PZC) of kaolinite, illite, muscovite, talc, and montmorillonite were at pH 2.7, 7, 4.6, 8.7, and 8.5, respectively. At the conditions where PZC is observed, the positively charged planes and negatively charged planes are in balance. Below this PZC, mineral surface is prone to the adsorption of OH^- ions from the solution onto positively charged surface, which results in a decrease in the pH of the solution and so ΔpH is to be positive. Conversely, above

this PZC, ΔpH is negative because H^+ ions from the solution are adsorbed onto the negatively charged surface, causing an increase in the pH of the solution. As a result, although Mular-Roberts titration technique doesn't provide the numerical estimate of the surface charge of the mineral, it can be concluded that kaolinite surface carries an overall negative charge at conditions above pH 2.7, and this is valid for other clay minerals at specific PZC. The difference existing between PZC and IEP values indicates the charge deviation from isotropic behavior, and the degree of charge anisotropy. The higher difference between the values is indicative of higher charge anisotropy. On the other hand, IEP and PZC values occurs at the same pH for isotropically charged minerals such as quartz and calcite (Johnson et al., 2000).

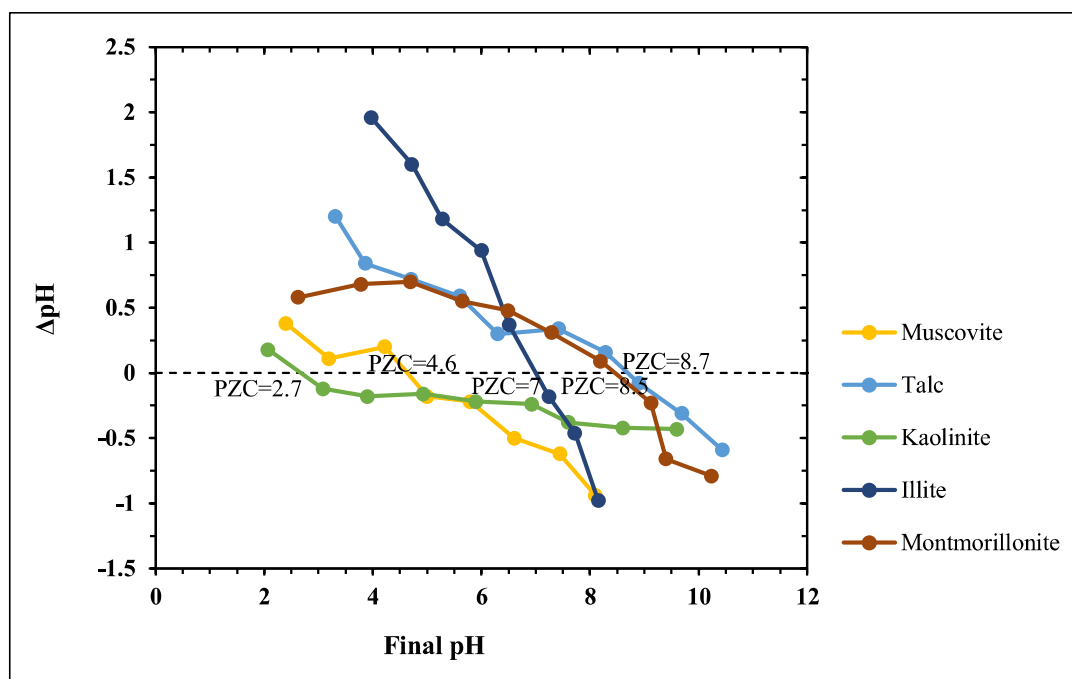


Figure 5.2 The potentiometric titration curves of clay minerals

Rheological tests on the tailings samples were conducted at ultra pure water which was in the range of pH 7-8. The test pH lies above the measured PZC of kaolinite (pH 2.7) and the measured PZC of muscovite (pH 4.6). This would result in the contribution of negative surface charge to tailings samples with kaolinite and muscovite because kaolinite and muscovite surfaces carry overall negative charges

at conditions above pH 2.7, and pH 4.6, respectively. The XRD pattern of the tailings samples shown in Figure 4.8 and 4.9 verified that muscovite mineral was higher in amount in the case of clayey vein sample than normal vein sample due to its higher peaks. This would result in the contribution of relatively higher negative surface charge of muscovite to tailings samples with muscovite mineral.

The test pH (pH 7-8) is close to the measured PZC of illite (pH 7). At this condition, it can be concluded that the overall charge is zero, or the particles are slightly negatively charged. The XRD pattern of the clayey tailings sample shown in Figure 4.9 verified the existence of illite mineral. This would result in the contribution of overall negative surface charge of illite to tailings samples with illite mineral because illite surface carries an overall negative charge at conditions above pH 7.

The measured PZC of talc (pH 8.7) and the measured PZC of montmorillonite (pH 8.5) lie above the test pH (pH 7-8). This would result in the contribution of overall positive surface charge of talc and montmorillonite to tailings samples because talc and montmorillonite surfaces carry overall negative charges at conditions above pH 8.7, and 8.5, respectively. The XRD pattern of the tailings samples shown in Figure 4.8 and 4.9 verified that montmorillonite mineral was higher in amount in the case of clayey vein sample than normal vein sample due to its intensive peaks. This would result in the contribution of relatively higher overall positive surface charge of montmorillonite to tailings samples.

5.2 Surface Charge Properties of Quartz and Calcite

The electrophoretic zeta potential measurements of quartz were performed as a function of pH over the range of pH 2- pH 12, with the results presented in Figure 5.3. The isoelectric point (IEP) was measured at pH 2.2, meaning the zeta potential is zero at pH 2.2. It can be seen that quartz particles were positively charged at low pH, but the increase in the suspension pH resulted in an increase in the negative charge of quartz. At low pH values, an excess of positive sites left on the surface of

quartz due to protonation provided to be positively charged. On the other hand, an excess of negative sites due to dissociation of H^+ at high pH values resulted in negatively charged surface. Quartz is a non-phyllsilicate mineral, which demonstrates isotropically charged behavior. In other words, IEP and PZC values occurs at the same pH 2.2. Different from quartz, the electrophoretic zeta potential measurements of calcite were performed as a function of pH over the range of pH 7- pH 12 due to the dissolution of calcite in acidic environment, with the results presented in Figure 5.3. The isoelectric point (IEP) was measured at pH 8.5, meaning the zeta potential is zero at pH 8.5. It can be seen that calcite particles were positively charged at low pH, but the increase in the suspension pH resulted in an increase in the negative charge of calcite. At low pH values, an excess of positive sites left on the surface of calcite due to protonation provided to be positively charged. On the other hand, an excess of negative sites due to dissociation of H^+ at high pH values resulted in negatively charged surface. Calcite demonstrates isotropically charged behavior different from phyllosilicate minerals. In other words, IEP and PZC values occurs at the same pH 8.5.

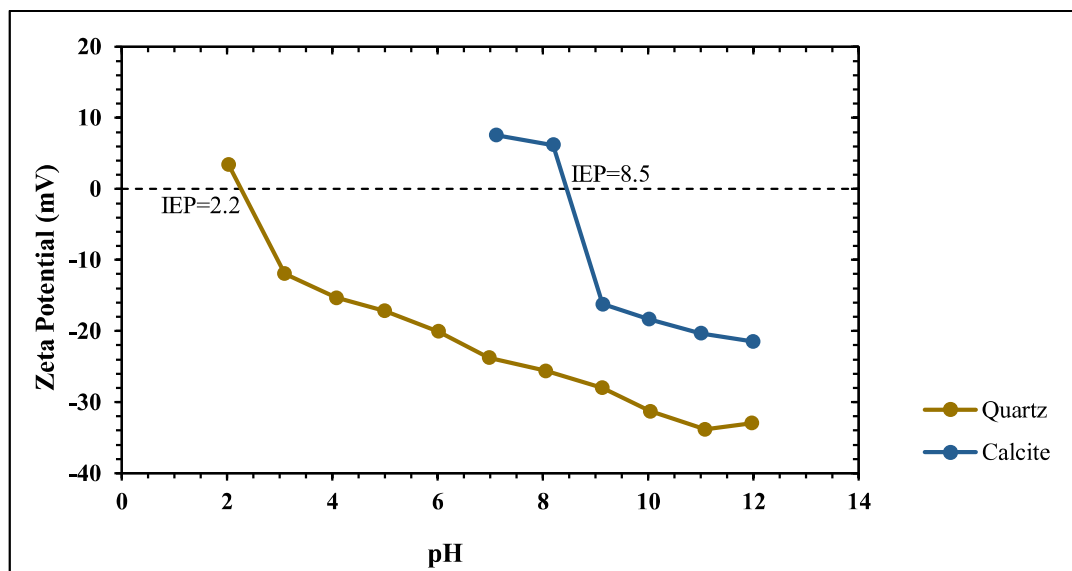


Figure 5.3 The zeta potential curves of quartz and calcite

In the lights of the findings obtained by the zeta potential curves of quartz and calcite, quartz particles are strongly negatively charged at test pH of 7-8, and it well dispersed in tailings samples with quartz mineral. Thus, because of its strong negative charge and charge isotropy, the effects of quartz on rheological properties can be disregarded when it is compared with distinct properties of clay minerals. On the other hand, the overall surface charge of calcite is zero, or the particles are slightly positively charged. Therefore, it was concluded that the effects of calcite on rheological properties of ore tailings suspensions can be disregarded.

5.3 Surface Charge Properties of Complex Gold Ore Tailings Samples

Zeta potential measurements of gold ore tailings samples with higher and less extent of clay minerals are given in Figure 5.4. Based on the results, zeta potentials of the clayey vein sample increased from approximately -1 mV to -25 mV with the rising pH from 2 to 12. On the other hand, there was an increase in the zeta potentials of the normal vein sample from approximately -5 mV to -30 mV with the rising pH from 2 to 12. It can be seen that both tailings samples were negatively charged at even low pH, and the increase in the suspension pH resulted in an increase in the negative surface charge of both tailings samples. The XRD patterns of tailings samples shown in Figure 4.8 and 4.9 verified the existence of montmorillonite, illite, and muscovite as clay minerals. Also, it was concluded that clay minerals were responsible for the most intense peaks in the case of clayey vein sample. The differences in zeta potential curves of both clayey vein sample and normal vein sample shown in Figure 5.4 comes from the existence of clay minerals in type and amount.

The surface charge properties are useful indicators of degree of aggregation and dispersion of particles within the suspensions. The higher values of surface charges of normal vein sample were observed in zeta potential measurements as compared to normal vein sample, as shown in Figure 5.4. The higher values of surface charges cause the more dispersed state whereas the particles with relatively lower values of surface charges are prone to interparticle interactions and agglomeration

in suspensions. As a result, this would result in more clayey suspensions of higher viscosity and yield stress than in the dispersed state.

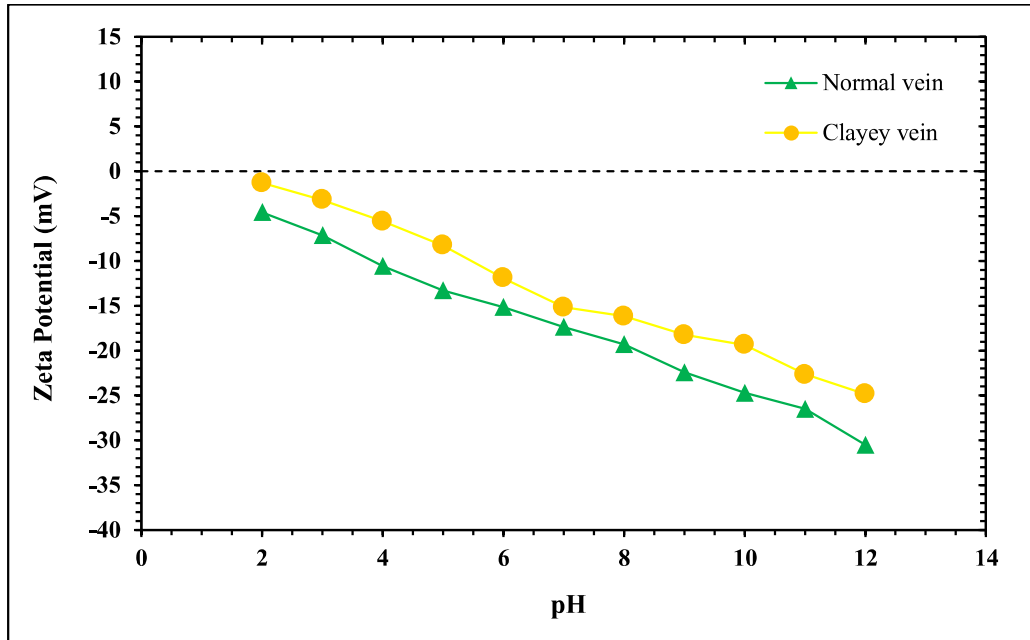


Figure 5.4 The zeta potential curves of ore tailings samples with higher and less extent of clay minerals

5.4 Rheological Properties of Complex Gold Ore Tailings Samples

5.4.1 Yield Stress of Clayey Vein Tailings Samples

The rheograms of ore tailings samples with higher clayey content including 35% solids by weight are presented in Figure 5.5 and Figure 5.6. The rheograms were evaluated based on “Bingham” and “Casson” rheological models. In this respect, yield stress of the samples including 35% solids by weight based on Bingham model is 15.10 dyn/cm², and 12.54 dyn/cm² for Casson model.

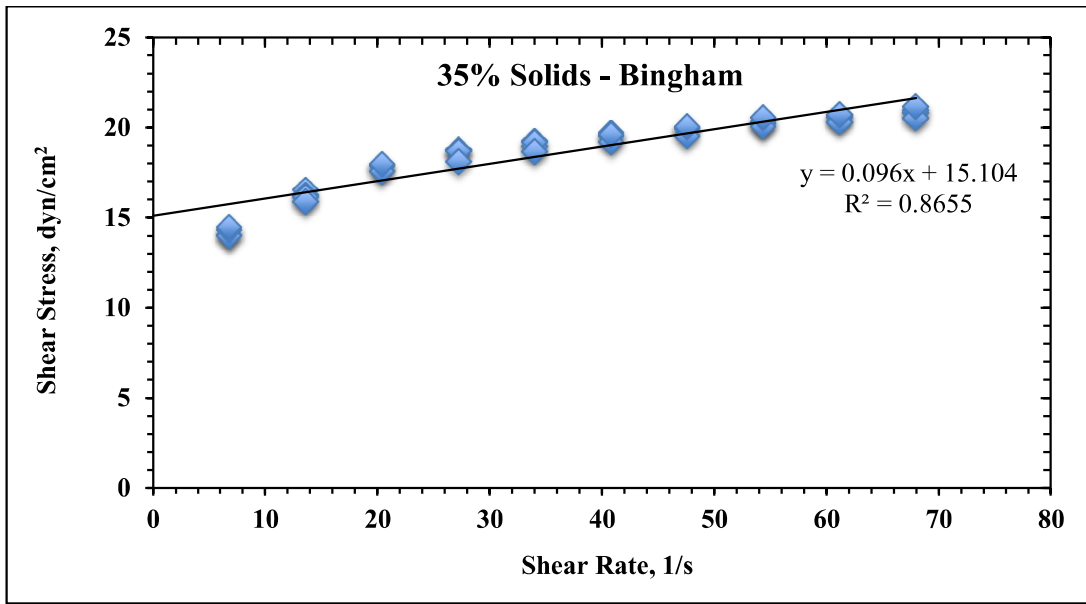


Figure 5.5 The plot of shear rate vs shear stress of clayey vein tailings sample including 35% solids by weight based on Bingham rheological model

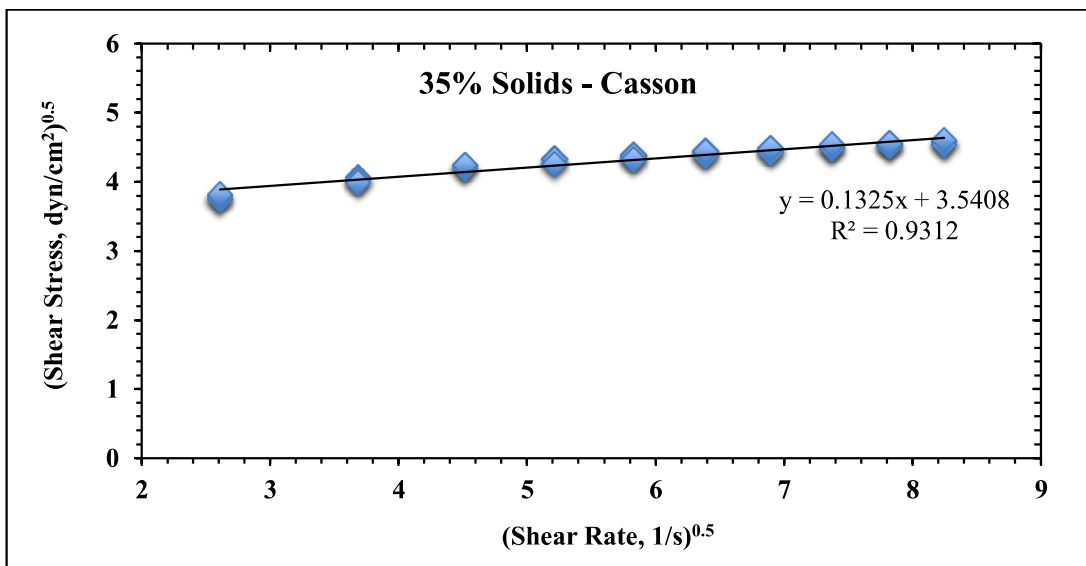


Figure 5.6 The plot of shear rate vs shear stress of clayey vein tailings sample including 35% solids by weight based on Casson rheological model

The rheograms of ore tailings samples with higher clayey content including 40% solids by weight are presented in Figure 5.7 and Figure 5.8. The rheograms were evaluated based on “Bingham” and “Casson” rheological models. In this respect, yield stress of the samples including 40% solids by weight based on Bingham model is 22.71 dyn/cm², and 19.27 dyn/cm² for Casson model.

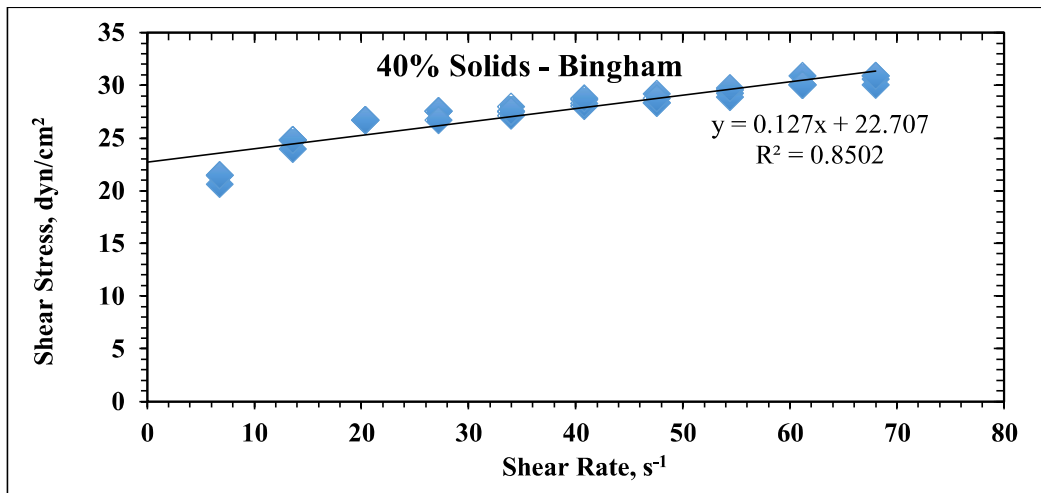


Figure 5.7 The plot of shear rate vs shear stress of clayey vein tailings sample including 40% solids by weight based on Bingham rheological model

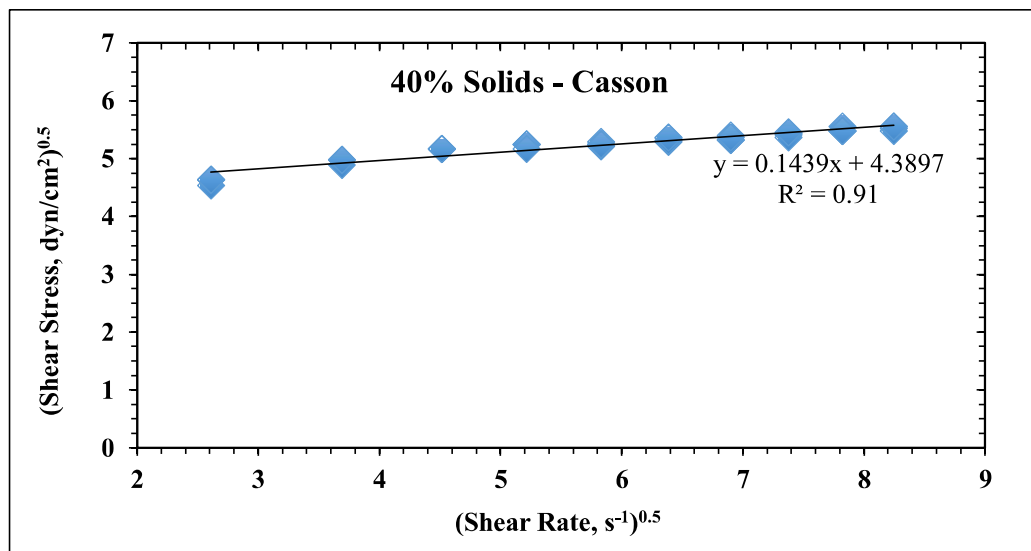


Figure 5.8 The plot of shear rate vs shear stress of clayey vein tailings sample including 40% solids by weight based on Casson rheological model

The rheograms of ore tailings samples with higher clayey content including 45% solids by weight are presented in Figure 5.9 and Figure 5.10. The rheograms were evaluated based on “Bingham” and “Casson” rheological models. In this respect, yield stress of the samples including 45% solids by weight based on Bingham model is 35.20 dyn/cm², and 30.48 dyn/cm² for Casson model.

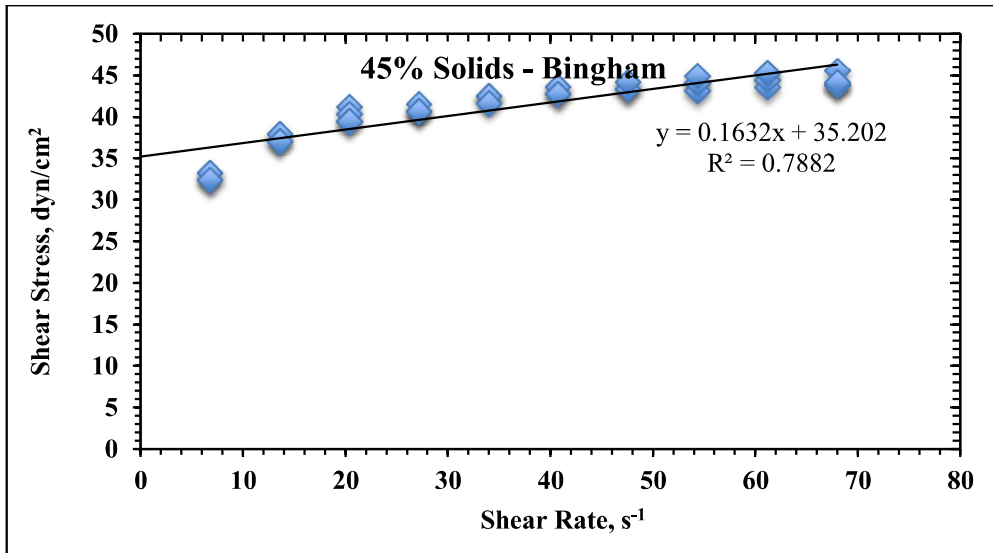


Figure 5.9 The plot of shear rate vs shear stress of clayey vein tailings sample including 45% solids by weight based on Bingham rheological model

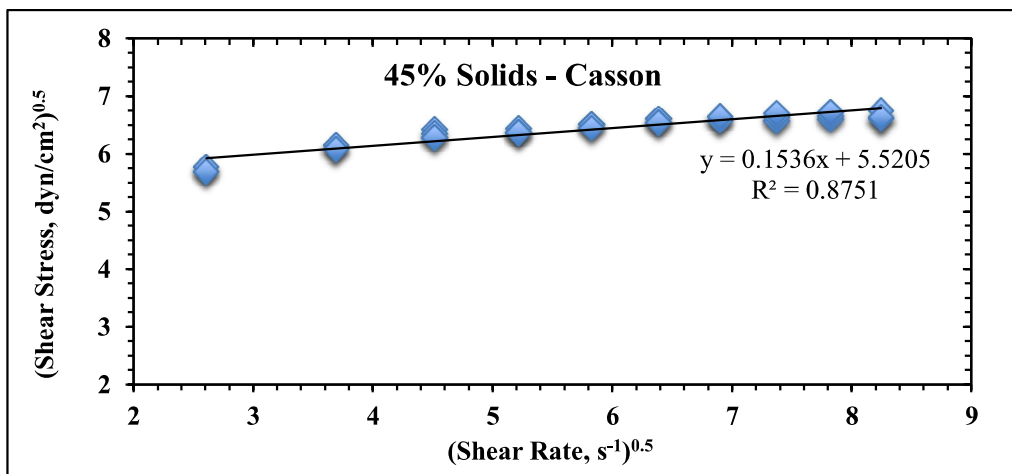


Figure 5.10 The plot of shear rate vs shear stress of clayey vein tailings sample including 45% solids by weight based on Casson rheological model

The rheograms of ore tailings samples with higher clayey content including 48% solids by weight are presented in Figure 5.11 and Figure 5.12. The rheograms were evaluated based on “Bingham” and “Casson” rheological models. In this respect, yield stress of the samples including 48% solids by weight based on Bingham model is 59.66 dyn/cm², and 51.85 dyn/cm² for Casson model.

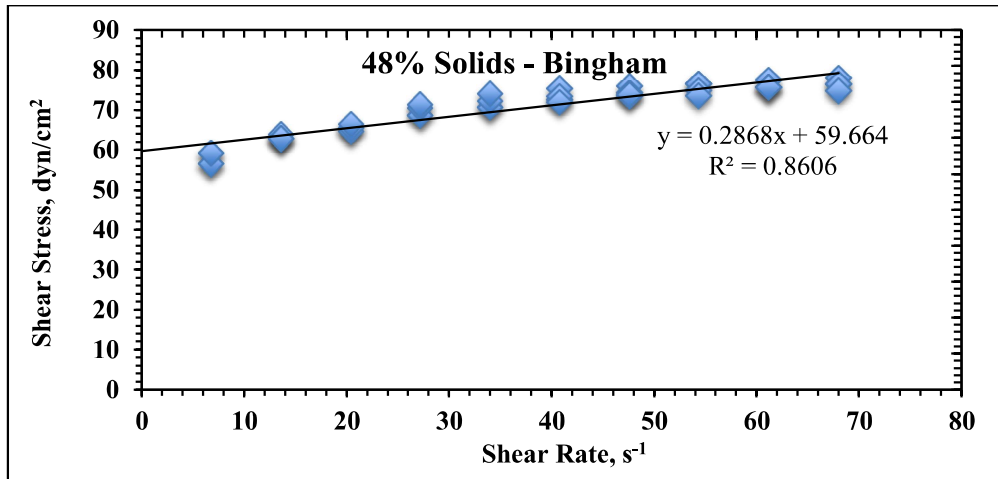


Figure 5.11 The plot of shear rate vs shear stress of clayey vein tailings sample including 48% solids by weight based on Bingham rheological model

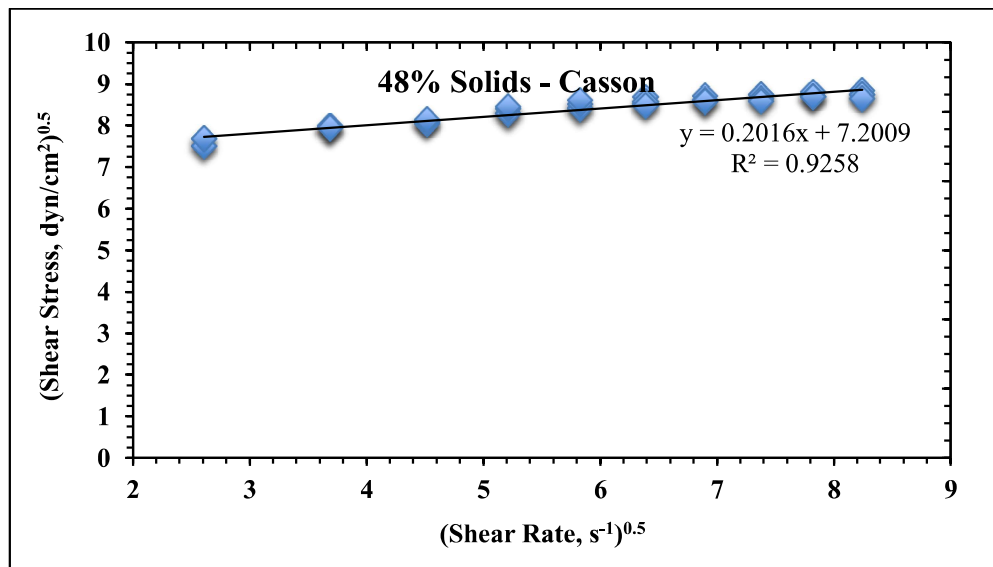


Figure 5.12 The plot of shear rate vs shear stress of clayey vein tailings sample including 48% solids by weight based on Casson rheological model

The rheograms of ore tailings samples with higher clayey content including 51% solids by weight are presented in Figure 5.13 and Figure 5.14. The rheograms were evaluated based on “Bingham” and “Casson” rheological models. In this respect, yield stress of the samples including 51% solids by weight based on Bingham model is 77.80 dyn/cm², and 66.54 dyn/cm² for Casson model.

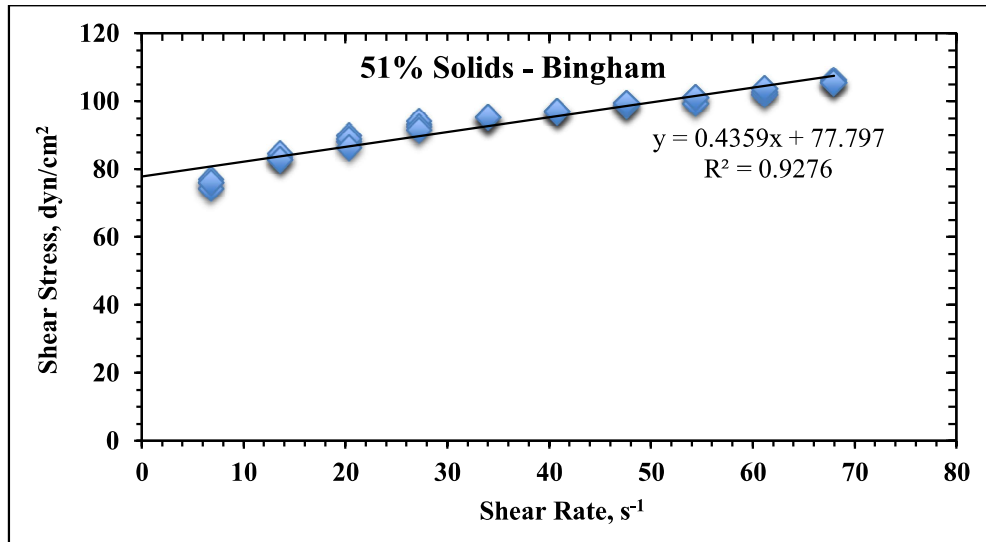


Figure 5.13 The plot of shear rate vs shear stress of clayey vein tailings sample including 51% solids by weight based on Bingham rheological model

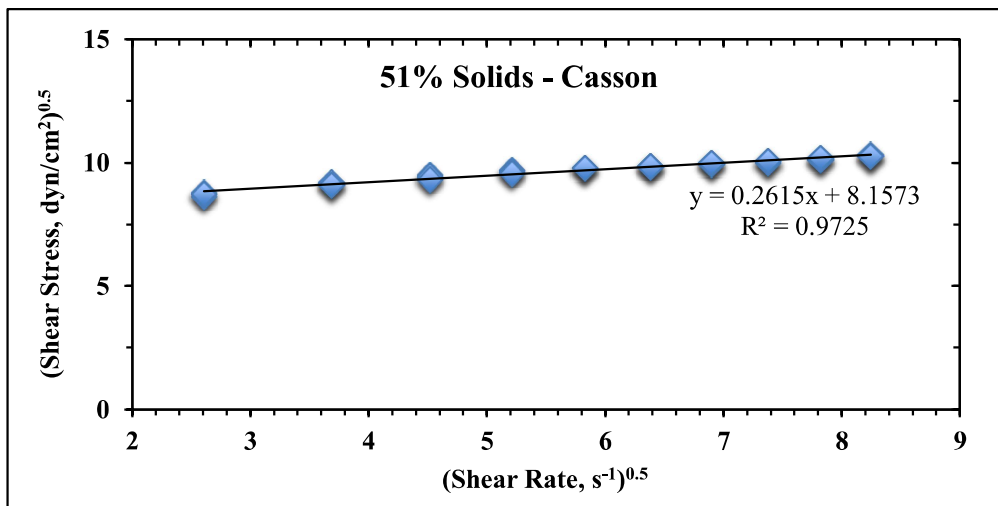


Figure 5.14 The plot of shear rate vs shear stress of clayey vein tailings sample including 51% solids by weight based on Casson rheological model

The rheograms of ore tailings samples with higher clayey content including 54% solids by weight are presented in Figure 5.15 and Figure 5.16. The rheograms were evaluated based on “Bingham” and “Casson” rheological models. In this respect, yield stress of the samples including 54% solids by weight based on Bingham model is 121.00 dyn/cm², and 95.34 dyn/cm² for Casson model.

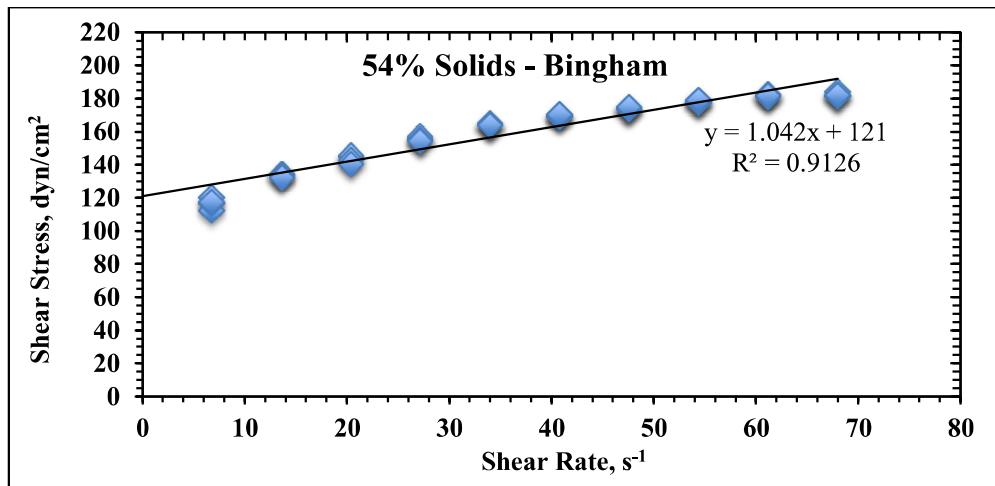


Figure 5.15 The plot of shear rate vs shear stress of clayey vein tailings sample including 54% solids by weight based on Bingham rheological model

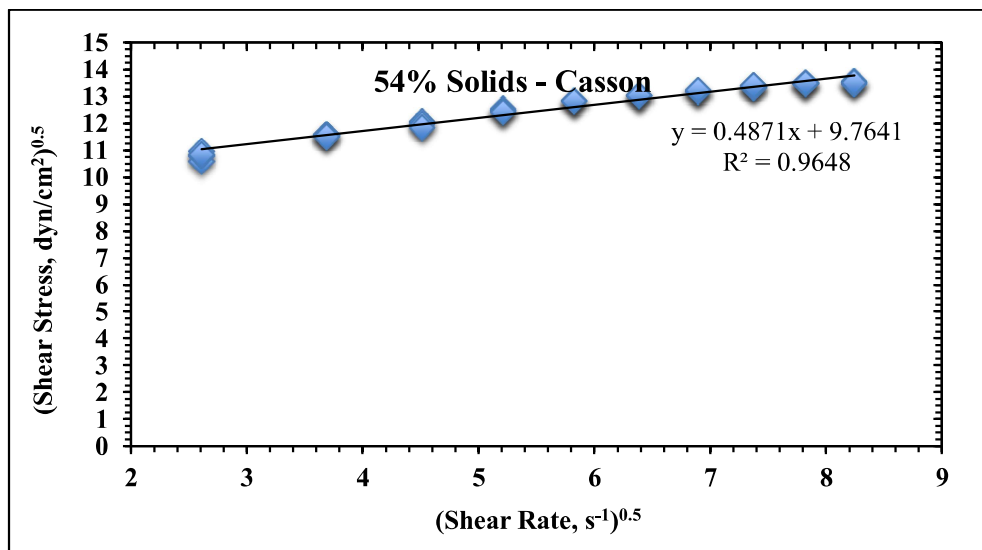


Figure 5.16 The plot of shear rate vs shear stress of clayey vein tailings sample including 54% solids by weight based on Casson rheological model

The rheograms of ore tailings samples with higher clayey content including 57% solids by weight are presented in Figure 5.17 and Figure 5.18. The rheograms were evaluated based on “Bingham” and “Casson” rheological models. In this respect, yield stress of the samples including 57% solids by weight based on Bingham model is 186.30 dyn/cm², and 167.13 dyn/cm² for Casson model.

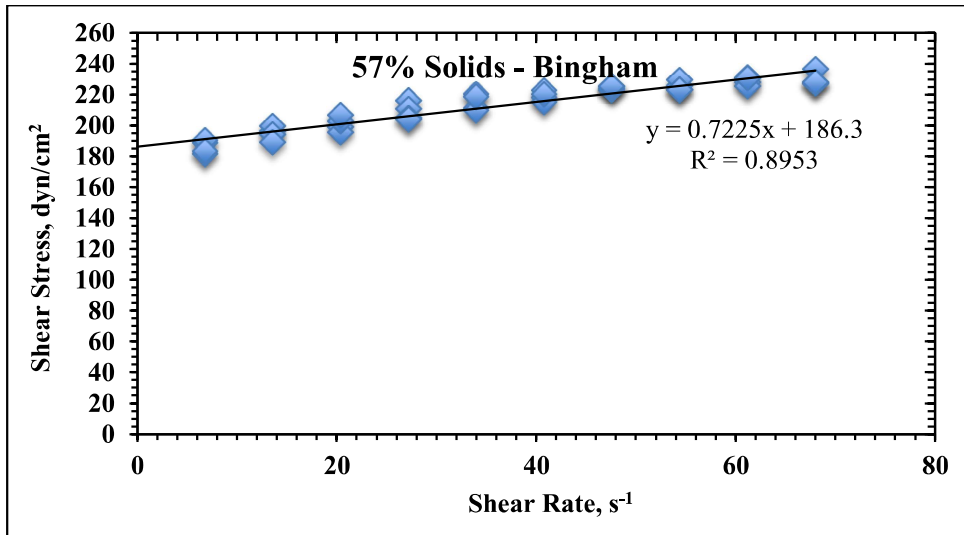


Figure 5.17 The plot of shear rate vs shear stress of clayey vein tailings sample including 57% solids by weight based on Bingham rheological model

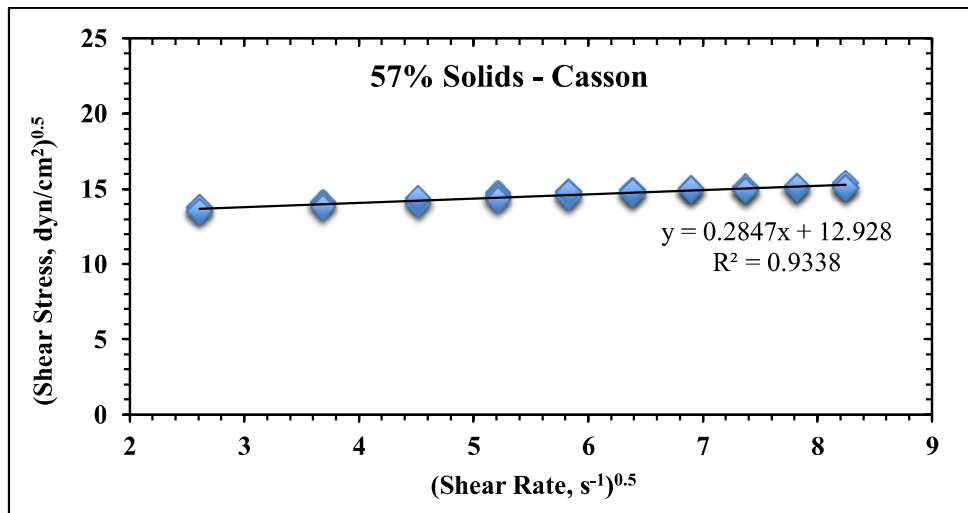


Figure 5.18 The plot of shear rate vs shear stress of clayey vein tailings sample including 57% solids by weight based on Casson rheological model

The rheograms of ore tailings samples with higher clayey content including 60% solids by weight are presented in Figure 5.19 and Figure 5.20. The rheograms were evaluated based on “Bingham” and “Casson” rheological models. In this respect, yield stress of the samples including 60% solids by weight based on Bingham model is 301.80 dyn/cm², and 260.24 dyn/cm² for Casson model.

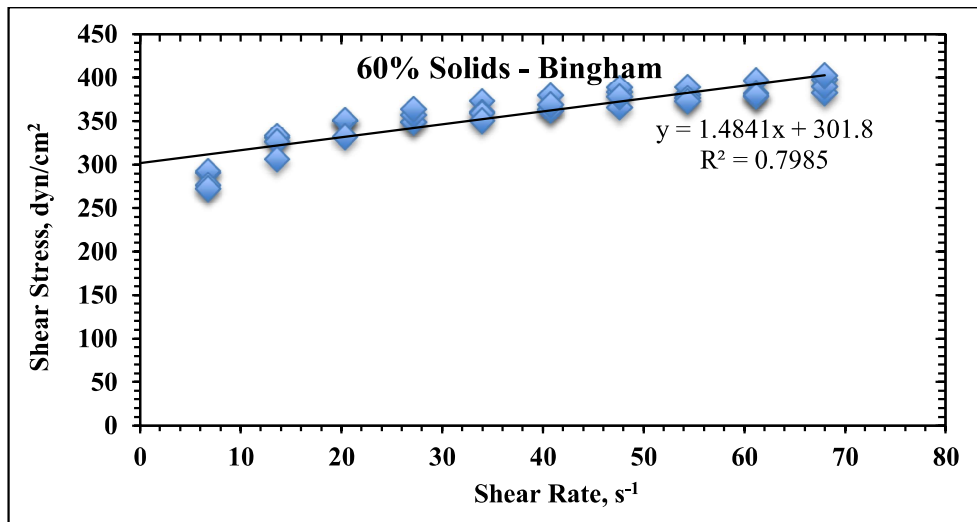


Figure 5.19 The plot of shear rate vs shear stress of clayey vein tailings sample including 60% solids by weight based on Bingham rheological model

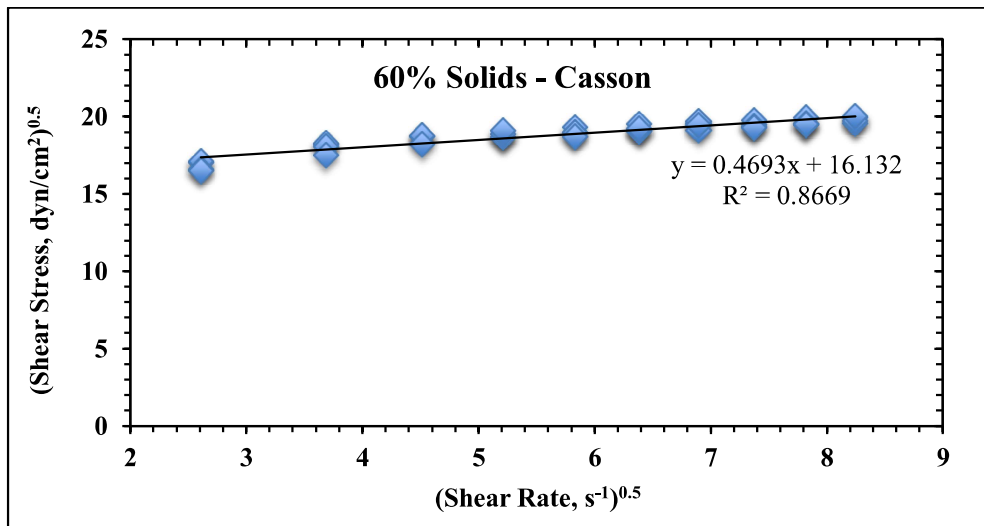


Figure 5.20 The plot of shear rate vs shear stress of clayey vein tailings sample including 60% solids by weight based on Casson rheological model

The rheograms of ore tailings samples with higher clayey content including 65% solids by weight are presented in Figure 5.21 and Figure 5.22. The rheograms were evaluated based on “Bingham” and “Casson” rheological models. In this respect, yield stress of the samples including 65% solids by weight based on Bingham model is 432.02 dyn/cm², and 288.15 dyn/cm² for Casson model.

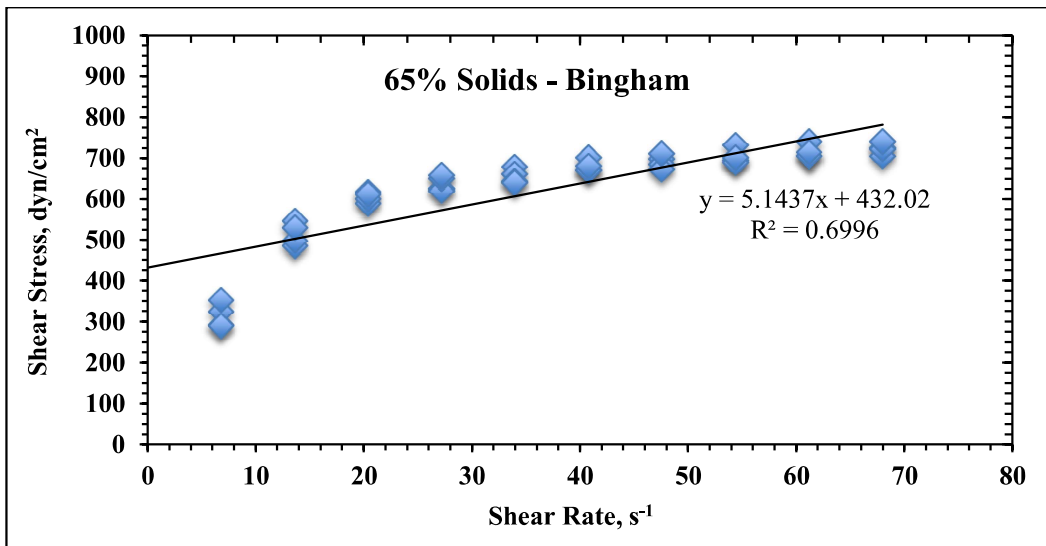


Figure 5.21 The plot of shear rate vs shear stress of clayey vein tailings sample including 65% solids by weight based on Bingham rheological model

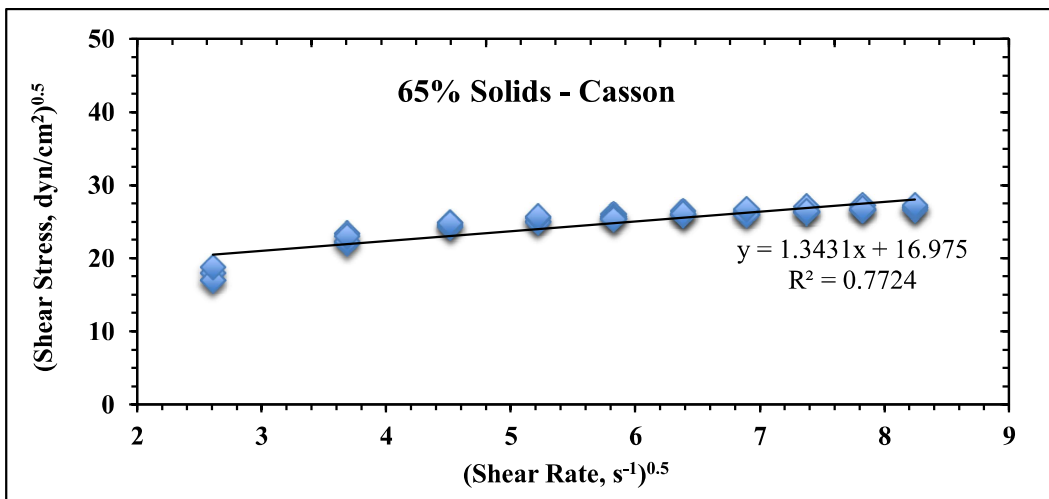


Figure 5.22 The plot of shear rate vs shear stress of clayey vein tailings sample including 65% solids by weight based on Casson rheological model

The rheograms of ore tailings samples with higher clayey content including 70% solids by weight are presented in Figure 5.23 and Figure 5.24. The rheograms were evaluated based on “Bingham” and “Casson” rheological models. In this respect, yield stress of the samples including 70% solids by weight based on Bingham model is 555.09 dyn/cm², and 391.68 dyn/cm² for Casson model.

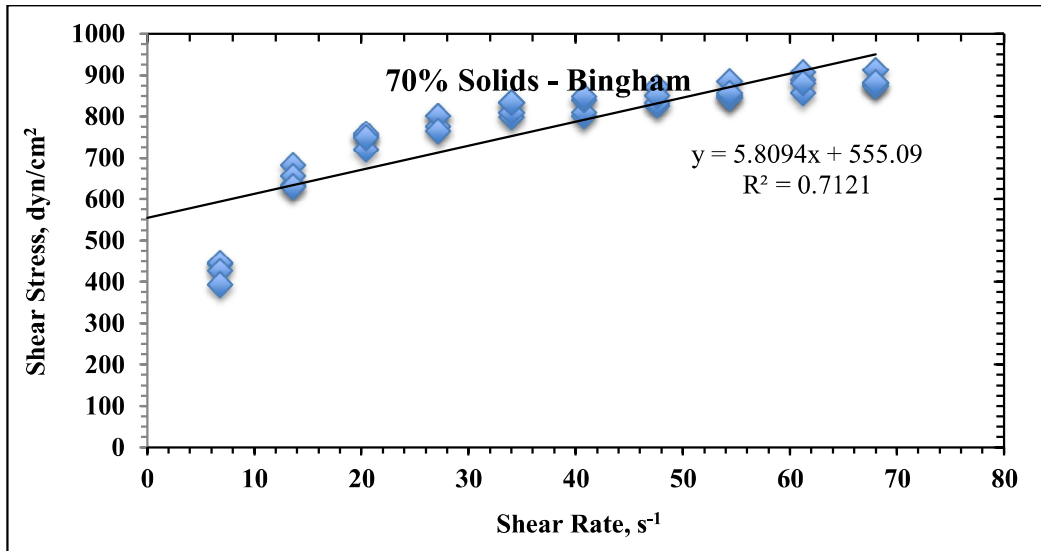


Figure 5.23 The plot of shear rate vs shear stress of clayey vein tailings sample including 70% solids by weight based on Bingham rheological model

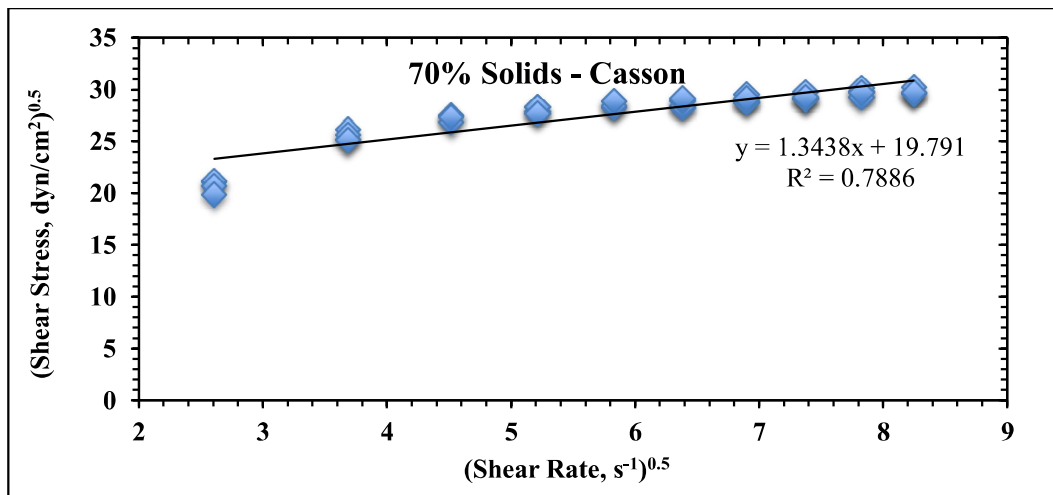


Figure 5.24 The plot of shear rate vs shear stress of clayey vein tailings sample including 70% solids by weight based on Casson rheological model

5.4.2 Yield Stress of Normal Vein Tailings Samples

The rheograms of ore tailings samples with less clayey content including 35% solids by weight are presented in Figure 5.25 and Figure 5.26. The rheograms were evaluated based on “Bingham” and “Casson” rheological models. In this respect, yield stress of the samples including 35% solids by weight based on Bingham model is 10.77 dyn/cm², and 9.73 dyn/cm² for Casson model.

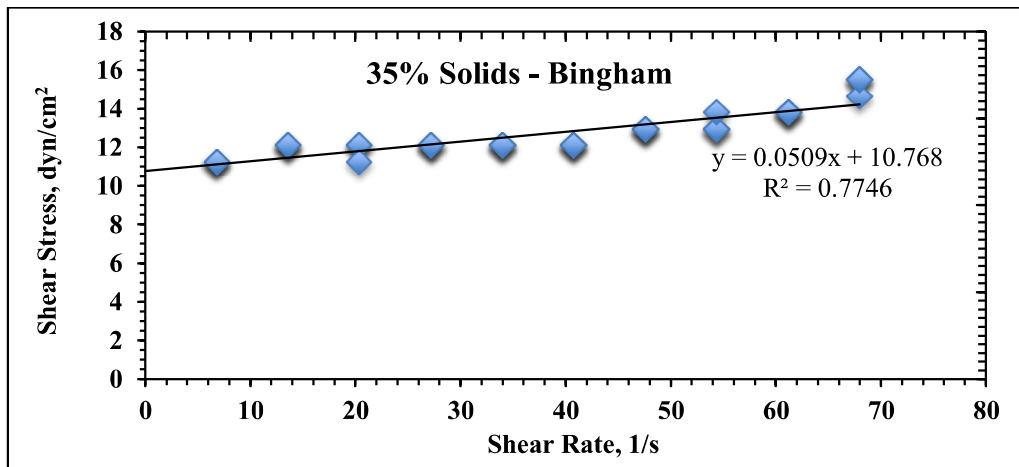


Figure 5.25 The plot of shear rate vs shear stress of normal vein tailings sample including 35% solids by weight based on Bingham rheological model

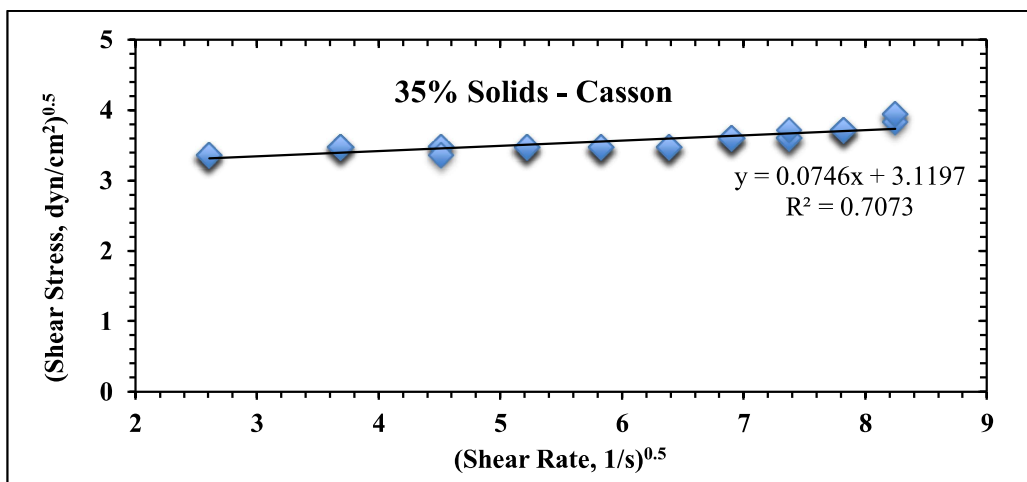


Figure 5.26 The plot of shear rate vs shear stress of normal vein tailings sample including 35% solids by weight based on Casson rheological model

The rheograms of ore tailings samples with less clayey content including 40% solids by weight are presented in Figure 5.27 and Figure 5.28. The rheograms were evaluated based on “Bingham” and “Casson” rheological models. In this respect, yield stress of the samples including 40% solids by weight based on Bingham model is 13.67 dyn/cm², and 11.74 dyn/cm² for Casson model.

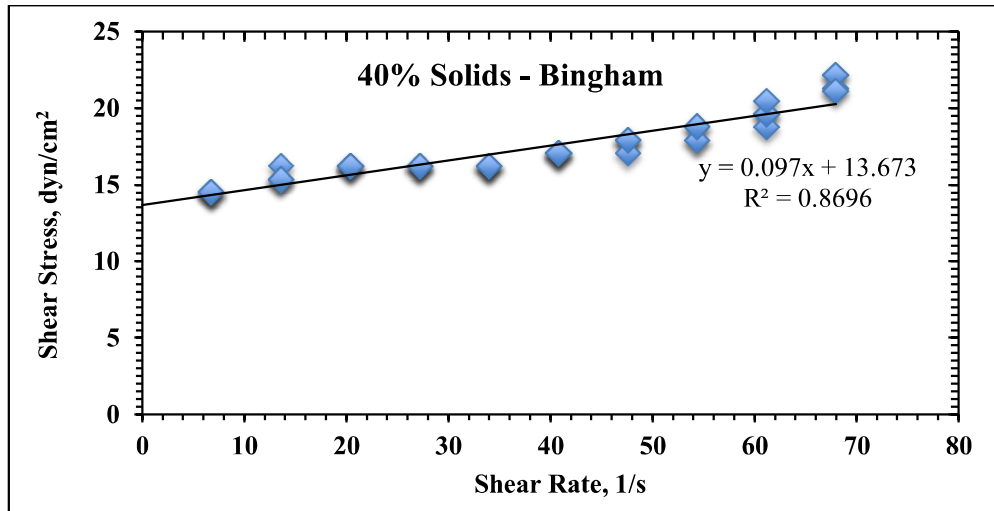


Figure 5.27 The plot of shear rate vs shear stress of normal vein tailings sample including 40% solids by weight based on Bingham rheological model

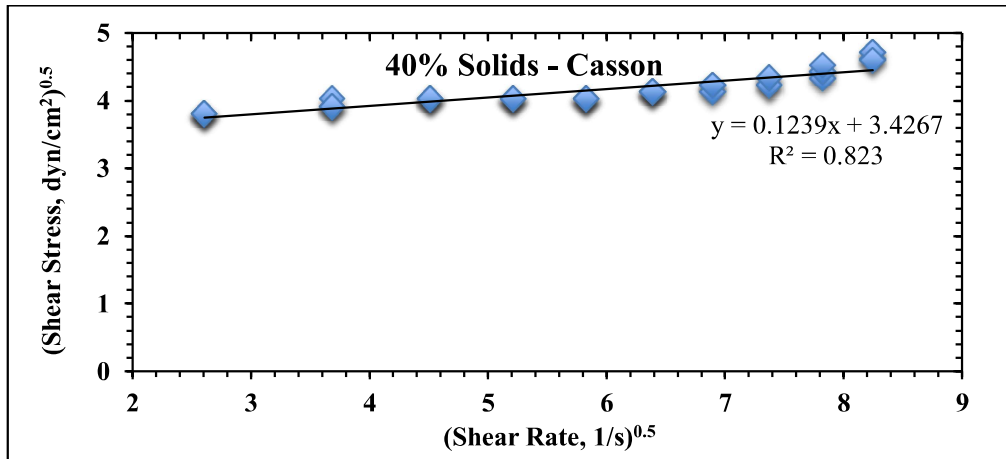


Figure 5.28 The plot of shear rate vs shear stress of normal vein tailings sample including 40% solids by weight based on Casson rheological model

The rheograms of ore tailings samples with less clayey content including 45% solids by weight are presented in Figure 5.29 and Figure 5.30. The rheograms were evaluated based on “Bingham” and “Casson” rheological models. In this respect, yield stress of the samples including 45% solids by weight based on Bingham model is 20.48 dyn/cm², and 18.64 dyn/cm² for Casson model.

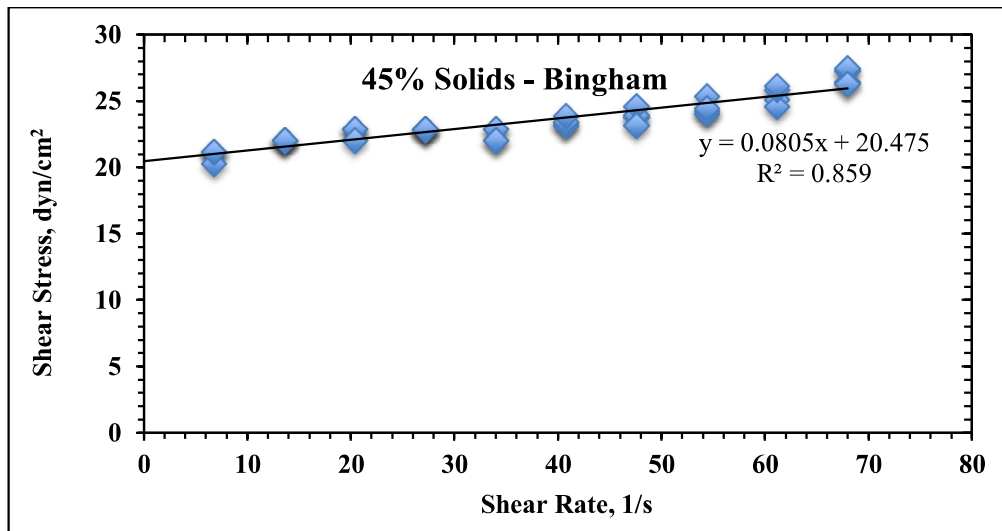


Figure 5.29 The plot of shear rate vs shear stress of normal vein tailings sample including 45% solids by weight based on Bingham rheological model

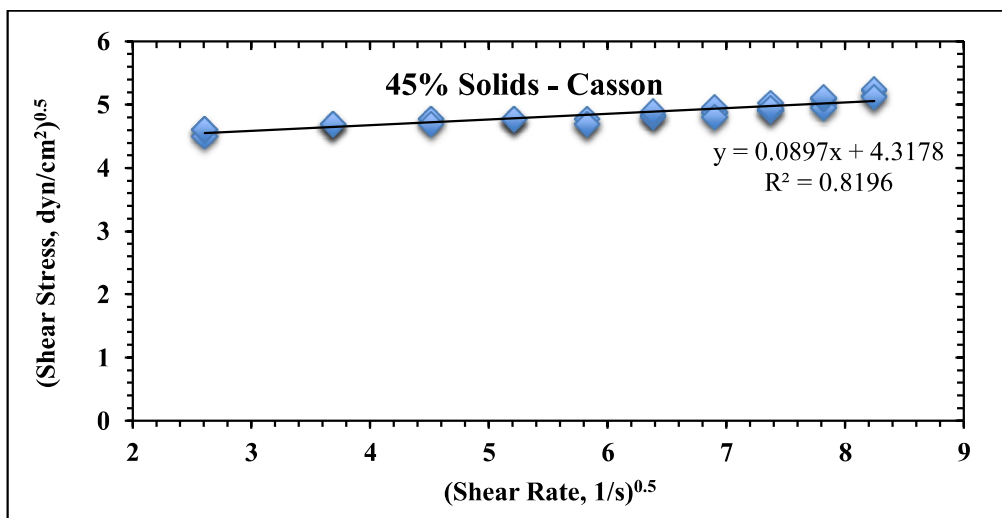


Figure 5.30 The plot of shear rate vs shear stress of normal vein tailings sample including 45% solids by weight based on Casson rheological model

The rheograms of ore tailings samples with less clayey content including 48% solids by weight are presented in Figure 5.31 and Figure 5.32. The rheograms were evaluated based on “Bingham” and “Casson” rheological models. In this respect, yield stress of the samples including 48% solids by weight based on Bingham model is 30.16 dyn/cm², and 27.98 dyn/cm² for Casson model.

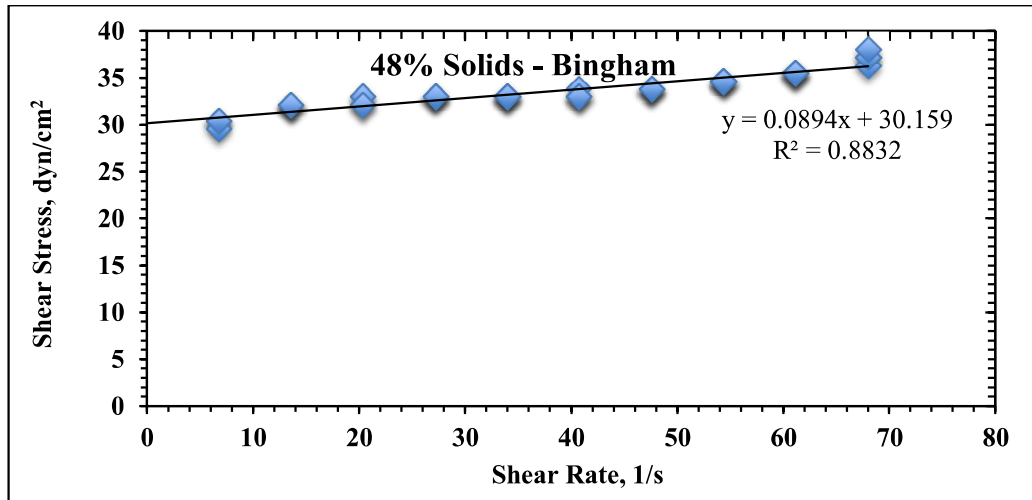


Figure 5.31 The plot of shear rate vs shear stress of normal vein tailings sample including 48% solids by weight based on Bingham rheological model

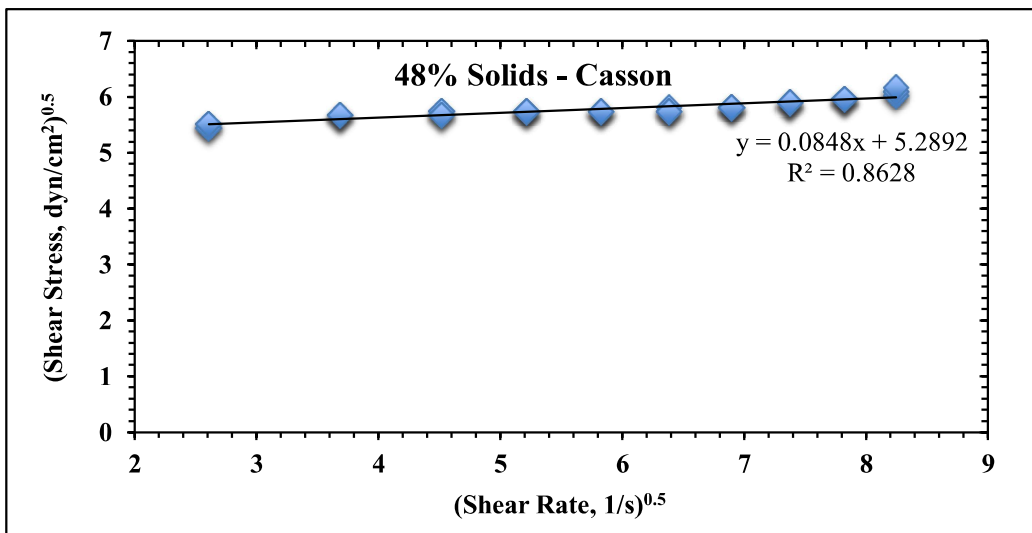


Figure 5.32 The plot of shear rate vs shear stress of normal vein tailings sample including 48% solids by weight based on Casson rheological model

The rheograms of ore tailings samples with less clayey content including 51% solids by weight are presented in Figure 5.33 and Figure 5.34. The rheograms were evaluated based on “Bingham” and “Casson” rheological models. In this respect, yield stress of the samples including 51% solids by weight based on Bingham model is 40.42 dyn/cm², and 36.10 dyn/cm² for Casson model.

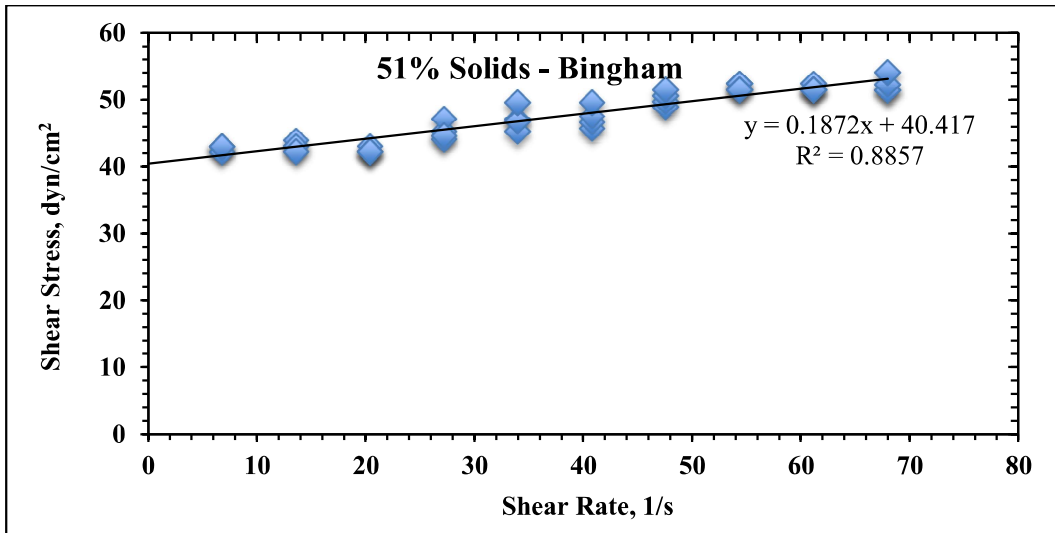


Figure 5.33 The plot of shear rate vs shear stress of normal vein tailings sample including 51% solids by weight based on Bingham rheological model

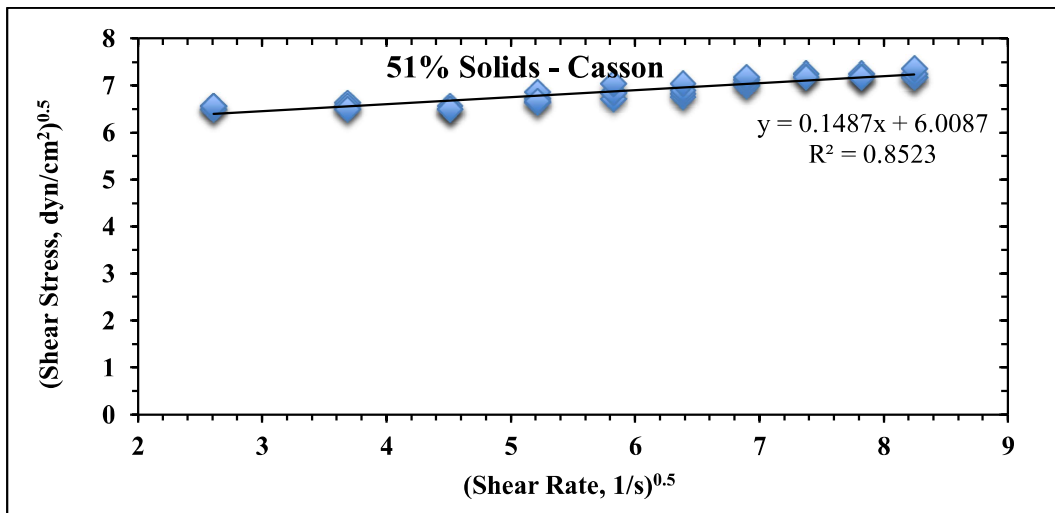


Figure 5.34 The plot of shear rate vs shear stress of normal vein tailings sample including 51% solids by weight based on Casson rheological model

The rheograms of ore tailings samples with less clayey content including 54% solids by weight are presented in Figure 5.35 and Figure 5.36. The rheograms were evaluated based on “Bingham” and “Casson” rheological models. In this respect, yield stress of the samples including 54% solids by weight based on Bingham model is 65.73 dyn/cm², and 60.73 dyn/cm² for Casson model.

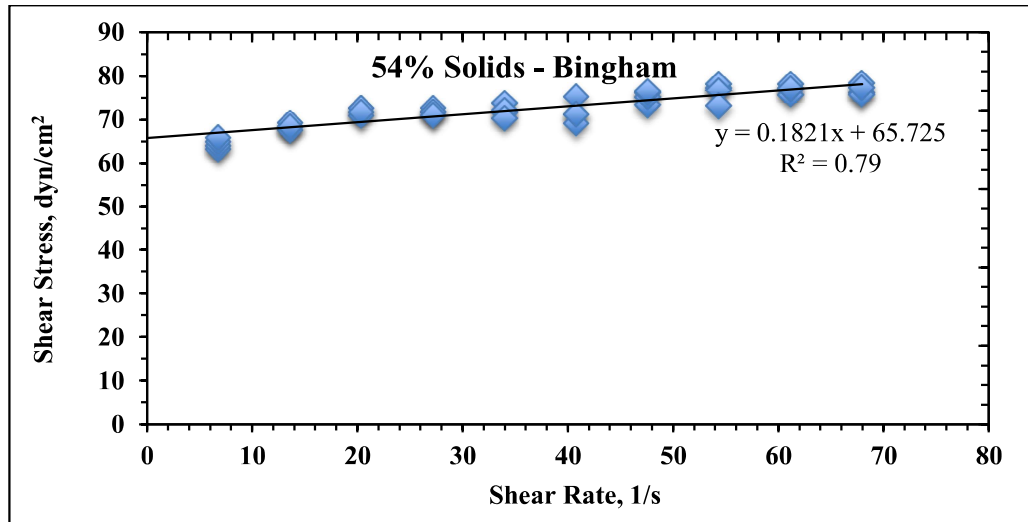


Figure 5.35 The plot of shear rate vs shear stress of normal vein tailings sample including 54% solids by weight based on Bingham rheological model

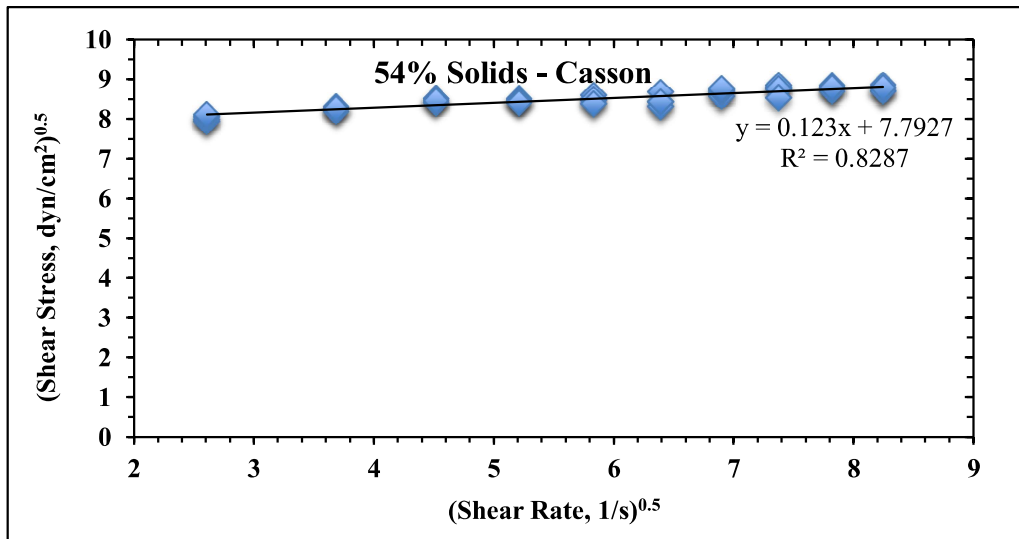


Figure 5.36 The plot of shear rate vs shear stress of normal vein tailings sample including 54% solids by weight based on Casson rheological model

The rheograms of ore tailings samples with less clayey content including 57% solids by weight are presented in Figure 5.37 and Figure 5.38. The rheograms were evaluated based on “Bingham” and “Casson” rheological models. In this respect, yield stress of the samples including 57% solids by weight based on Bingham model is 96.79 dyn/cm², and 93.32 dyn/cm² for Casson model.

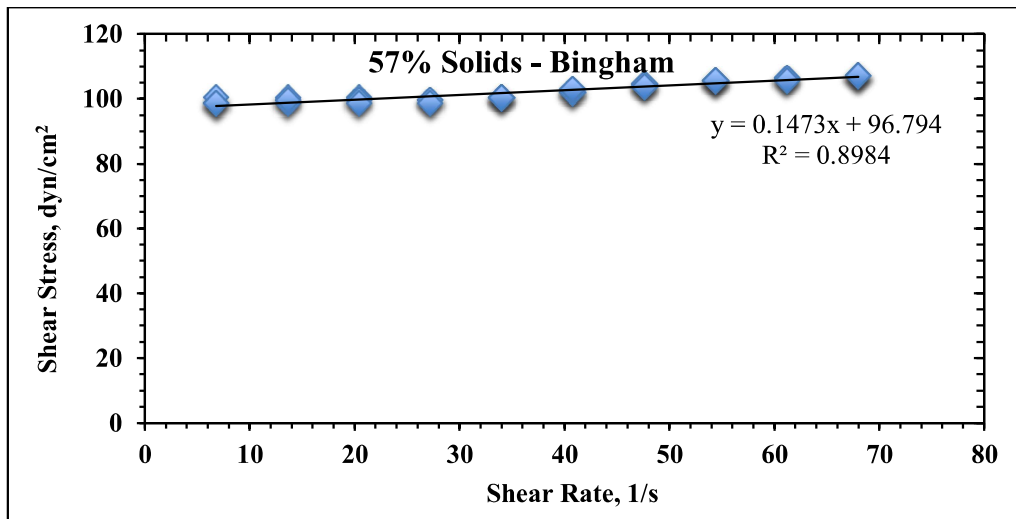


Figure 5.37 The plot of shear rate vs shear stress of normal vein tailings sample including 57% solids by weight based on Bingham rheological model

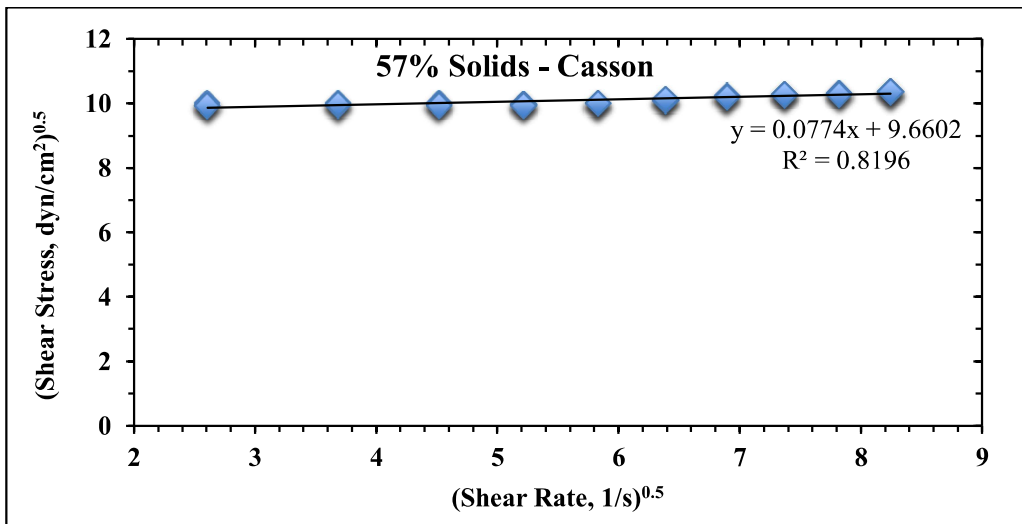


Figure 5.38 The plot of shear rate vs shear stress of normal vein tailings sample including 57% solids by weight based on Casson rheological model

The rheograms of ore tailings samples with less clayey content including 60% solids by weight are presented in Figure 5.39 and Figure 5.40. The rheograms were evaluated based on “Bingham” and “Casson” rheological models. In this respect, yield stress of the samples including 60% solids by weight based on Bingham model is 140.53 dyn/cm², and 123.88 dyn/cm² for Casson model.

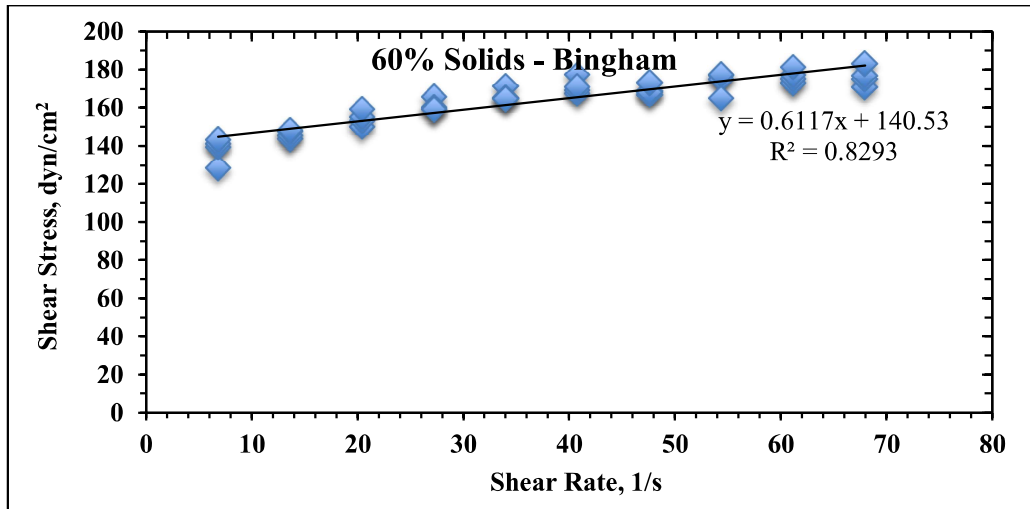


Figure 5.39 The plot of shear rate vs shear stress of normal vein tailings sample including 60% solids by weight based on Bingham rheological model

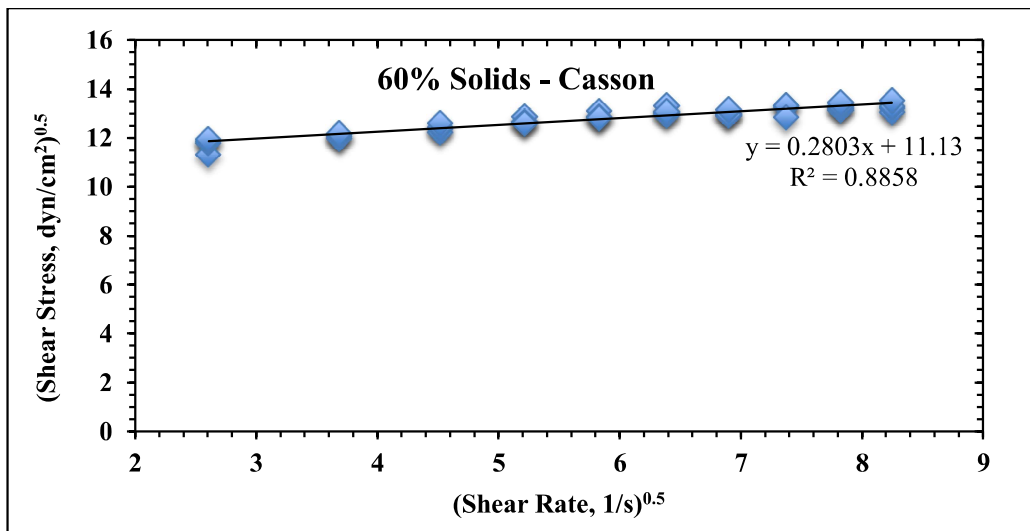


Figure 5.40 The plot of shear rate vs shear stress of normal vein tailings sample including 60% solids by weight based on Casson rheological model

The rheograms of ore tailings samples with less clayey content including 65% solids by weight are presented in Figure 5.41 and Figure 5.42. The rheograms were evaluated based on “Bingham” and “Casson” rheological models. In this respect, yield stress of the samples including 65% solids by weight based on Bingham model is 241.29 dyn/cm², and 192.54 dyn/cm² for Casson model.

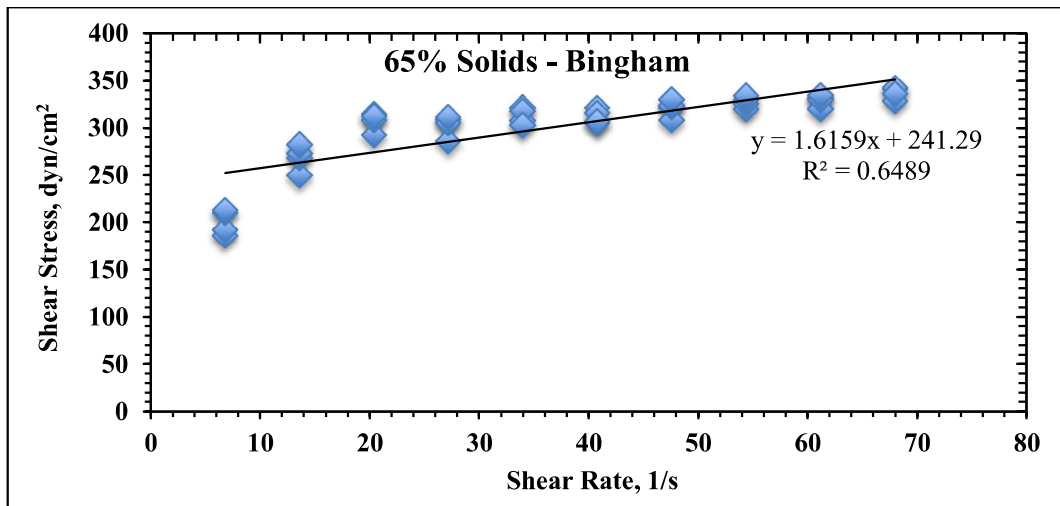


Figure 5.41 The plot of shear rate vs shear stress of normal vein tailings sample including 65% solids by weight based on Bingham rheological model

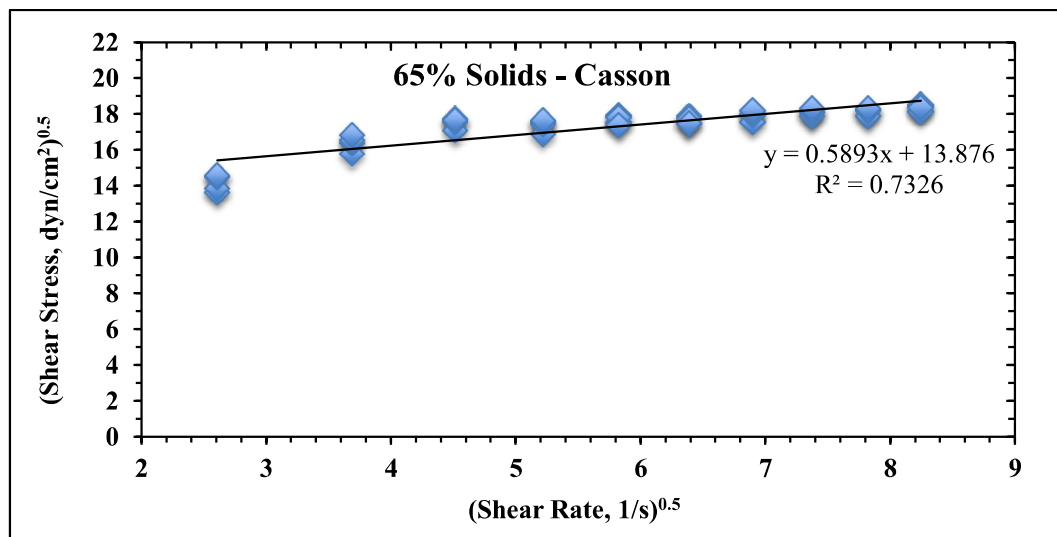


Figure 5.42 T The plot of shear rate vs shear stress of normal vein tailings sample including 65% solids by weight based on Casson rheological model

The rheograms of ore tailings samples with less clayey content including 70% solids by weight are presented in Figure 5.43 and Figure 5.44. The rheograms were evaluated based on “Bingham” and “Casson” rheological models. In this respect, yield stress of the samples including 70% solids by weight based on Bingham model is 385.26 dyn/cm², and 229.64 dyn/cm² for Casson model.

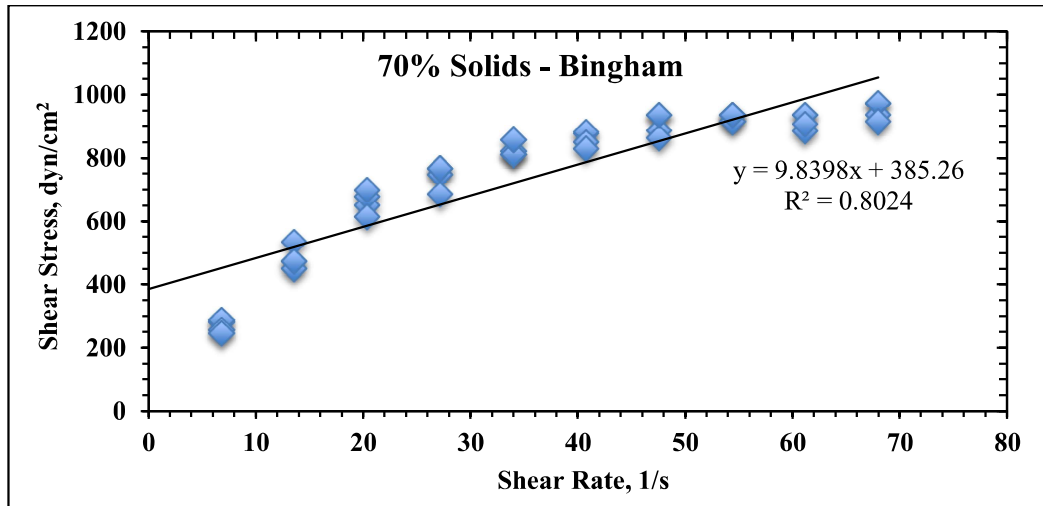


Figure 5.43 The plot of shear rate vs shear stress of normal vein tailings sample including 70% solids by weight based on Bingham rheological model

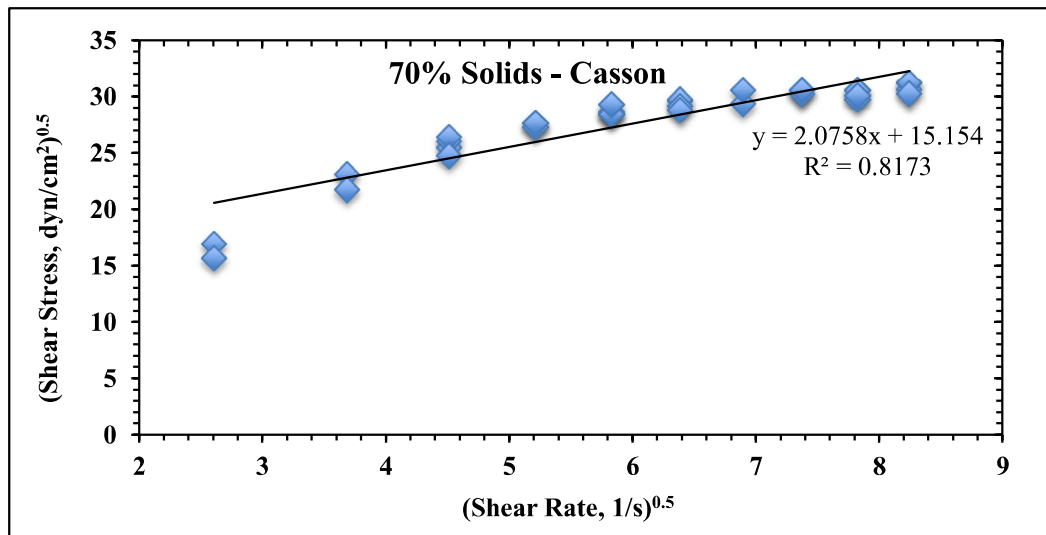


Figure 5.44 The plot of shear rate vs shear stress of normal vein tailings sample including 70% solids by weight based on Casson rheological model

As a result of the measurements, yield stress of ore tailings samples from different veins of the same deposit and obtained from thickener underflow are given in Table 5.1. Also, the changes in yield stress values depending on the solid content of clayey vein tailings and normal vein tailings based on Bingham and Casson rheological models are given in Figure 5.45 and Figure 5.46, respectively.

Table 5.1 Yield stress values depending on solid contents of clayey and normal vein tailings samples obtained from thickener underflow

Solid Content (by wt. %)	Clayey tailings sample		Normal tailings sample	
	Yield Stress (dyn/cm ²)		Yield Stress (dyn/cm ²)	
	Bingham Plastic Model	Casson Model	Bingham Plastic Model	Casson Model
35	15.10	12.54	10.77	9.73
40	22.71	19.27	13.67	11.74
45	35.20	30.48	20.48	18.64
48	59.66	51.85	30.16	27.98
51	77.80	66.54	40.42	36.10
54	121.00	95.34	65.73	60.73
57	186.30	167.13	96.79	93.32
60	301.80	260.24	140.53	123.88
65	432.02	288.15	241.29	192.54
70	555.09	391.68	385.26	229.64

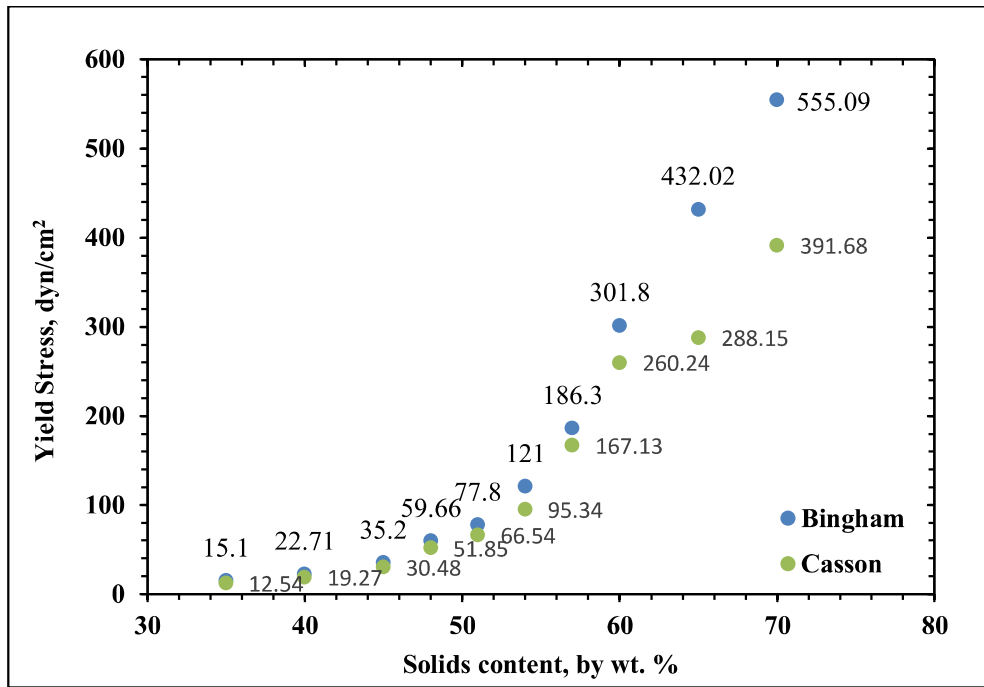


Figure 5.45 The changes in yield stress values depending on the solid content of clayey vein tailings based on Bingham and Casson models

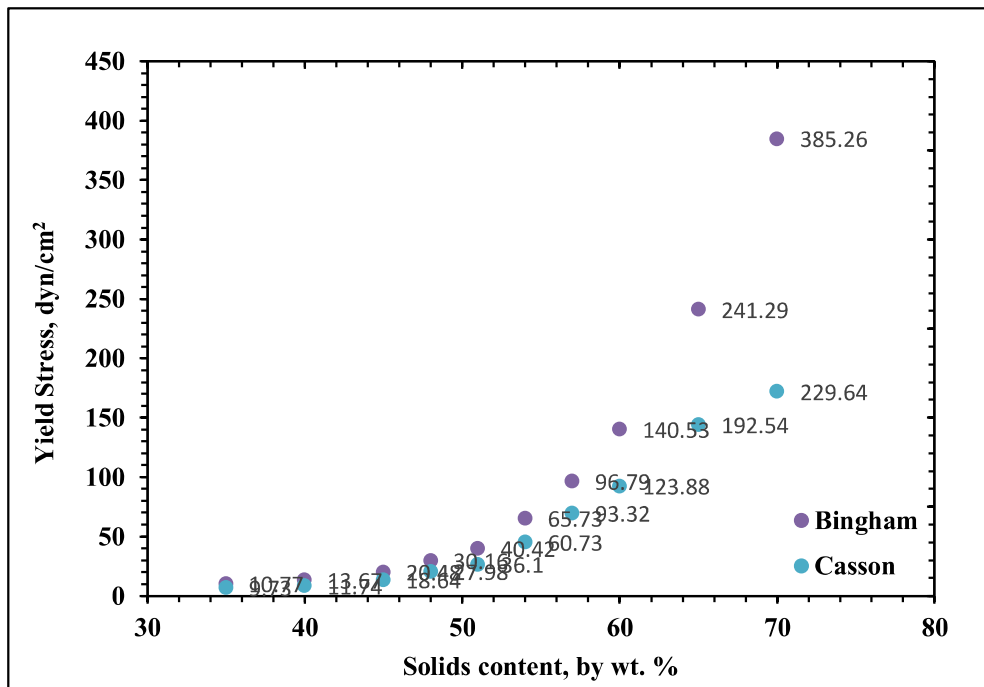


Figure 5.46 The changes in yield stress values depending on the solid content of normal vein tailings based on Bingham and Casson models

Based on the obtained results, the behavior of yield stress is similar for Bingham and Casson model in both tailings samples. The solid content and yield stress relationship obtained in these models confirms each other. In the case of both tailings samples, it was observed that yield stress tends to increase significantly while solid content is increased especially from 54% by weight in Bingham and Casson model. The behavior also shows that there is an exponential relationship between yield stress and solid content. In the case of ore tailings sample with higher clay content, yield stress values obtained by Bingham and Casson models up to 51% solid content are close to each other. As the solid content rises above 51%, the difference between yield stress values increases in both models. On the other hand, yield stress values obtained by both models are close each other up to 57% solid content in the case of ore tailings samples with less clay content, however, the difference between yield stress values rises when solid content is above 57%. In the light of yield stress values, it can be observed that 51% and 57% solid content by weight is a critical point for the tailings samples with higher clay mineral content, and with less clay mineral content, respectively. The increase in solid content above this value causes difficulty to initiate flow. The results show that yield stress values of the clayey and normal vein tailings samples are quite different when compared (Table 5.1). It was revealed that the mineralogical characteristics of clayey vein tailings samples cause higher yield stress values at each solid content condition. In some solid content conditions, it was observed that yield stress values of clayey vein samples are two times higher than normal vein samples. The XRD pattern of the clayey tailings sample shown in Figure 4.9 verified the existence of illite, muscovite and montmorillonite as clay minerals. Furthermore, the surface charge properties of the mentioned clay minerals were discussed in Section 5.1 individually. It was concluded that the contribution of overall positive surface charge of montmorillonite, the overall negative surface charge of illite and muscovite to clayey tailings sample in the test pH resulted in the relatively lower values of surface charges as discussed in Section 5.3, which are prone to interparticle interactions and agglomeration in suspensions. As a result, this resulted in higher yield stress values in clayey suspensions as indicated.

5.4.3 Viscosity of Ore Tailings Samples

Ore tailings samples having different mineralization characteristics and different solid contents were studied to determine viscosity values. The plots of viscosity versus time of these samples are given in Figure 5.47-5.50. It was observed from the graphs that relative viscosity of the samples become constant after 800 seconds of the experiments. The relative viscosity values of the samples are given in Table 5.2.

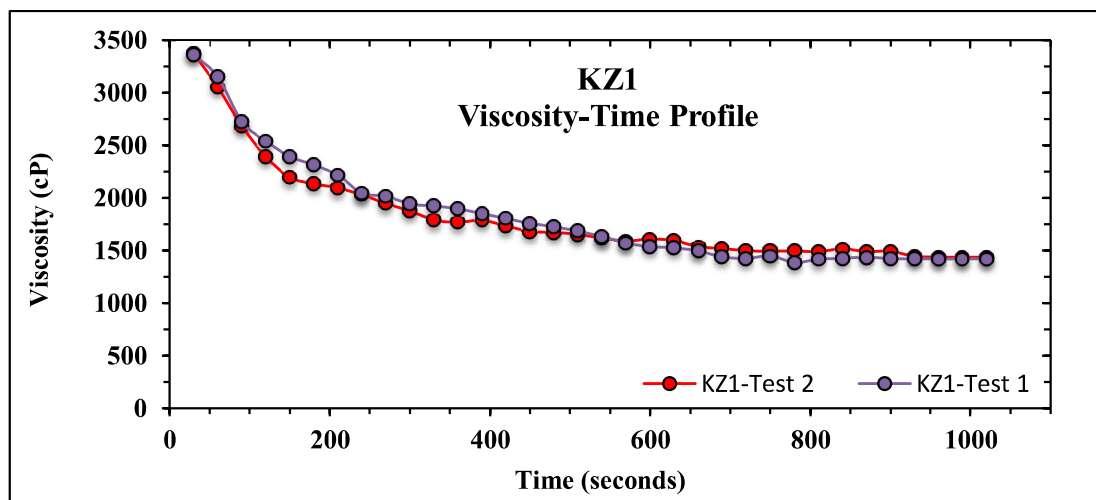


Figure 5.47 Viscosity-time graph of tailings sample having higher extent of clay with 65.58% solids by wt. – Test 1 and Test 2

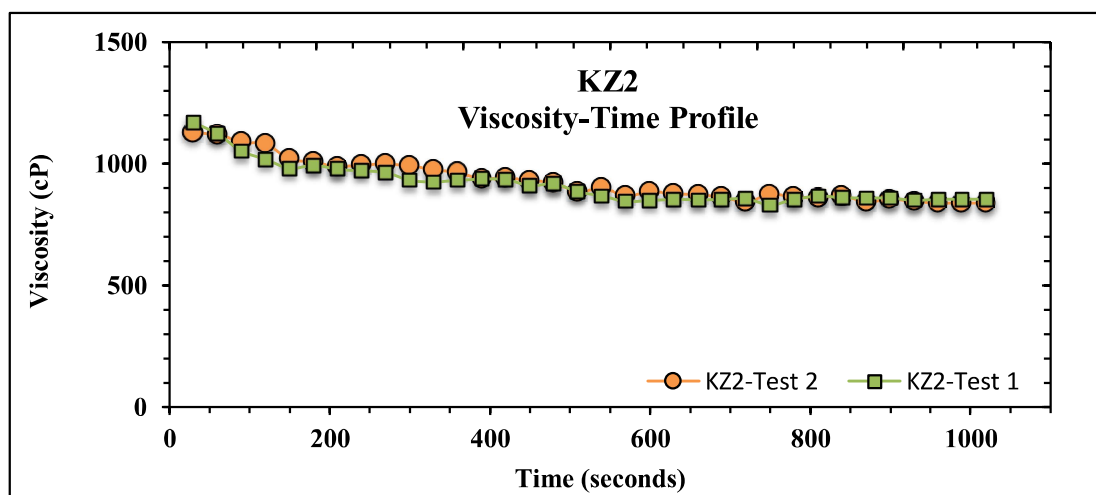


Figure 5.48 Viscosity-time graph of tailings sample having higher extent of clay with 54.60% solids by wt. – Test 1 and Test 2

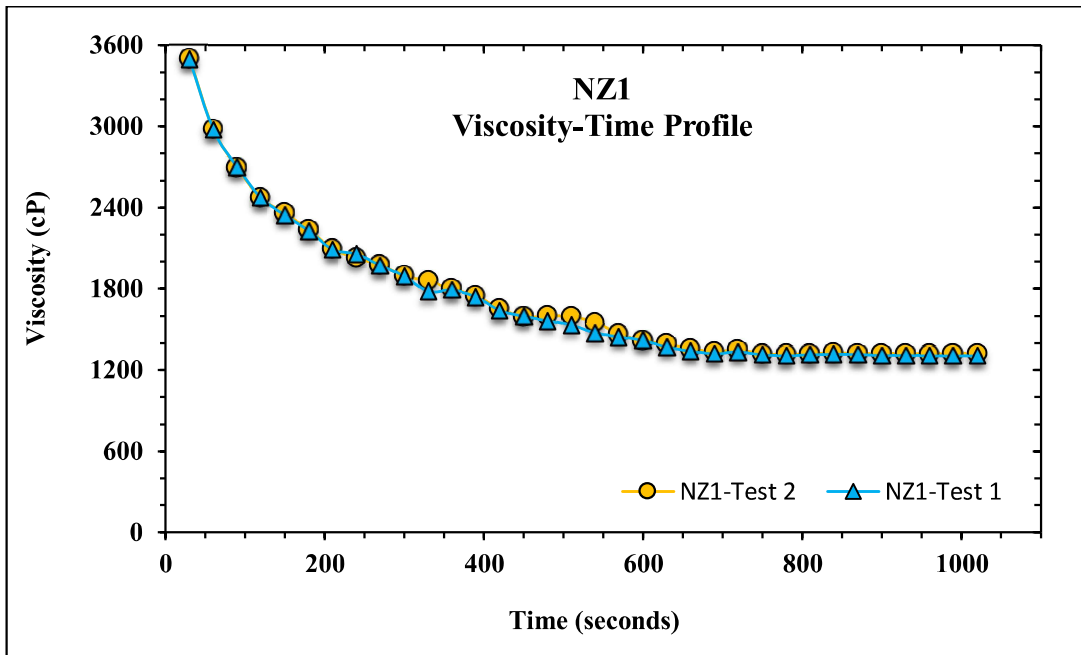


Figure 5.49 Viscosity-time graph of tailings sample having less extent of clay with 65.36% solids by wt. – Test 1 and Test 2

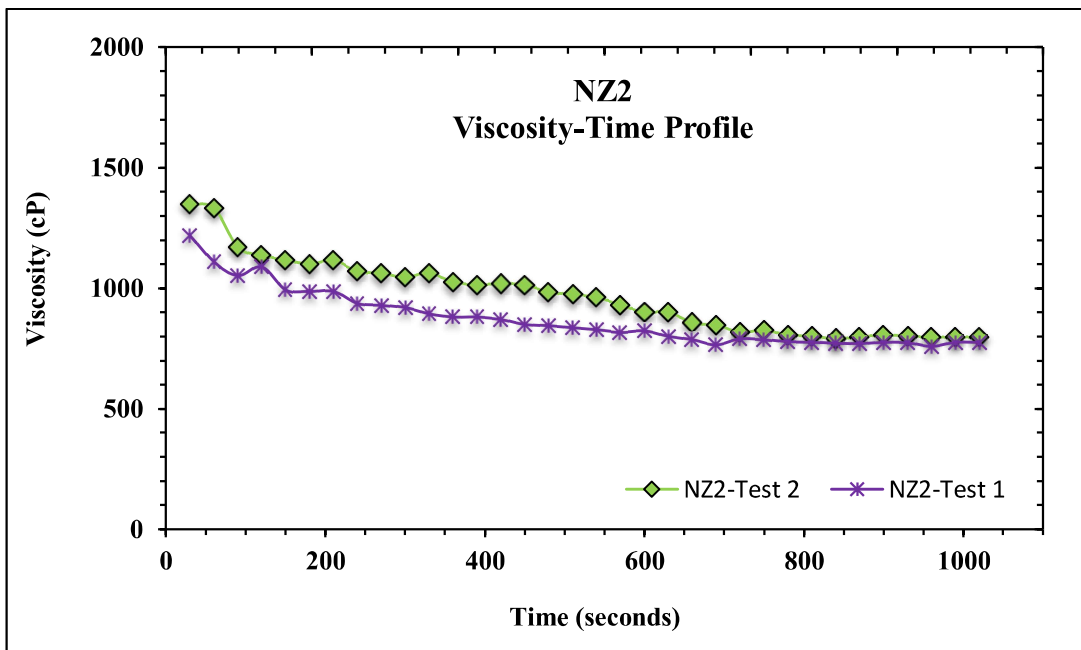


Figure 5.50 Viscosity-time graph of tailings sample having less extent of clay with 54.43% solids by wt. – Test 1 and Test 2

Table 5.2 Relative viscosity values of ore tailings samples with higher and less extent of clay minerals

	NZ1	NZ2	KZ1	KZ2
Samples	(65.36% solids)	(54.43% solids)	(65.58% solids)	(54.60% solids)
Test 1, Viscosity (cP)	1305	776	1420	854
Test 2, Viscosity (cP)	1322	798	1438	839
Average viscosity (cP)	1314	787	1429	847

The results show that viscosity of both ore tailings samples tend to decrease as a function of time as illustrated in Figure 5.47-5.50. The decrease in the viscosity continues until approximately 800 seconds for both tailings samples, and it reaches a constant value (as given in Table 5.2). The decrease in viscosity as a function of time can be explained by thixotropic behavior showed by the gold ore tailings samples obtained by thickener underflow.

In the light of the results in Table 5.2, the tailings samples obtained by clayey vein having 54.60% solids by weight (KZ2) were examined, and average viscosity was found as 847 cP. When solid content is increased from 54.60% to 65.58% by wt as in sample KZ1, there was a significant increase in average viscosity from 847 cP to 1429 cP. This shows that the increase in the solid content affects the flow behavior of clayey suspensions negatively. In the case of the tailings samples obtained by normal vein, average viscosity of NZ2 sample containing 54.43% solids by wt was found as 787 cP. On the other hand, NZ1 sample containing more solid (65.36% by wt) were investigated to obtain average viscosity, and it was found as 1314 cP. As a results, it was observed that the higher solid content significantly increases viscosity of the sample by affecting the flow behavior even if there exist a 11% increase in the solid content.

It is possible to obtain important results when two gold ores from different veins of the same deposit are examined comparatively. Although they have similar solid contents, there are differences between viscosity values. The tailings samples obtained by clayey vein in both solid contents showed higher viscosity values than that of the tailings samples with less extent of clay mineral. In the first group having approximately 54% solids by wt, viscosity of the sample of clayey vein (KZ2) is 847 cP whereas viscosity of the sample of normal vein (NZ2) is 787 cP. However, in the second group having approximately 65% solids by wt, the difference between viscosity values is higher, and the viscosity values are 1314 cP and 1429 cP for the samples of normal vein and clayey vein, respectively (Table 5.2).

The XRD pattern of the clayey tailings sample shown in Figure 4.9 verified the existence of illite, muscovite and montmorillonite as clay minerals. Furthermore, the surface charge properties of the mentioned clay minerals were discussed in Section 5.1 individually. It was concluded that the contribution of overall positive surface charge of montmorillonite, the overall negative surface charge of illite, the overall negative charge of muscovite to clayey tailings sample in the test pH resulted in the relatively lower values of surface charges as discussed in Section 5.3, which are prone to interparticle interactions and agglomeration in suspensions. As a result, this resulted in higher viscosity values in clayey suspensions as indicated.

CHAPTER 6

CONCLUSION AND RECOMMENDATION

Through the study, rheological characteristics of tailings samples from different veins of the same deposit with respect to the ore mineralogy and with special emphasis to the presence of clay minerals was investigated for the backfill purposes of tailings from mineral processing plants. In this context, zeta potential measurements and potentiometric titration measurements were conducted on pure mineral suspensions and gold ore tailings slurries. In addition to surface charge property experiments, the rheological properties of the ore tailings samples with higher and less extent of clay minerals were examined to enable the real simulations of rheological properties of clay minerals in complex multicomponent ore systems where different clay particles locked in valuable mineral particles.

The significant findings were obtained thanks to rheological measurements. First of all, regardless of the vein of the ore tailings samples, the ore tailings samples showed thixotropic behavior. In other words, it was understood that during the transportation of tailings, they continue to flow easily and increasingly until some period of time after initiating the flow, then they reach stable rheological behavior, and they flow with a lower viscosity than they were initiated. Secondly, it was obtained that solid content plays an important role in viscosity regardless of which veins the tailings samples were sourced. Also, it was concluded that the small amount of increase in the solid content cause the significant decrease in the flow by increasing viscosity. Therefore, the detailed analysis of the rheological behavior of ore tailings slurries depending on solid content should be taken into account to prevent possible clogging and collapse in the transportation lines, and the increase in the energy and transportation costs.

In addition to these findings, it was revealed that the mineralogical characteristics have a significant effect on rheological behavior of ore tailings slurries. In this context, the ore tailings sample from clayey vein of the deposit showed higher viscosity than that of normal vein of the same deposit despite of similar solid content. The higher values of surface charges caused the more dispersed state whereas the particles with relatively lower values of surface charges were prone to interparticle interactions and agglomeration in suspensions. As a result, this would result in suspensions of higher viscosity and yield stress than in the dispersed state.

To sum up, this indicates that the transportation of “clayey” tailings is more challenging. Therefore, it becomes more critical to optimize rheological behavior of ore tailings slurries by arranging solid content especially for “clayey” tailings. As a result, mineralogical characteristics of ore tailings s, and the processing conditions are critical for the transportation of the tailings from minerals processing plant for backfill purposes. Therefore, the real simulation and the optimization of the rheological behavior of ore suspensions are of great importance so that the problems encountered during the transportation of tailings can be eliminated, and the desired processing plant conditions with high command can be provided.

In the light of the findings of this thesis, the work conducted in this study should be extended to other clay minerals for broader classification. For a better understanding of the rheological behavior of clay minerals, they should be analysed individually in simple mineral system. In future studies, the influence of clay mineral rheological behavior on parameters different from solid content should be investigated. The mentioned parameters can be pH, particle size, particle shape, and ionic strength.

REFERENCES

- Adamson, A. W., & Gast, A. P. (1997). *Physical chemistry of surfaces* (Sixth). John Wiley & Sons, Inc.
- Alderman, N. J., Meeten, G. H., & Sherwood, J. D. (1991). Vane rheometry of bentonite gels. *Journal of Non-Newtonian Fluid Mechanics*, *39*, 291–310.
- Allagui, A., Benaoum, H., & Olendski, O. (2021). On the Gouy–Chapman–Stern model of the electrical double-layer structure with a generalized Boltzmann factor. *Physica A: Statistical Mechanics and Its Applications*, *582*. <https://doi.org/10.1016/j.physa.2021.126252>
- Barnes, H. A. (1999). The yield stress-a review or 'panta roi'-everything flows? *Journal of Non-Newtonian Fluid Mechanics*, *81*, 133–178.
- Barnes, H. A., Hutton, J. F., & Walters, K. (1989). *An introduction to rheology* (First). Elsevier Science.
- Becker, M., Harris, P. J., Wiese, J. G., & Bradshaw, D. J. (2009). Mineralogical characterisation of naturally floatable gangue in Merensky Reef ore flotation. *International Journal of Mineral Processing*, *93*, 246–255. <https://doi.org/10.1016/j.minpro.2009.10.004>
- Bobicki, E. R., Liu, Q., & Xu, Z. (2014). Effect of microwave pre-treatment on ultramafic nickel ore slurry rheology. *Minerals Engineering*, *61*, 97–104. <https://doi.org/10.1016/j.mineng.2014.03.025>
- Boger, D. v. (2000). Rheology and the minerals industry. *Mineral Processing and Extractive Metallurgy Review*, *20*(1), 1–25.
- Boylu, F., Çinku, K., Esenli, F., & Çelik, M. S. (2010). The separation efficiency of Na-bentonite by hydrocyclone and characterization of

- hydrocyclone products. *International Journal of Mineral Processing*, 94(3–4), 196–202. <https://doi.org/10.1016/j.minpro.2009.12.004>
- Brown, T. J., Idoine, N. E., Raycraft, E. R., Shaw, R. A., Hobbs, S. F., Everett, P., Deady, E. A., & Bide, T. (2018). *World Mineral Production (2012-2016)*.
- Brown, T. J., Idoine, N. E., Wrighton, C. E., Raycraft, E. R., Hobbs, S. F., Shaw, R. A., Everett, P., Deady, E. A., & Kresse, C. (2021). *World Mineral Production (2015-2019)*. British Geological Survey.
- Burdukova, E., Becker, M., Bradshaw, D. J., & Laskowski, J. S. (2007). Presence of negative charge on the basal planes of New York talc. *Journal of Colloid and Interface Science*, 315, 337–342. <https://doi.org/10.1016/j.jcis.2007.06.067>
- Chen, P.-Y. (1977). *Table of Key Lines in X-ray Powder Diffraction Patterns of Minerals in Clays and Associated Rocks*.
- Chryss, A. (2017). Effects of clay in tailings handling and storage. In *Clays in the Minerals Processing Value Chain* (pp. 381–399). Cambridge University Press. <https://doi.org/10.1017/9781316661888.011>
- Concha, F. (2014). Suspension Rheology. In *Solid-Liquid Separation in the Mining Industry* (Vol. 105, pp. 341–372). Springer.
- Cruz, N., Forster, J., & Bobicki, E. R. (2019). Slurry rheology in mineral processing unit operations: A critical review. *The Canadian Journal of Chemical Engineering*, 97(7), 2102–2120.
- Cruz, N., Peng, Y., Wightman, E., & Xu, N. (2015). The interaction of clay minerals with gypsum and its effects on copper-gold flotation. *Minerals Engineering*, 77, 121–130. <https://doi.org/10.1016/j.mineng.2015.03.010>

- de Kretser, R., Scales, P. J., & Boger, D. v. (1997). Improving Clay-Based Tailings Disposal: Case Study on Coal Tailings. *AIChE Journal*, *43*, 1894–1903.
- de Moraes, A. S., Carneiro Neto, E. B., & Lopes, M. C. (2021). Simulation of the Impedance of the Electrical Double Layer and Evaluation of the Surface Excess Concentration by Finite Element Analysis. *Orbital: The Electronic Journal of Chemistry*, *13*(2), 108–114. <https://doi.org/10.17807/orbital.v13i2.1453>
- Deer, W. A. (William A., Howie, R. A. (Robert A., & Zussman, J. (2013). *An introduction to the rock-forming minerals*.
- Dinkgreve, M., Paredes, J., Denn, M. M., & Bonn, D. (2016). On different ways of measuring “the” yield stress. *Journal of Non-Newtonian Fluid Mechanics*, *238*, 233–241.
- Farrokhpay, S. (2012). The importance of rheology in mineral flotation: A review. *Minerals Engineering*, *36–38*, 272–278.
- Farrokhpay, S., Morris, G. E., Fornasiero, D., & Self, P. (2010). Stabilisation of titania pigment particles with anionic polymeric dispersants. *Powder Technology*, *202*, 143–150.
- Farrokhpay, S., Ndlovu, B., & Bradshaw, D. (2018). Behavior of talc and mica in copper ore flotation. *Applied Clay Science*, *160*, 270–275. <https://doi.org/10.1016/j.clay.2018.02.011>
- Fatehah, M. O., Aziz, H. A., & Stoll, S. (2014). Nanoparticle Properties, Behavior, Fate in Aquatic Systems and Characterization Methods. *Journal of Colloid Science and Biotechnology*, *3*(2), 1–30. <https://doi.org/10.1166/jcsb.2014.1090>
- Fisher, D. T., Clayton, S. A., Boger, D. v., & Scales, P. J. (2007). The bucket rheometer for shear stress-shear rate measurement of industrial suspensions. *Journal of Rheology*, *51*(5), 821–831.

- Forbes, E., & Chryss, A. (2017a). Fundamentals of clays: Surface and colloid science, and rheology. In *Clays in the Minerals Processing Value Chain* (pp. 81–110). Cambridge University Press.
- Forbes, E., & Chryss, A. (2017b). Fundamentals of clays: Surface and colloid science, and rheology. In *Clays in the Minerals Processing Value Chain* (pp. 81–110). Cambridge University Press.
- Gao, M.-W., & Forssberg, E. (1993). A study on the effect of parameters in stirred ball milling. *International Journal of Mineral Processing*, 37, 45–59.
- George, H. F., & Qureshi, F. (2013). Newton's Law of Viscosity, Newtonian and Non-Newtonian Fluids. In *Encyclopedia of Tribology*. Springer US. <https://doi.org/10.1007/978-0-387-92897-5>
- Gräfe, M., McFarlane, A., & Klauber, C. (2017). Clays and the minerals processing value chain (MPVC). In *Clays in the Minerals Processing Value Chain* (pp. 1–80). Cambridge University Press. <https://doi.org/10.1017/9781316661888.003>
- Gregory, J. (2006). *Particles in Water : Properties and Processes*. IWA Pub.
- Gungoren, C., Guven, O., Cinar, M., & Ozdemir, O. (2020). An investigation of the effect of clay type on coal flotation along with DLVO theoretical analyses. *International Journal of Coal Preparation and Utilization*, 40(3), 210–222. <https://doi.org/10.1080/19392699.2019.1603146>
- He, M., Wang, Y., & Forssberg, E. (2004). Slurry rheology in wet ultrafine grinding of industrial minerals: A review. *Powder Technology*, 147(1–3), 94–112.
- Hiemenz, P. C., & Rajagopalan, R. (1997). *Principles of Colloid and Surface Chemistry* (Third).

- Hoffman, R. L. (1972). Discontinuous and Dilatant Viscosity Behavior in Concentrated Suspensions. I. Observation of a Flow Instability. *Transactions of the Society of Rheology: Journal of Rheology*, 16(1), 155–173.
- Johnson, S. B., Franks, G. v, Scales, P. J., Boger, D. v, & Healy, T. W. (2000). Surface chemistry-rheology relationships in concentrated mineral suspensions. *International Journal of Mineral Processing*, 58, 267–304.
- Jorjani, E., Barkhordari, H. R., Tayebi Khorami, M., & Fazeli, A. (2011). Effects of aluminosilicate minerals on copper-molybdenum flotation from Sarcheshmeh porphyry ores. *Minerals Engineering*, 24(8), 754–759.
- Kelessidis, V. C., & Maglione, R. (2008). Yield stress of water-bentonite dispersions. *Colloids and Surfaces A: Physicochemical and Engineering Aspects*, 318, 217–226.
- Klein, C., & Hurlbut, C. S. (1993). *Manual of Mineralogy*. Wiley & Sons.
- Liptak, B. G., & Kim, C. H. (2003). Viscometers—Application and Selection & Laboratory. In B. G. Liptak (Ed.), *Instrument Engineers' Handbook: Process Measurement and Analysis* (4th ed., Vol. 1, pp. 1700–1722). CRC Press.
- Luckham, P. F., & Rossi, S. (1999). The Colloidal and Rheological Properties of Bentonite Suspensions. *Colloid and Interface Science*, 82, 43–92.
- Malvern. (2013). *Zetasizer Nano User Manual*. Malvern Instruments Ltd.
- McFarlane, A., Bremmell, K., & Addai-Mensah, J. (2005). Microstructure, rheology and dewatering behaviour of smectite dispersions during orthokinetic flocculation. *Minerals Engineering*, 18(12), 1173–1182. <https://doi.org/10.1016/j.mineng.2005.06.013>

- Ndlovu, B. (2013). *The Effect of Phyllosilicate Mineralogy and Surface Charge on the Rheology of Mineral Slurries*.
- Ndlovu, B., Becker, M., Forbes, E., Deglon, D., & Franzidis, J.-P. (2011). The influence of phyllosilicate mineralogy on the rheology of mineral slurries. *Minerals Engineering*, 24(12), 1314–1322.
- Ndlovu, B., Farrokhpay, S., & Bradshaw, D. (2013). The effect of phyllosilicate minerals on mineral processing industry. *International Journal of Mineral Processing*, 125, 149–156.
- Ndlovu, B., Forbes, E., Farrokhpay, S., Becker, M., Bradshaw, D., & Deglon, D. (2014). A preliminary rheological classification of phyllosilicate group minerals. *Minerals Engineering*, 55, 190–200.
- Nelson, M. G. (2019). Viscosity and Rheology. In C. Robert, Kawatra S., & C. Young (Eds.), *SME Mineral Processing and Extractive Metallurgy Handbook* (pp. 161–171). Society for Mining, Metallurgy, and Exploration (SME).
- Nguyen, Q. D., & Boger, D. v. (1983). Yield Stress Measurement for Concentrated Suspensions. *Journal of Rheology*, 27(4), 321–349.
- Nguyen, Q. D., & Boger, D. v. (1985a). Direct Yield Stress Measurement with the Vane Method. *Journal of Rheology*, 29(3), 335–347.
- Nguyen, Q. D., & Boger, D. v. (1985b). Thixotropic behaviour of concentrated bauxite residue suspensions. *Rheologica Acta* , 24, 427–437.
- Oldham, K. B. (2008). A Gouy-Chapman-Stern model of the double layer at a (metal)/(ionic liquid) interface. *Journal of Electroanalytical Chemistry*, 613(2), 131–138. <https://doi.org/10.1016/j.jelechem.2007.10.017>
- Parker, S. P. (1991). *McGraw-Hill Dictionary of Science and Technology* (4th ed.). McGraw-Hill.

- Prestidge, C. A. (1997). Rheological investigations of ultrafine galena particle slurries under flotation-related conditions. *International Journal of Mineral Processing*, 51, 241–254.
- Rao, M. A. (2014). Flow and functional models for rheological properties of fluid foods. In *Rheology of Fluid, Semisolid, and Solid Foods* (pp. 27–61). Springer.
- Robinson, M. (1996). *Chambers 21st Century Dictionary*. W.R. Chambers.
- Schramm, G. (2000). *A Practical Approach to Rheology and Rheometry* (2nd ed.). Thermo Haake Rheology.
- Shaw, D. J. (1992). *Introduction to Colloid and Surface Chemistry* (4th ed.). Butterworth Heinemann.
- Shi, F. N., & Napier-Munn, T. J. (2002). Effects of slurry rheology on industrial grinding performance. *International Journal of Mineral Processing*, 65, 125–140.
- Tadros, T. F. (2010). *Rheology of Dispersions: Principles and Applications* (First). Wiley-VCH.
- Tilton, J. N. (2008). Fluid and Particle Dynamics. In D. W. Green & R. H. Perry (Eds.), *Perry's Chemical Engineers' Handbook* (8th ed.). McGraw-Hill.
- Verkerk, C. G., & Marcus, R. D. (1988). The Pumping Characteristics and Rheology of Paste Fills. In *Backfill in South African Mines* (pp. 221–233). Johannesburg, SAIMM.
- Wills, B. A., & Finch, J. A. (2016). Classification. In *Will's Mineral Processing Technology: An Introduction to the Practical Aspects of Ore Treatment and Mineral Recovery* (pp. 199–221).

- Xu, Z., Liu, J., Choung, J. W., & Zhou, Z. (2003). Electrokinetic study of clay interactions with coal in flotation. *International Journal of Mineral Processing*, *68*, 183–196.
- Yuan, D., Cadien, K., Liu, Q., & Zeng, H. (2019). Separation of talc and molybdenite: challenges and opportunities. *Minerals Engineering*, *143*.
<https://doi.org/10.1016/j.mineng.2019.105923>
- Zhang, M., & Peng, Y. (2015). Effect of clay minerals on pulp rheology and the flotation of copper and gold minerals. *Minerals Engineering*, *70*, 8–13.